Modelling Hydrodynamic Transport and Larval Dispersal in North-East Atlantic Shelf Seas

Thesis submitted in accordance with the requirements of
the University of Liverpool for the degree of Doctor in Philosophy
by

Jack J. C. Phelps

September 20, 2015

Abstract

This thesis presents a series of numerical modelling studies into hydrodynamic transport and larval dispersal. The initial investigation seeks to evaluate retention timescales in Liverpool Bay. The flushing time and residence time are equal to 136 days and 103 days respectively, however small concentrations of seawater are retained over several years due to vigorous tidal mixing. The age distribution is shown to be highly variable and dependent upon tracer input duration, however salinity can be used to estimate the mean age, which is not directly observable in practice.

Chapters 3, 4 and 5 all focus upon the dispersal of meroplanktonic larvae and aim to determine how larval behaviour affects their transport. Vertical migration is a significant influence upon larval dispersal within each case study, although the effect of this behaviour is conditional upon local hydrodynamic conditions. For example diel vertical migration promotes dispersal in the western Irish Sea, however the identical swimming pattern facilitates local retention in the eastern Irish Sea. The ecological implications of these findings are discussed.

This thesis concludes with an investigation into the impact of large CO_2 leakages on the marine carbonate system at potential carbon sequestration sites in the North Sea. Perturbations to seawater pH are found to vary according to the rate, duration and location of CO_2 input. The northern North Sea is particularly vulnerable to large perturbations ($>$ 1 pH units) during the summer months, as the strong seasonal thermocline suppresses CO_2 outgasing.

Contents

Acknowledgements

First and foremost I would like to thank Dr. Jeff Polton, whose guidance, patience and humour have been invaluable. It has been a genuine privilege to work alongside Jeff, and I consider myself extremely lucky to have had such a knowledgeable and considerate supervisor. I am also indebted to Prof. Alejandro Souza and Dr. Leonie Robinson for their vital support throughout my studies, and particularly for their helpful comments on the drafts of our published manuscripts. Their input has certainly resulted in many significant improvements to this thesis, and for that I am very grateful. Almost everyone at the National Oceanography Centre Liverpool has assisted me at some point over the past few years, but in particular I would like to thank Dr. Jason Holt and Dr. Jenny Brown for their insight during my two research placements. Likewise I thank Jerry Blackford for his assistance during my time on the QICS project. I would also like to acknowledge the Natural Environment Research Council for funding my studentship (NE/I528042/1) and making this research possible.

To Mum, thanks for promoting my research amongst the nursery nurses and primary school teachers of Rotherham, a key demographic that is often overlooked by many scientific minds. Your roast dinners helped too. To Dad, thanks for managing to muster some pride in my work despite the fact that it doesn't involve wearing overalls. I suppose Edd and Lucy are oreyt an' all.

Finally to Siân, who knows how grateful I am, thank you for cheering me up when I needed it most.

About This Thesis

Funding Sources

Chapters 2, 3 and appendix A are closely based upon three published manuscripts (see overleaf for details). The former two articles (Phelps et al., 2013, 2015a) were entirely funded by Natural Environment Research Council (NERC) postgraduate studentship funding (NE/I528042/1). The final article (Phelps et al., 2015b) derives from a short report written during a temporary placement at the National Oceanography Centre, as part of the QICS (Quantifying and monitoring potential ecosystem Impacts of geological Carbon Storage) project funded by RCUK/NERC grants (NE/H013849/1 and NE/H013962/1). Much of the preperation and original model simulations were conducted during this placement. Postgraduate studentship funding (NE/I528042/1) enabled Jack Phelps to carry out the additional simulations, data analyses, figure creation and scientific writing that were required in order to develop this work into a publishable manuscript. As such this material is included as an appendix rather than a full thesis chapter.

Publications

Jack J. C. Phelps, Jeff A. Polton, Alejandro J. Souza, Leonie A. Robinson
Hydrodynamic Timescales in a Hyper-tidal Region of Freshwater Influence
Continental Shelf Research, 63, 13-22, 2013.
DOI: 10.1016/j.csr.2013.04.027

Jack J. C. Phelps, Jeff A. Polton, Alejandro J. Souza, Leonie A. Robinson
The Influence of Behaviour on Larval Dispersal in Shelf Sea Gyres: *Nephrops norvegicus* in the Irish Sea
Marine Ecology Progress Series, 518, 177-191, 2015a.
DOI: 10.3354/meps11040

Jack J. C. Phelps, Jerry C. Blackford, Jason T. Holt, Jeff A. Polton
Modelling Large-Scale CO2 Leakages in the North Sea
International Journal of Greenhouse Gas Control, 38, 210-220, 2015b.
DOI: 10.1016/j.ijggc.2014.10.013

Chapter 1

Introduction

1.1 Introduction to Larval Dispersal

Marine benthic invertebrate taxa generally adopt one of three larval development strategies, commonly referred to as direct (or non-pelagic) development, lecithotrophy and planktotrophy (Vance, 1973; Todd and Doyle, 1981; Lalli and Parsons, 1997). Direct developers have no planktonic larval stage, and hatch as benthic juveniles that often closely resemble the adult form. Lecithotrophic larvae are planktonic and feed upon yolk stored in the egg during the larval stage. These larvae hatch in relatively small numbers from large eggs, and have a short pelagic larval duration (PLD) that typically ranges from less than a day to a few weeks. Finally, planktotrophic larvae are also planktonic, however they feed upon planktonic food throughout the larval stage. They tend to hatch in much greater numbers than either direct developers or lecithotrophic larvae, and they generally have a longer PLD that may range from a couple of weeks to several months. Altogether, approximately 70 % of benthic invertebrate species are said to have a planktonic larval phase early in their life cycle (Lalli and Parsons, 1997).

Lecithotrophic and planktotrophic larvae hatch at a spawning site inhabited by the adult population, and these propagules are subsequently advected by ocean currents. Upon reaching the end of their PLD, the larvae return to the seabed in order to locate an appropriate substrate and develop into

a juvenile. As many invertebrate larvae have limited swimming capabilities, larval transport is often largely determined (or at least heavily influenced) by the local hydrodynamic circulation, and individuals may be advected great distances between hatching and settlement. This transport of planktonic larvae from a spawning ground to a settlement site by dynamic processes in the marine environment is referred to as larval dispersal (Pineda et al., 2007).

1.2 Applications of Larval Dispersal

1.2.1 Population Connectivity

The length of time spent in the plankton is strongly correlated with dispersal distance (Shanks et al., 2003; Shanks, 2009). Although there are many notable exceptions to the rule, a short PLD often restricts the dispersal potential of lecithotrophic larvae, whereas the long PLD of planktotrophic larvae may lead to dispersal over hundreds of kilometres. It is also possible for larvae to be dispersed between geographically isolated subpopulations. This exchange of individuals between subpopulations is known as connectivity. In some marine environments, the dynamical regime may not favour local retention of larvae, therefore subpopulations of benthic invertebrates may rely upon recruitment of larvae from external sources for sustainability. Alternatively if local populations are sufficiently isolated, the circulation is retentive, or the PLD is very short, there may be no significant larval exchange between them, and they may rely entirely upon local recruitment.

Most benthic invertebrates are highly sedentary throughout their adult life, and many taxa such as mussels and barnacles are sessile, meaning they permanently or semi-permanently attached to the substrate. Larval dispersal is therefore critical for population dynamics and connectivity as the temporary larval stage is often the only opportunity for any significant migration between local populations. If there is no appreciable larval exchange between distinct local populations, they are referred to as closed populations (see figure 1.1), whereas if larvae are widely dispersed between local populations they are known as open populations (Cowen and Sponaugle, 2009).

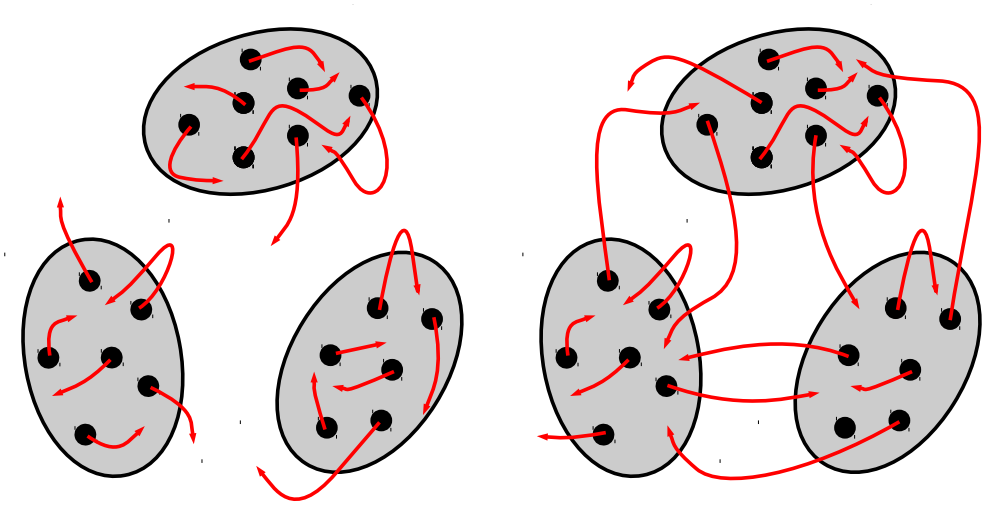

(a) Closed populations (b) Open populations

Figure 1.1: Schematic illustrating the concepts of connectivity, open and closed populations. Grey blocks represent local populations, red arrows represent larval trajectories.

Connectivity is a fundamental concept in marine ecology, and determining whether a local population is open or closed can have important implications for marine management (Cowen et al., 2000). Furthermore, insufficient or incorrect information about population connectivity can potentially lead to poor marine management decisions (Carr and Reed, 1993). It has been suggested that open populations may be more resilient to fishing pressure than closed populations, and they may be less susceptible to species loss as they are able to recruit individuals from external sources (e.g. Roberts, 1997).

Although the focus here has thus far been upon benthic invertebrate larvae, planktonic dispersal is also relevant for the eggs and larvae of many marine fish taxa, which are collectively termed ichthyoplankton. Fish larvae may be dispersed downstream from their spawning site into a nursery ground such as and estuary, seagrass meadow or mangrove forest (Rijnsdorp et al., 1985; Beck et al., 2001; Bolle et al., 2009). These nursery grounds typically have conditions that are favourable for development, and tend to have

high densities of juveniles (Beck et al., 2001). Additionally, the dispersal of ichthyoplankton can also be important for population connectivity. Despite the fact that adult fish are nektonic, meaning that they are capable swimmers and are able to swim independently of the local currents, many species (particularly coral reef fish) remain remarkably close to their settlement site throughout adulthood, restricting their activity to a "home range" that may be a kilometre in length or shorter (Kramer and Chapman, 1999).

1.2.2 Marine Protected Areas

Interest in larval dispersal and connectivity has risen sharply over the past 25 years, and investigations into the subject are now highly frequent within many marine ecology journals (Levin, 2006; Jones et al., 2009). One of the primary applications fuelling this growing interest is in the design of effective networks of marine protected areas (MPAs) and marine reserves.

A MPA is defined by the OSPAR Recommendation 2003/3 as "an area within the maritime area for which protective, conservation, restorative or precautionary measures, consistent with international law have been instituted for the purpose of protecting and conserving species, habitats, ecosystems or ecological processes of the marine environment", although various other competing definitions are available (Agardy et al., 2003). The term "marine reserve" is usually used to describe marine regions where any fishing or other extraction activities are entirely prohibited. Networks of MPAs and marine reserves have been widely advocated as a potential tool for conserving marine biodiversity and managing fisheries (Roberts et al., 2001; Agardy et al., 2003; Gell and Roberts, 2003; Christie et al., 2010), and larval dispersal is regarded as an important consideration in their design. There have been various recommendations and discussions on the size and spacing of MPAs in relation to local larval dispersal (e.g. Shanks et al., 2003; Palumbi, 2003; Jones et al., 2009; Roberts et al., 2010), and there is an emerging consensus on certain aspects of network design.

Ideally MPAs should be large enough so that sufficient numbers of larvae are retained within the protected site to sustain the local population. Typical

"rule of thumb" recommendations are for MPAs to have a minimum diameter of at least 5 to 10 km in order to protect a self-sustaining local population, although the exact requirements would be dependent upon each species and local hydrodynamic conditions. Clearly this may not be feasible if resident larvae have great dispersal potential (e.g. due to a long PLD or highly non-retentive local circulation) and the local population is heavily reliant upon larval import from external sources. In such cases it is recommended that MPAs are placed in relatively close proximity to one another in order to allow larvae with a high dispersal potential to migrate between adjacent protected nodes. MPAs should also be small enough to allow a degree of larval export to unprotected areas where fishing is permitted.

The design of MPA networks requires careful consideration of the various requirements of different stakeholders (Gleason et al., 2010). The ultimate objective of an MPA network should be to maximise the protection of biodiversity in the marine environment without restricting sustainable use of marine resources. Although balancing these competing requirements can be a difficult task, larval export from MPAs may actually lead to an increase in the fishery yield in nearby unprotected areas (Palumbi, 2003). Therefore larval dispersal studies can play an important role in designing and managing MPA networks to achieve mutual benefits.

It is the aim of the OSPAR Commission to establish an ecologically coherent network of marine protected areas in the north-east Atlantic, which should be far more effective at conserving marine biodiversity than isolated sites. By the end of 2012 there were a total of 333 MPAs in the region (figure 1.2), however the network was still not judged to be ecologically coherent (OSPAR Commission, 2012). Whilst there there is no precise formal definition of the term "ecological coherence", and it is open to some interpretation, connectivity of protected sites is one of the main assessment criteria. Larval dispersal studies will therefore be an essential tool in the assessment of the effectiveness of the MPA network in the north-east Atlantic as the network continues to grow.

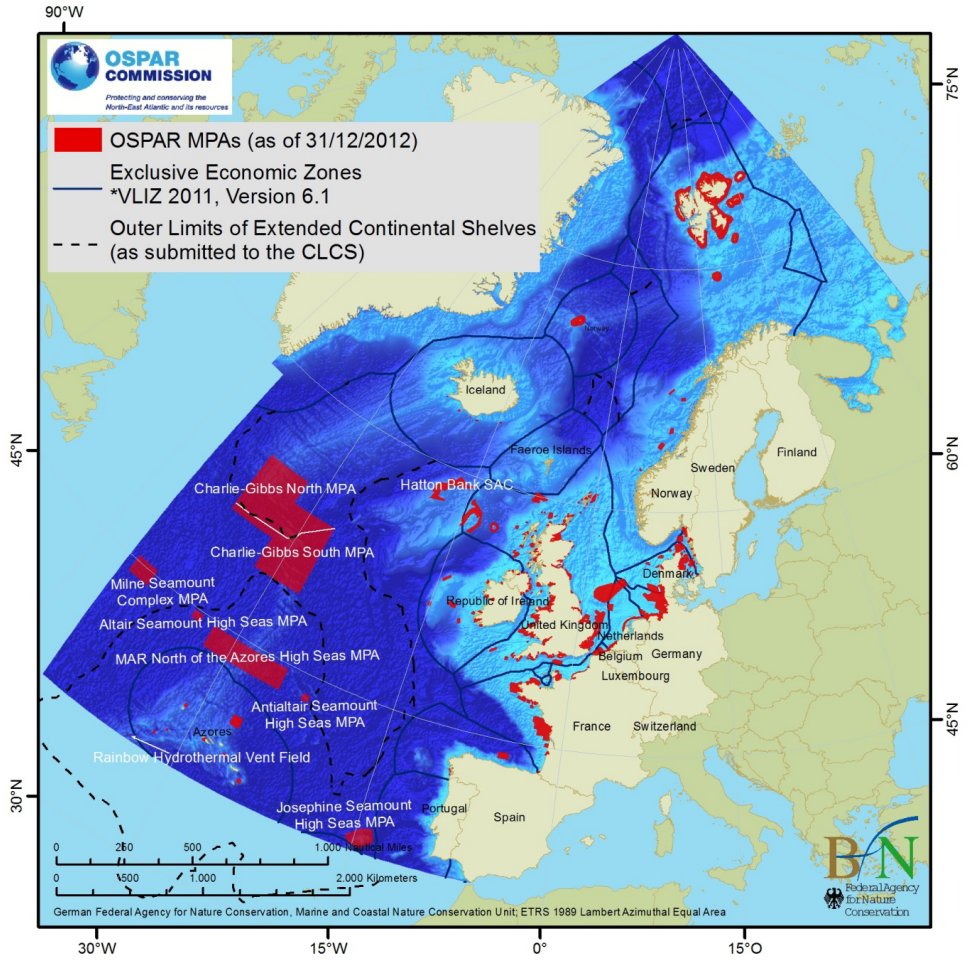

Figure 1.2: Distribution of OSPAR MPAs across OSPAR Regions (as of 31 December 2012), reproduced with permission from OSPAR Commission 2012 Status Report on the OSPAR Network of Marine Protected Areas. This figure was originally produced for the OSPAR Commission by the German Federal Agency for Nature Conservation, Marine and Coastal Nature Conservation Unit

1.2.3 Invasive Species

Another relatively common motivation for studying larval dispersal is to understand the spread of invasive species in the marine environment. Marine

organisms may be transported great distances whilst fixed upon the hull of ships, or within ballast water (Carlton and Geller, 1993). As ships circumnavigate the globe, non-indigenous species can be introduced into new environments where they are able to establish populations.

Invasive species can be detrimental to community structure as they consume indigenous biota, and compete with others for limited resources such as food and habitat. Such increased predation and competition may ultimately lead to local extinctions of indigenous populations (Mack et al., 2000). The pressure from invasive species has increased dramatically over recent centuries in line with the rise in shipping activity (Ruiz et al., 2000). Identifying invasive species and implementing effective measures to prevent their associated deleterious impacts is regarded as one of the greatest challenges to marine biodiversity (Mack et al., 2000; Molnar et al., 2008).

Notable examples of successful invasions in north-east Atlantic shelf seas include the barnacle *Elminius modestus* and the mussel *Mytilus galloprovincialis*. *E. modestus* is native to Australasia, however it was first observed on the south coast of England in 1945 (Bishop, 1947). Pelagic larval dispersal enabled *E. modestus* to advance rapidly along the coasts of Great Britain and continental Europe over the subsequent years, displacing the indigenous barnacle *Semibalanus balanoides* (Crisp, 1958). *M. galloprovincialis* naturally inhabits the Mediterranean coast, although it has now successfully established populations in several locations across the globe including South Africa, Japan and Hawaii (reviewed by Branch and Steffani, 2004). *M. galloprovincialis* have also formed a population in south-west England where they interbreed with *M. edulis* to create a hybrid population (Gilg and Hilbish, 2003a,b).

Whilst the initial introduction of invasive species in the marine environment is generally a consequence of shipping and other human activity, the subsequent development of newly established populations is often rendered possible due to pelagic larval dispersal (e.g. Crisp, 1958; Branch and Steffani, 2004). Larval dispersal studies have been used to predict the rate and direction of the expansion of invasive species populations (McQuaid and Phillips,

2000), and have the potential to inform coastal management and effective preventative measures. Conversely, distributions of invasive species may also be monitored in order to derive information about larval dispersal more generally (Shanks, 2009).

1.3 Observational Methods

It is extremely difficult to monitor larval dispersal directly using the traditional mark and recapture techniques that are highly effective in terrestrial and fisheries ecology because most species release millions of minuscule larvae. Furthermore larval densities decrease rapidly with distance from the source due to advective and diffusive physical processes, and also over time due to high mortality rates. Despite this intrinsic difficulty, several methods have been used to either observe larval dispersal patterns directly, or to infer them from observational data with varying degrees of success (see Thorrold et al., 2002; Palumbi, 2003; Levin, 2006; Thorrold et al., 2007; Hedgecock et al., 2007; Cowen and Sponaugle, 2009; Jones et al., 2009; Carson et al., 2013, for comprehensive reviews of various methods). Three of the most commonly used methods are artificial (or chemical) tags, geochemical (or environmental) tags and direct genetic analyses.

Artificial chemical tags involve marking larvae prior to dispersal and recapturing them at a later date to monitor their migration. This typically requires eggs or developing larvae to be immersed within fluorescent compounds or other chemical solutions that adhere to the individuals (e.g. Jones et al., 1999). Whilst such studies may provide direct evidence of larval retention or transport, there are several significant drawbacks. It is difficult to ensure that significant handling effects have not been introduced whilst tagging the eggs or larvae, and it is often difficult to recover tagged individuals (Thorrold et al., 2002). Furthermore it is not possible to evaluate connectivity statistics without first estimating the proportion of the population that were chemically tagged.

Recent investigations have begun transgenerational marking (Thorrold

et al., 2006; Almany et al., 2007), which involves injecting adult females with stable isotopes which are passed onto their offspring. This approach is certainly less laborious than immersing eggs and larvae in chemical solutions, and it may enable a greater proportion of the population to be tagged. However there are conflicting reports on the extent that such tagging affects larval development (Williamson et al., 2009; Starrs et al., 2014), therefore it is possible that tagged larvae may not be representative of the population.

Geochemical tags, (or environmental tags) arise from the fact that variations in temperature, salinity or seawater chemical composition are often naturally recorded by marine organisms, particularly in calcified structures such as the shells or statoliths of invertebrates (Fodrie et al., 2011) or the otoliths of fish (Vasconcelos et al., 2007; Cuveliers et al., 2010). If for example the elemental composition of the shell of a juvenile invertebrate does not reflect the surrounding habitat, then this may indicate that the individual was imported from an external source, and it may be possible to identify its origin.

There are benefits to this method over the artificial chemical approach, notably that the entire population is naturally marked, and the lack of an artificial marking procedure ensures that no adverse handling effects are introduced. Drawbacks include the fact that geochemical markers can be ambiguous and difficult to analyse (Thorrold et al., 1998; Martin et al., 2004). Furthermore as this approach relies upon strong regional gradients in the physical or geochemical properties of seawater, it may be particularly useful in estuarine and coastal environments, however it is generally not suitable for measuring dispersal in more spatially uniform environments such as the open ocean.

Genetic approaches to investigating larval dispersal rely on genetic differentiation amongst marine populations and can be either direct or indirect. Direct genetic methods involve analysing genetic data and conducting statistical analyses in order to deduce either a likely population of origin (Gilg and Hilbish, 2003a) or the exact parentage (Jones et al., 2005; Planes et al., 2009; Christie et al., 2010; Berumen et al., 2012) of an individual. Indi-

rect genetic techniques are used to study connectivity over evolutionary time scales (Hedgecock et al., 2007). Unfortunately even low levels of migration between subpopulations often diminish genetic differentiation substantially, rendering some genetic methods unsuitable (Hellberg et al., 2002; Palumbi, 2003).

Whilst each of these observational methods can be effective and may provide direct evidence of dispersal or retention of larvae, they are generally labour intensive, and thorough experiments are expensive to conduct. No single observational technique is universally suitable to study larval dispersal in all species and environments, and most of these methods are only suited to monitoring one spawning event. Furthermore each method involves making various assumptions, for example regarding the proportion of larvae that are tagged, larval mortality rates or population genetic structure. Because of the numerous drawbacks to observational approaches, many marine ecologists utilise numerical hydrodynamic models to predict larval dispersal patterns.

1.4 Passive Dispersal Models

Early numerical investigations that addressed larval dispersal were generally based upon the premise of passive transport by the ambient local circulation. Whilst some of these studies utilise Eulerian tracer concentrations within idealised advection-diffusion or advection-diffusion-mortality models to research aspects of larval dispersal in a general context (Hill, 1990; Cowen et al., 2000), most focus upon a specific geographical area, incorporating spatial and temporal variability of the local circulation into their calculations in order to assess dispersal at a regional level (Dight et al., 1990; Black, 1993; Davidson and deYoung, 1995; Jenkins et al., 1997; Roberts, 1997; Huggett et al., 2003).

Typically numerical hydrodynamic models are used to generate velocity fields in the region of interest, and these data are used to force an "offline" particle tracking model. Particles representing larvae are released at a known (or often assumed) spawning site, and are advected and diffused for a length of time corresponding to the PLD of the species under investigation (figure

1.3). The final particle locations are then assumed to represent potential settlement sites for juvenile invertebrates or fish. The trajectories of the passive particles can then be analysed to estimate dispersal distances and connectivity statistics.

Aside from obvious reductions in costs and resources there are several other advantages to using numerical techniques over observational methods. Modelling studies can release many millions of particles, whereas genetic parentage studies for example may only succeed in identifying a handful of parent-offspring pairs (Christie et al., 2010). This ability to generate a wealth of dispersal data is highly valuable when conducting statistical analyses. With regular model output, numerical modellers are also able to pinpoint the exact location of each particle throughout their entire pelagic stage, whilst observational studies are usually only able to estimate a spawning site and settlement site. Furthermore it is usually relatively straight forward to run simulations under different seasonal conditions, atmospheric forcing, or even use future climate projections to estimate how climate change might affect larval dispersal. On the other hand, these numerical methods are not without their shortcomings, and many early modelling studies have received strong criticism for making the major simplifying assumption of passive dispersal, neglecting larval behaviour. As with all numerical models they must be carefully validated.

1.5 Larval Behaviour

It has long been established that the meroplanktonic larvae of coral reef fish and large oceanic invertebrates are capable of actively influencing their transport and should not be regarded as passive particles by ocean modellers (Roe, 1984; Paris and Cowen, 2004). There is now substantial evidence that the larvae of many smaller marine invertebrates in temperate coastal environments display similar characteristics (Hillis, 1974; Pennington and Emlet, 1986; Lindley et al., 1994; Hays et al., 1996; Irigoien et al., 2004; Knights et al., 2006).

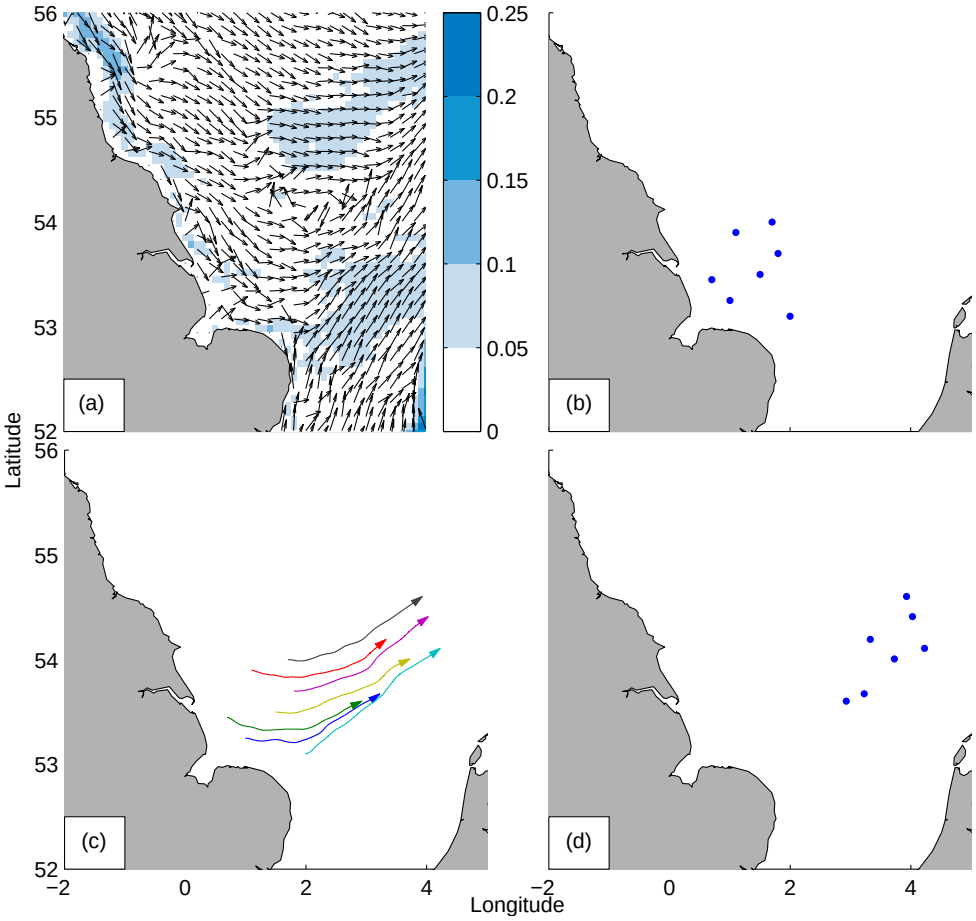

Figure 1.3: A schematic illustrating the steps involved in passive larval dispersal modelling. (a) Step 1: Use a hydrodynamic model to produce velocity fields at regular intervals. This panel depicts surface velocity (m s^{-1}) off the eastern English coastline in January 2002, calculated by the POLCOMS MRCS model. Direction is indicated by the arrows, absolute velocity is indicated by the colour axis. (b) Step 2: Initialise the particle locations at an assumed adult spawning ground. (c) Step 3: Advect and diffuse the particles in the model for a period of time corresponding to the PLD of the species under investigation. (d) Step 4: Output the final particle distribution, which represents potential larval settlement sites, and derive dispersal distances, connectivity statistics etc.

Many larvae are able to regulate their position in the water column. This normally involves active vertical swimming to either maintain a desired depth throughout the planktonic phase or migrate vertically in response to physical and biological cues such as light intensity, tidal state or larval stage (Kingsford et al., 2002). If such behaviour is adopted within vertically sheared flows, larvae will modify their dispersal pathway significantly, even if swimming velocities are several orders of magnitude smaller than the local circulation (Hill, 1991, 1998; Smith and Stoner, 1993; Cronin and Forward, 1979; North et al., 2008). If vertical gradients in horizontal velocity are substantial, swimming just a few metres in the vertical may result in vastly different dispersion scenarios (Vikebo et al., 2005).

Perhaps the most widely documented form of vertical migration amongst larvae and other zooplankton is diel vertical migration (DVM), whereby larval depths fluctuate within the water column with a twenty four hour period. The most common DVM strategy is referred to as nocturnal (or normal) DVM, and it is characterised by a daily vertical ascent to the surface waters at sunset, followed by a descent into deeper waters at sunrise (Lalli and Parsons, 1997). There are also many reports of two other DVM strategies, particularly amongst holoplanktonic copepods, referred to as twilight DVM (or midnight sinking) and reverse DVM (or nocturnal descent). Twilight diel vertical migration is characterised by plankton that rise to the surface at dusk and slowly descend around midnight, followed by a second ascent at the end of the night and a final descent at dawn (Cushing, 1951), whilst reverse diel vertical migration involves plankton residing in the surface waters by day and deep waters by night (Ohman et al., 1983).

Considerable effort has made to understand the adaptive significance of this behaviour and several hypotheses have been proposed in an attempt to explain the underlying motives. There is a large body of evidence to support the argument that some zooplankton reside within darker sub-surface waters during the day in order to avoid visually hunting predators, and return to the surface waters at night as that is where food is most abundant (Zaret and Suffern, 1976; Gliwicz, 1986; Neill, 1990; Hays, 2003). Similarly Ohman

et al. (1983) suggests that the reverse DVM strategy is used by the marine copepod *Pseudocalanus* sp. to avoid non-visually feeding nocturnal predators. Other proposed explanations for DVM include metabolic advantages (McLaren, 1963) or a reduction in the risk of harmful ultraviolet radiation (Pennington and Emlet, 1986; Leech and Williamson, 2001). Whilst it is highly likely that no single universal driver, it is believed that evasion of visually hunting predators is probably the ultimate motive for most zooplankton that perform DVM (Hays, 2003).

Ontogenetic vertical migration is another widespread form of vertical swimming behaviour, where larval depths are dependent upon larval stage. Amongst benthic invertebrate larvae, older late-stage larvae are often found in deeper waters than their newly hatched counterparts (e.g Hillis, 1974), presumably as they descend towards the seabed in order to locate a suitable habitat for settlement. Some species are known to display rather more complex ontogenetic behaviour patterns, such as a modification to the regular DVM during certain larval stages (Shanks, 1986).

Yet another relatively common vertical migration scheme is circatidal migration, which is characterised by swimming vertically in synchronisation with tidal state. Some larvae are able to exploit the vertical shear in tidal currents in order to manipulate their horizontal transport. This is achieved by ascending in the water column during one stage of the tide to be advected by the tidal flow, and returning to deeper waters (where tidal velocities are weaker) or attach themselves to the seabed on the opposite tidal stage. By utilising a single tidal stage in this manner, larvae can increase net advection dramatically to promote dispersal. Alternatively, in estuarine and coastal environments, larvae may ascend during the flood tide to reduce dispersal and ensure local retention, or even migrate further up an estuary (Cronin and Forward, 1979; DeVries et al., 1994; Knights et al., 2006). This process is referred to as selective tidal stream transport (STST) (Forward and Tankersley, 2001).

It is not clear whether larvae that exhibit circatidal migration respond to changes in pressure, salinity, turbulence or another physical cue (Kingsford

et al., 2002). Although circatidal migration behaviour is similar to DVM, horizontal transport is apparently the purpose of circatidal migration, rather than an indirect consequence.

Vertical swimming may be particularly important in determining the fate of planktonic larvae in shelf seas as vertical gradients in horizontal velocity can be substantial. Strong tidal currents and shallow depths result in sharp vertical gradients in tidal flow in the bottom boundary layer. Large riverine flow into regions of freshwater influence (ROFIs) (Simpson, 1997) result in strong salinity-mediated horizontal density gradients that drive an estuarine circulation (Heaps, 1972; Heaps and Jones, 1977; Simpson et al., 1990), and can be seen to influence bottom current direction and sediment transport (Brown et al., 2015). Cold water pools can develop in bathymetric depressions beneath seasonal thermoclines, and the associated sharp bottom horizontal density gradients drive seasonal jets and gyres that dominate the local mean flow (Hill et al., 1994; Hill, 1996; Brown et al., 2003; Horsburgh et al., 2000). These conspicuous geostrophic baroclinic features are often found in shelf seas.

Whilst much of the modelling focus has been placed upon incorporating vertical swimming into particle tracking models, this is only one (albeit very important) aspect of larval behaviour. Some larger larvae are also capable of directed horizontal swimming at considerable speeds; late stage coral reef fish larvae are able to swim at velocities of tens of centimetres per second (Leis et al., 1996; Leis and Carson-Ewart, 1997; Fisher et al., 2005). Such horizontal swimming capabilities could either greatly enhance dispersal or ensure local retention depending upon the swimming orientation.

Predation and mortality are also important considerations. Not only does mortality reduce the overall number of larvae that survive through to adulthood, but if there are spatial variations to mortality, for example due to predator abundance, or food availability, then this can affect the overall spatial pattern of dispersal and connectivity.

Another feature that is common amongst many marine taxa is the influence of physical properties, particularly temperature upon larval growth.

Typically warmer seawater temperatures lead to faster development, and therefore a shorter PLD (O'Connor et al., 2007). Some larvae also develop at different rates according to seawater salinity (Thiyagarajan et al., 2003). As shorter PLDs are typically associated with shorter dispersal distances (Shanks et al., 2003), these effects can be important for larval dispersal and connectivity. Other important considerations include competition for resources, substrate availability and tolerances to physical properties such as temperature and salinity.

This is certainly far from an exhaustive account of all aspects of larval behaviour that influence dispersal (see Kingsford et al., 2002, for further details), however it is apparent that larvae cannot be assumed to behave as passive particles in numerical models unless there is sufficient evidence for the contrary. Although marine modellers are often limited by the scarcity of species-specific quantitative biological data, every effort should be taken to ensure that numerical models take proper account (as best as possible) of the particular behaviour of the species under investigation. Failure to do so may lead to erroneous results, and potentially poor marine management decisions.

1.6 Biophysical Models

In recent years larval dispersal studies have developed from two dimensional passive particle tracking models to complex three dimensional biophysical models that incorporate many of aspects of larval behaviour. Models that include some form of vertical migration are now commonplace (e.g. Emsley et al., 2005; Marta-Almeida et al., 2006; van der Molen et al., 2007; Vikebo et al., 2007; North et al., 2008; Fox et al., 2009; Bolle et al., 2009; Ospina-Alvarez et al., 2012; Robins et al., 2013), although the parametrisation of this behaviour varies considerably.

Simulated vertical swimming behaviour ranges from relatively simple schemes where particle depth or swimming velocity is prescribed as either a sinusoidal or piecewise constant function of time (Robins et al., 2013), to

complex stochastic vertical swimming sub-models where particles respond to physical cues such as a halocline (North et al., 2008). It is known that the precise numerical parametrisation of vertical migration behaviour can influence results (Sundelof and Jonsson, 2012). Complex stochastic vertical swimming sub-models are generally considered to be superior providing that they can be validated against observational data, however straightforward swimming schemes are more appropriate if swimming behaviour is not fully understood, or for generic larval dispersal studies that do not focus upon a particular species.

Recently there have been numerous attempts to include directed horizontal swimming into modelling studies (reviewed by Staaterman and Paris, 2014). This is now a promising and growing area of research, however directed horizontal swimming is clearly more difficult to simulate accurately than a regular vertical oscillation. Other elements of larval behaviour and physiology that have been successfully incorporated into numerical models include e.g. temperature-dependent larval development rates (Vikebo et al., 2005; Ospina-Alvarez et al., 2012; Nicolle et al., 2013; Phelps et al., 2015a).

Significant advances in computational power and affordability have also led to increasingly sophisticated modelling techniques. For example early larval dispersal studies often relied upon the Euler method of integration to calculate particle advection; this technique has now largely been superseded by advanced numerical schemes such as the Runge-Kutta 4^{th} order method (North et al., 2008) or the Adams-Bashforth / Adams-Moulton predictor-corrector method (Peliz et al., 2007). Such methods are well known to be considerably more accurate at calculating particle advection (Ramsden and Holloway, 1991; North et al., 2009; Qiu et al., 2011).

The number of particles simulated in typical studies has also risen sharply (Willis, 2011), and modern studies now regularly use upwards of one million particles, and sometimes considerably more. Greater numbers of particles ensure that the results are not overly influenced by outliers. Ideally one should conduct statistical tests to ensure that the number of particles is sufficient for the investigation (Brickman and Smith, 2002; Simons et al.,

2013).

There have also been significant developments in the treatment of diffusion in larval dispersal models. Hunter et al. (1993) highlighted the fact that non-uniform diffusivity can lead to artificial particle accumulation in regions of low diffusivity. In order to ensure that the well-mixed condition is met (i.e. a uniform distribution of particles remains uniform at all time, see Brickman and Smith, 2002, for details) additional terms are added to the stochastic diffusion equation. This problem has since been addressed by Visser (1997) and Ross and Sharples (2004), who also highlight the importance of the time step selection and boundary conditions. Further information on the recommended practice for modelling planktonic eggs and larvae and their behaviour is provided by North et al. (2009), Willis (2011) and Staaterman and Paris (2014).

Whilst this vast research field has seen some significant developments over the past decade, it is clear that certain aspects of larval dispersal remain poorly understood, and there is still plenty of scope for further improvements. It is vital for effective marine management that future investigations utilise appropriate research methods to discern the extent of dispersal and connectivity, particularly in exploited coastal regions.

Each study method from genetic parentage analyses to numerical models have their own benefits and drawbacks, and no single method can be considered universally superior. Several investigations have successfully supplemented modelling simulations with observational data (Gilg and Hilbish, 2003b; Galindo et al., 2010; Christie et al., 2010). It would appear likely that combining methodologies in this manner will be critical in working towards a general understanding of larval dispersal in the marine environment.

1.7 Hydrodynamic Transport Timescales

Although the principal focus of this thesis is upon the dispersal of planktonic larvae, chapter 2 is dedicated to a numerical investigation into hydrodynamic transport timescales. Transport timescales such as age, residence time and

flushing time have found widespread application within marine science (e.g. Waugh et al., 2004; Zhang et al., 2010; Olbert et al., 2011). In this investigation these timescales are each evaluated in Liverpool Bay, a shallow coastal marine region with artificially enriched nutrient concentrations.

This chapter serves as an effective introduction to both the study region and the POLCOMS hydrodynamic model. It also introduces many physical processes in coastal oceanography, such as estuarine circulation, advection of dissolved passive tracers, turbulent mixing and strain-induced periodic stratification. Whilst this investigation does not directly deal with larval dispersal, the residence time of a coastal region is known to influence larval dispersal, with longer residence times favouring greater local retention.

Chapter 2

Hydrodynamic Timescales in a Hyper-tidal Region of Freshwater Influence.

This chapter is based upon Phelps, J. J. C., Polton, J. A., Souza, A. J. and Robinson, L. A. Hydrodynamic timescales in a hyper-tidal region of freshwater influence. *Continental Shelf Research*, 63: 13-22, 2013.

Abstract

This study uses a three dimensional hydrodynamic model to investigate transport timescales in Liverpool Bay, a shallow hyper-tidal region of freshwater influence (ROFI) with a density-driven baroclinic residual circulation. Flushing time, residence time and age are evaluated, providing rigorously defined parameters to describe the rate of offshore freshwater transport and basin replenishment. Additional challenges encountered when assessing these timescales in a tidally mixed regime are highlighted by idealised models.

Climatological river gauge data reveals that the numerous local rivers contribute an average of 203 m^3s^{-1} of freshwater to Liverpool Bay. Based upon the mean salinity distribution, this would suggest a flushing time of approximately 136 days. The mean residence time of the region is approximately 103 days although small concentrations of water are retained over

several years due to vigorous tidal mixing.

Age in the region is highly variable with regular oscillations caused by tidal advection, whilst long term fluctuations are governed by river flow rates. The mean age gradient is directed offshore, approximately parallel to both the salinity gradient and the major axis of the tidal ellipse, with basin wide average magnitude of 6 days km^{-1}. It is shown that salinity may be used to estimate the age of freshwater, which is not directly observable in practice.

2.1 Introduction

Concerns about the exposure of marine ecosystems to anthropogenically enriched fluvial nutrient concentrations, toxic metals and other pollutants have led to a drive within biological and geochemical research to investigate the fate of freshwater in shelf seas. A thorough understanding of the transport of freshwater runoff is essential for effective marine management and proper protection of the coastal zone. With increasingly sophisticated numerical hydrodynamic models, together with modern advances in Constituent-oriented Age and Residence time Theory (CART) (Delhez et al., 1999; Deleersnijder et al., 2001; Delhez and Deleersnijder, 2002; Delhez et al., 2004), there is an unprecedented opportunity to properly assess the vulnerability of coastal waters to the stresses of anthropogenic activity.

Although the impacts of marine pollution upon a coastal ecosystem are diverse, eutrophication represents one of the greatest threats to the biodiversity of many shallow shelf regions. Undesirable disturbances associated with eutrophication include harmful algal blooms and depletion of dissolved oxygen, which may have a devastating impact upon fish and invertebrate populations (Hallegraeff, 1993). Additionally, blooms of toxin producing algae may ultimately result in human illnesses, and potentially human fatalities through the consumption of seafood (Hallegraeff, 1993). The risk of eutrophication is amplified when the local hydrography is retentive (Schindler, 2006) and as such freshwater transport timescales are fundamental properties when considering the potential effects of nutrient enrichment.

Three of the most frequently utilised methods of quantifying transport time in a marine environment are flushing time, residence time and age (Monsen et al., 2002). Flushing time is defined as the ratio of the mass of a scalar in a bounded system to the rate of renewal of that scalar. In this investigation flushing time serves as an elementary method to approximate the time taken to completely replenish the freshwater content of a basin. The residence time of a water parcel is defined as the length of time that it will remain within the region before exiting through an offshore boundary. This describes the typical exposure of the basin to any dissolved constituent or contamination and acts as a quantitative measure of how retentive the local hydrography is. Finally the age of a water parcel refers to the length of time that has elapsed since it entered the system through a source point (Zimmerman, 1976). In coastal marine modelling this source point is typically an estuary. This study aims to evaluate these three timescales in Liverpool Bay, a coastal marine region with a history of nutrient enrichment.

Liverpool Bay has been the subject of numerous biological and geochemical investigations, (e.g. Gowen et al., 2000; Gowen and Stewart, 2005; Gowen et al., 2008; Greenwood et al., 2011; Panton et al., 2012) many of which primarily conducted to observe the elevated nutrient concentrations in the basin, and to assess the risk of coastal eutrophication and other deleterious impacts. Heightened concentrations of nitrogen and phosphorus are found throughout the winter months, particularly in the vicinity of the estuaries, this is attributed to the impact of industrial and domestic effluent. There is also substantial evidence to suggest that nutrient enrichment contributes to an elevated biomass in the region (although not necessarily an undesirable disturbance), and as such the necessity to closely monitor the region continues.

2.2 Study Region

Liverpool Bay is a shallow coastal sub-region of the semi-enclosed Irish Sea (figure 2.1). Liverpool Bay was closely monitored for eight years by

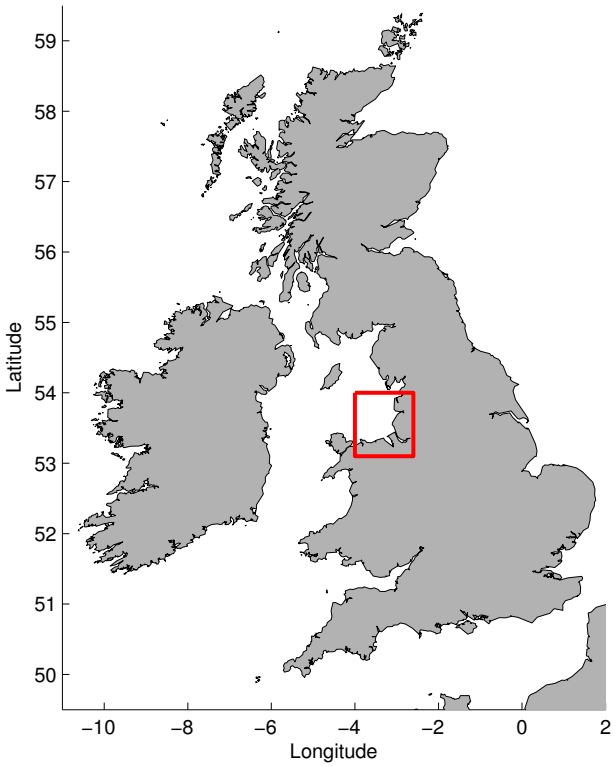

Figure 2.1: Location of Liverpool Bay (highlighted in red) in relation to Great Britain and Ireland.

the coastal observatory (Howarth and Palmer, 2011) led by the Proudman Oceanographic Laboratory (now part of the National Oceanography Centre). Observational data collected by routine CTD surveys, fixed moorings, coastal tide gauges, satellite data and instrumented ferries are supplemented by numerical simulations with the objective of gaining insight into the response of a shelf sea to natural forcing and the consequences of human activity.

Freshwater enters the bay at discrete point sources through several rivers, including the Mersey, Ribble, Dee, Conway and Clwyd (shown in figure 2.2). These rivers collectively maintain a strong, quasi-stable offshore salinity gradient (figure 2.3), resulting in a zonal offshore density gradient of approximately 0.12 kg m^{-3} km^{-1} (Verspecht et al., 2009b). Liverpool Bay is described as a Region Of Freshwater Influence (ROFI) (Simpson, 1997).

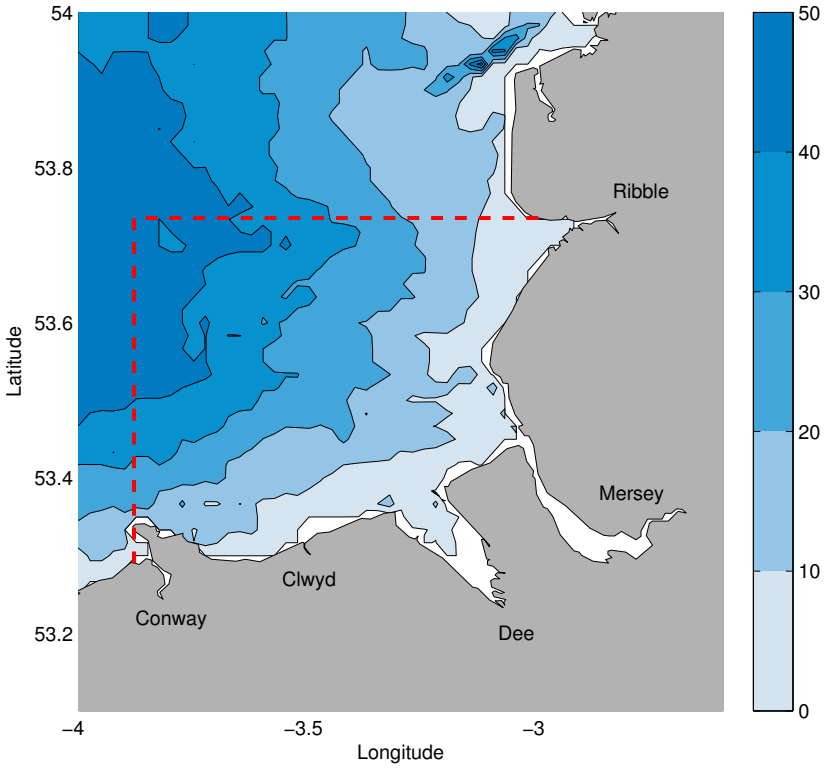

Figure 2.2: POLCOMS Irish Sea model bathymetry (m) data in Liverpool Bay. Major rivers are labelled and the domain boundary is highlighted in red.

Liverpool Bay experiences a temperate climate and temperature gradients are directed onshore during summer and offshore during winter. The seasonal variability in the direction of the temperature gradient is due to the fact that shallow coastal waters respond faster to atmospheric temperature changes than deeper offshore waters (Polton et al., 2011). This variable temperature distribution has a relatively weak influence upon the density field in contrast to the salinity distribution.

Liverpool Bay is categorised as a hyper-tidal region, with semi-diurnal tidal currents that reach 1 m s^{-1}, and an exceptionally large tidal range that occasionally exceeds 10 m during spring tides. Tidal flow is approximately rectilinear within Liverpool Bay, taking the form of a standing wave,

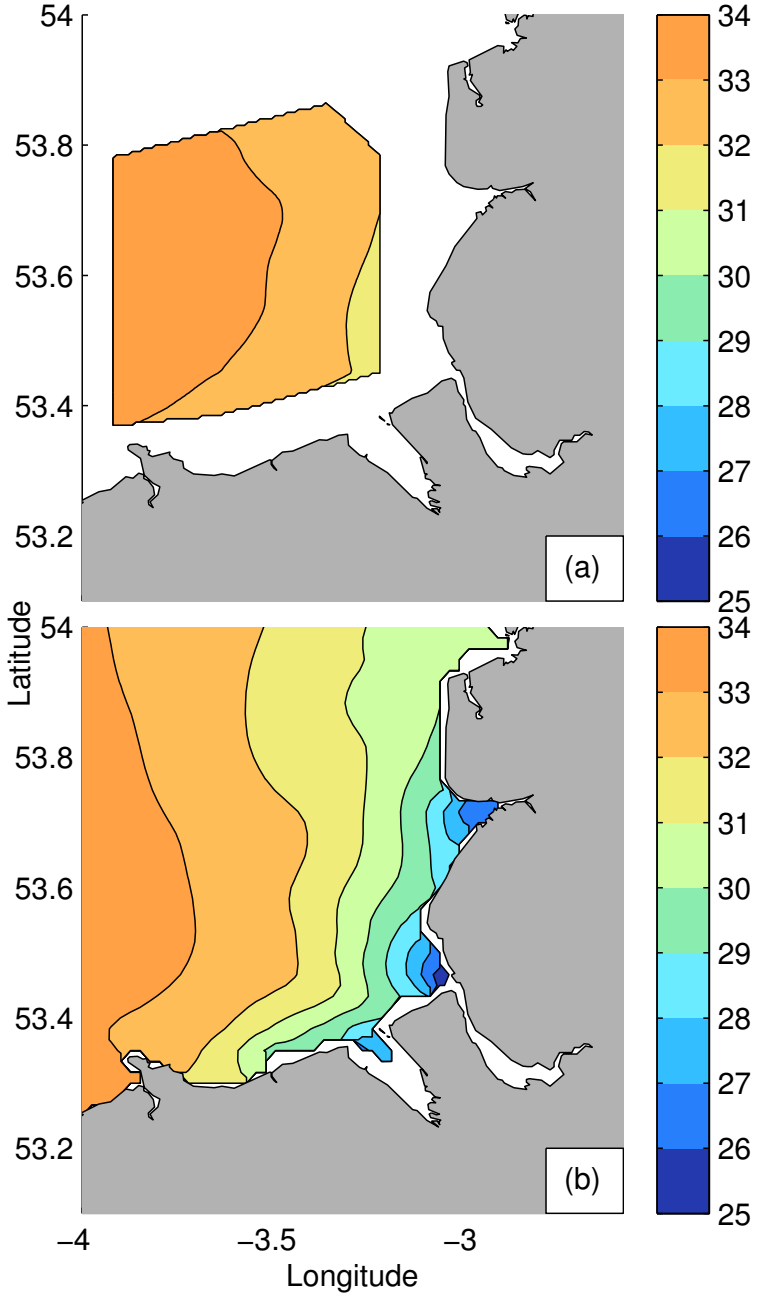

Figure 2.3: The average surface salinity (psu) distribution in Liverpool Bay. (a) Calculated from observational salinity data, collected from a series of 68 coastal observatory cruises. (b) Calculated from POLCOMS hydrodynamic model salinity output, forced with meteorological data from the year 1999.

propagating almost parallel to the density gradient (Polton et al., 2011).

Water column stability in Liverpool Bay fluctuates according to tidal state and tidal phase due to the strain-induced periodic stratification (SIPS) process (Simpson et al., 1990). Buoyant brackish water is advected over the denser ambient water during the ebb tide due to the interaction between horizontal density gradient and vertical shear in tidal velocity, resulting in a stratified water column. On the flood tide the process is reversed and the water column reverts to a vertically mixed state. Whilst this phenomenon has been observed in other macro-tidal ROFIs (e.g. the Rhine ROFI Souza and Simpson, 1996), it is particularly pronounced here due to the mutual alignment of the density gradient and the major axis of the tidal ellipse. SIPS is found in Liverpool Bay on most tidal cycles, however enduring stratification can persist over the flood tide during neaps (Simpson et al., 1990; Verspecht et al., 2009a; Palmer and Polton, 2011).

Observations and modelling studies demonstrate that wind stress also has an important influence upon the residual circulation and the development of stratification in Liveprool Bay (Verspecht et al., 2009a,b). The mean surface flow is strengthened during periods of offshore (south-easterly) winds, whereas onshore (north-westerly) winds lead to a significant reduction in the strength of the surface flow, and occasionally a reverse in the direction. Similarly wind straining may either facilitate or restrict the development of stratification depending upon wind direction. Offshore winds enhance SIPS on the ebb tide and slow the breakdown of stratification on the flood tide, whilst onshore winds have the opposite effect.

Although the tidal flow dominates the kinetic energy budget in Liverpool Bay, it is the residual circulation that is of primary importance for long-term freshwater transport. The long-term mean circulation in Liverpool Bay is spatially variable, but it broadly consists of a northward offshore surface flow of approximately 0.04 m s^{-1} that rotates with depth, culminating in a southward onshore bottom flow of around 0.02 m s^{-1} (Polton et al., 2013). The principal component of this residual flow is a result of the salinity-controlled baroclinic density field, that introduces a horizontal pressure gradient, which

in turn induces an estuarine circulation under the influence of rotation. This component of the mean flow was described by Heaps (1972) as an approximate balance between the pressure gradient, Coriolis and frictional forces. Freshwater input is therefore paramount to the local hydrodynamic regime.

There have been some notable recent developments upon the work of Heaps (1972), which attempt to eliminate the discrepancy between theory and observations. Verspecht et al. (2009b) analysed five years of acoustic doppler current profiler (ADCP) measurements and found that the periodic stratification in Liverpool Bay further complicates the mean circulation through its effect upon the eddy viscosity. As the water column stratifies towards the end of the ebb tide, vertical mixing is suppressed, and the density driven flow strengthens. Tidal flow therefore ultimately reinforces the offshore transport of freshwater through nonlinear rectification of the mean flow. Whilst the necessary assumption of Heaps (1972) of a constant eddy viscosity is unrealistic, Verspecht et al. (2009b) found that by reducing the viscosity from 0.0234 $m^2\ s^{-1}$ (which is typical of a mixed water column) to 0.0129 $m^2\ s^{-1}$ the model error can be reduced significantly.

Polton et al. (2013) also built upon this work by adjusting the model to be constrained by surface velocity, which can be readily deduced from high frequency (HF) radar observations, rather than freshwater flow and the horizontal density gradient, which are not as well understood. By using this method, two-dimensional surface flow data can be combined with the analytical model to infer a relatively accurate spatially variable three-dimensional velocity field.

Another component of the mean circulation arises from a modification to the barotropic tide. Although the tide in Liverpool Bay is generally almost entirely rectilinear, stratification decouples the upper and lower mixed layers, resulting in counter rotating tidal ellipses in the surface and bottom waters (Verspecht et al., 2010; Palmer, 2010). During periodic stratification this tidal modification will introduce a brief northward surface flow and southward bottom flow (Palmer, 2010; Palmer and Polton, 2011), therefore complimenting the density driven flow. This mechanism is referred to as

SIPS pumping.

An additional contribution to the transport of freshwater in Liverpool Bay comes in the form of tidally induced shear dispersion (Bowden, 1965). Shear dispersion occurs due to the interaction between vertical turbulent mixing and the vertical gradient in the horizontal velocity profile, resulting in an effective horizontal diffusion. In Liverpool Bay, this will lead to a reinforced horizontal diffusion in the east-west direction, parallel to the major axis of the tidal ellipse.

Whilst the density-driven residual flow is believed to be the primary control upon the fate of freshwater in Liverpool Bay, the nonlinear influence of tidal circulation can clearly not be ignored. For a thorough contemporary introduction to physical and dynamical oceanography in Liverpool Bay the reader is referred to Polton et al. (2011).

Flushing time and residence time can only be defined for bounded domains, and whilst the coastline provides clear eastern and southern boundaries of Liverpool Bay, there are no universally accepted offshore boundaries. For the purpose of this investigation, Liverpool Bay shall henceforth refer to the coastal region bounded to the north by the latitude of the Ribble estuary, and bounded to the west by the longitude of the Conway estuary (shown in figure 2.2). It should be noted that this choice of boundaries will affect the timescales evaluated in this study, and that larger domains are associated with longer timescales.

2.3 Methodology

2.3.1 Model Description

This investigation used the Proudman Oceanographic Laboratory Coastal Ocean Modelling System (POLCOMS) Irish Sea model, a high resolution ($\sim$ 1.8 km), three dimensional hydrodynamic model of a shelf region containing the whole Irish Sea (7° to 2.6° W, 51° to 56° N). POLCOMS is formulated upon a staggered Arakawa B-grid (Arakawa and Lamb, 1977), and vertical discretisation is achieved using terrain following $\sigma-$coordinates, with the

water column divided into 32 cells of equal depth. The model utilises the piecewise parabolic method (PPM) advection scheme (Colella and Woodward, 1984), which allows for artificial steepening of gradients during the advection process, making it highly non-diffusive in comparison to linear advection schemes (James, 1996). Due to both the grid choice and advection scheme, POLCOMS is particularly suitable for modelling the tidal mixing fronts and river plumes found within the Irish Sea.

POLCOMS is coupled to the General Ocean Turbulence Model (GOTM), and the $k-\epsilon$ turbulence closure scheme of Canuto et al. (2001) was adopted throughout the present study to calculate eddy viscosity and diffusivity. This is widely regarded as a physically sound and computationally efficient turbulence closure scheme (Burchard and Bolding, 2001).

River forcing is simulated by increasing sea surface elevation and reducing salinity according to the volume flux at the river input grid cell. Temperature is also modified throughout the water column to account for the temperature difference between river and shelf sea. Volume fluxes are taken from the Environment Agency river gauge data, archived at the Centre for Ecology and Hydrology (CEH), which are then scaled to include unmeasured rivers and tributaries and other accumulation of freshwater downstream of the river gauges (CEH, 2003).[1] Whilst this approach to river forcing neglects the transfer of momentum from estuary to shelf sea, the receiving basin is subject to strong tidal currents and volumetric flow rates are very small compared to that of Liverpool Bay. The impact of neglecting estuarine momentum transfer is therefore expected to be minimal at this resolution.

This method is partially validated by the good qualitative agreement with the field data, however in a detailed comparison between simulations and observations Polton et al. (2011) found that the model does overestimate the strength of both the horizontal salinity gradient and the vertical stratification. This is believed to be due to river flow uncertainty and weaknesses in the turbulence closure scheme in replicating a coastal environment. Whilst

[1] As there was no available data for the Conway this was taken into account by linearly scaling the Clwyd flow rates in the same manner as other unmeasured tributaries.

it is difficult to determine precisely how these weaknesses in the model might affect the timescales assessed in this study, they do lead to an overestimation of the strength of the density driven mean flow (Polton et al., 2013), and one might expect this to ultimately result in an underestimation of the age and residence time in the region. Further comparisons between the model and observations in Liverpool Bay are given by Polton et al. (2011); O'Neill et al. (2012), and in the southern North Sea by Holt et al. (2005). For a more thorough technical description of the model the reader is directed to Holt and James (2001).

2.3.2 Flushing Time

Flushing time is defined as the ratio of the mass of a scalar in a bounded system to the rate of renewal of the scalar (Monsen et al., 2002). In a ROFI the scalar is frequently taken to be the freshwater content of the system. Assuming an input salinity of s_i and a background salinity s_b, the volume of freshwater V_f within a volume V with salinity s may be calculated according to

$$V_f = V\left(\frac{s - s_b}{s_i - s_b}\right). \tag{2.1}$$

The flushing time T_F is then taken as the volume of freshwater divided by the average volumetric freshwater input rate Q,

$$T_F = \frac{V_f}{Q}. \tag{2.2}$$

Whilst it is possible to estimate the flushing time from salinity observations, the CTD grid in Liverpool Bay does not extend to the coast (see figure 2.3a) so some inference would be necessary to approximate coastal salinity values. Other available observational data do not provide sufficient spatial or temporal coverage, therefore a modelling approach is therefore adopted. In this study the freshwater volume is estimated from the salinity distribution as predicted by the POLCOMS model. Climatological mean river flow data are used in the model run as flushing time is highly sensitive to river flow rates, which fluctuate rapidly in Liverpool Bay (see figure 2.4). The total

volume of freshwater is then calculated according to equation 2.1 once every 300 s.

2.3.3 Residence Time

The residence time of a particle is defined by Zimmerman (1976) as the length of time taken for the particle to be removed from the bounded system. In a hyper-tidal environment, a water parcel will be thoroughly mixed by turbulent diffusion and different concentrations will leave the region at different times, so it is not possible to assign a single residence time to a volume of water. The following Eulerian definition of residence time given by Takeoka (1984) is adopted.

Suppose a water parcel located at $\mathbf{x}$ is injected with a passive tracer at time t_0, and let $m(\mathbf{x}, t)$ be the mass of this tracer remaining within the bounded system at time t. The remnant function $r(\mathbf{x}, t)$ is defined as the ratio of the remaining tracer mass to the initial tracer mass,

$$r(\mathbf{x}, t) = \frac{m(\mathbf{x}, t)}{m(\mathbf{x}, t_0)}. \tag{2.3}$$

The mean residence time at location $\mathbf{x}$ and time t_0 is given by the integral of the remnant function over time,

$$T_R(\mathbf{x}, t_0) = \int_{t_0}^{\infty} r(\mathbf{x}, t)\, \mathrm{d}t. \tag{2.4}$$

This definition can be interpreted as the mass weighted mean residence time of a water parcel.

Calculating the residence time with a fine spatial resolution requires either numerous model runs or the transport of multiple tracer fields. This would come at a considerable computational cost. Whilst this problem may be overcome by utilising the adjoint method of Delhez et al. (2004), this procedure involves running the model backwards and is not adopted here. Instead, spatial variability has been sacrificed in favour of computational efficiency, and a single tracer is injected throughout the domain at an initial

time step. The spatially averaged remnant function $\langle r \rangle$ is evaluated at every time step by taking a global sum of the tracer remaining within Liverpool Bay. As such a single mean residence time $\langle T_R \rangle$ is obtained for the whole bounded region. A similar approach has been taken previously in both experimental (Jefferies et al., 1982) and computational (Dabrowski et al., 2010) investigations.

Some previous studies in the Irish Sea (e.g. Jefferies et al., 1982) have assumed tracer loss to be proportional to the remaining tracer mass, therefore allowing the remnant function to be approximated by an exponential curve,

$$\langle r\left(\mathbf{x},t\right)\rangle \approx r_1(t) = e^{-At}, \tag{2.5}$$

where t is time after the initial tracer input in days and A is a constant to be determined for each individual case. Similarly Dabrowski and Hartnett (2008) found that the exponential model of Murakami (1991), equivalent to

$$\langle r\left(\mathbf{x},t\right)\rangle \approx r_2(t) = e^{-(Bt)^C}, \tag{2.6}$$

where B and C are constants to be determined, can be used to represent the remnant function rather accurately in the Irish Sea. In the current investigation, both models are fitted to the remnant function in order to compare their ability to accurately predict the loss of water masses in Liverpool Bay. Both curves are optimised to fit the remnant function using an iterative approach to minimise the mean squared error, thus maximising the coefficient of determination R^2. As highlighted by Kvalseth (1985), there are several forms of R^2 that are used in published scientific literature, not all of which are appropriate for nonlinear models. The following definition of R^2 is used in this study

$$R^2 = 1 - \frac{\sum\left(y_i - \hat{y}_i\right)^2}{\sum\left(y_i - \overline{y}\right)^2}, \tag{2.7}$$

where y_i are the values derived from POLCOMS model output, $\overline{y}$ is the mean value of y_i, and $\hat{y}_i$ are the predicted values given by the simplified models in equations 2.5 and 2.6.

2.3.4 Age

The age of a particle is defined as the length of time that has elapsed since it entered the domain. Once again this Lagrangian definition is inappropriate when describing the age of larger water parcels in a turbulent environment and an Eulerian description of age is adopted, given by Deleersnijder et al. (2001).

The age concentration spectrum $c(\mathbf{x}, t, \tau)$ is defined as the concentration of the water at location $\mathbf{x}$ and time t that has an age of τ. The mass weighted mean age $a(\mathbf{x}, t)$ is defined as the first moment of the age concentration spectrum with respect to age

$$a(\mathbf{x}, t) = \frac{\alpha\left(\mathbf{x}, t\right)}{C\left(\mathbf{x}, t\right)}, \tag{2.8}$$

where

$$C\left(\mathbf{x}, t\right) = \int_0^\infty c(\mathbf{x}, t, \tau)\, \mathrm{d}\tau, \tag{2.9}$$

$$\alpha\left(\mathbf{x}, t\right) = \int_0^\infty \tau c(\mathbf{x}, t, \tau)\, \mathrm{d}\tau. \tag{2.10}$$

Assuming that freshwater concentration sources P have a prescribed age of zero and that there are no freshwater sinks, the evolution of α and C is governed by the following transport equations,

$$\frac{\partial C}{\partial t} = P - \nabla \cdot (\mathbf{u}C) + \nabla \cdot (\mathbf{K} \cdot \nabla C), \tag{2.11}$$

$$\frac{\partial \alpha}{\partial t} = C - \nabla \cdot (\mathbf{u}\alpha) + \nabla \cdot (\mathbf{K} \cdot \nabla \alpha), \tag{2.12}$$

where $\mathbf{u}$ is the velocity vector and $\mathbf{K}$ is the diffusivity tensor. Full derivation of these equations[2] and further details may be found in Deleersnijder et al. (2001) .

[2]Note that equations 2.11 and 2.12 differ slightly from the corresponding equations (2.17) and (2.30) of Deleersnijder et al. (2001) because tracer destruction is neglected ($D_i = 0$ and $\delta_i = 0$), all tracer input is assumed to have an age of zero ($\pi_i = 0$), and different constituents are not considered separately (so the subscript i is dropped).

In this study the age distribution is estimated in Liverpool Bay using the POLCOMS model with real daily river gauge data (i.e. not climatological mean data). The tracer source term P is proportional to the temporally variable volumetric freshwater flux at each of the numerous rivers. Each river is weighted equally, and the age may be interpreted as the mean length of time that has elapsed since the freshwater content at a given location entered Liverpool Bay through one of the estuaries.

Equations 2.11 and 2.12 are solved using the standard time-splitting PPM advection and vertical diffusion subroutines written in POLCOMS. Horizontal diffusion is neglected in the model. An explicit tracer source term was used for P in equation 2.11 and an implicit ageing term C in equation 2.12 following the guidance of Mercier and Delhez (2010). Although it has been noted that non-linear advection schemes such as PPM may lead to some non-physical behaviour (such as an age in excess of the model run time) due to differently shaped sub-grid-cell profiles of C and α (Mercier and Delhez, 2010), this was only observed where C was extremely small (attributed to numerical diffusion). In such regions the age was artificially limited to prevent it exceeding the tracer input duration.

2.4 Results

2.4.1 Flushing Time

River gauge data revealed that the average volumetric flow rates for the Mersey, Ribble, Clwyd and Dee (along with associated tributaries) were 70, 50, 43 and 40 $m^3\ s^{-1}$ respectively between the years 1950 and 2005. Collectively these rivers contributed an average freshwater budget of 203 $m^3\ s^{-1}$ to Liverpool Bay, with an annual total of 6.4 km^3. Climatological data shows that river flow is typically around 3 times greater during winter than during summer (figure 2.4a). However in any given year the river flow rates fluctuate dramatically (figure 2.4b). River flow rates in the distinct rivers are clearly closely correlated, particularly between rivers with directly adjacent catchment areas (e.g. Clwyd and Dee) (see table 2.1). The cumulative volumetric

river flow can reach 1000 m^3 s^{-1} or greater during significant rain events.

Unsurprisingly the freshwater volume was found to oscillate dramatically during the POLCOMS simulation according to tidal state and freshwater input rates. This is due to large volumes of freshwater advancing beyond the bounded system during the ebb tide, and the strong influence of river flow rates upon the salinity distribution in Liverpool Bay. During a single year model run the volume of freshwater within the bounded system varied between 1.5 and 3.8 km^3, based upon an assumed input salinity of 0 and a background salinity of 34, typical of the central Irish Sea. This gives rise to a flushing time ranging from 88 to 215 days. The annual mean freshwater volume in Liverpool Bay was found to be 2.4 km^3, giving an average flushing time of 136 days.

2.4.2 Residence Time

The POLCOMS model was run with real river gauge data for a full decade in order to ensure that the region had been entirely replenished, beginning with an initial tracer injection on the first high tide of 1^{st} January 1991. Any tracer quantities remaining beyond the decade were deemed negligible. It took 37 days, 330 days and 1140 days for the remnant function to permanently fall below values of 0.5, 0.1 and 0.01 respectively (figure 2.5). The remnant function fluctuated with semi-diurnal tidal frequency as tracer masses oscillated over the offshore domain boundaries. There were occasional periods when the remnant function increased noticeably, suggesting a certain degree of recirculation in the region. The mean residence time in Liverpool Bay was found to be 103 days.

The closest representation of the remnant function by equation 2.5 was found with $A = 0.0151$ $days^{-1}$, giving a root mean squared error of 0.0457 and a coefficient of determination of $R^2 = 0.819$. The closest fit of equation 2.6 to the remnant function was found with values $B = 0.0196$ $days^{-1}$ and $C = 0.509$, giving a root mean squared error of 0.0132 and a coefficient of determination of $R^2 = 0.993$. With these values equations 2.5 and 2.6 give residence time estimates of 66.2 and 101.9 days respectively. It is clear

River	Mersey	Ribble	Clwyd	Dee
Mersey	1	0.806	0.780	0.779
Ribble	0.806	1	0.624	0.668
Clwyd	0.780	0.624	1	0.904
Dee	0.779	0.668	0.904	1

Table 2.1: Matrix of correlation coefficients for the volumetric river flow in the rivers Mersey, Ribble, Clwyd and Dee. Daily mean river flow data were collected between the years 1950 and 2005 inclusive.

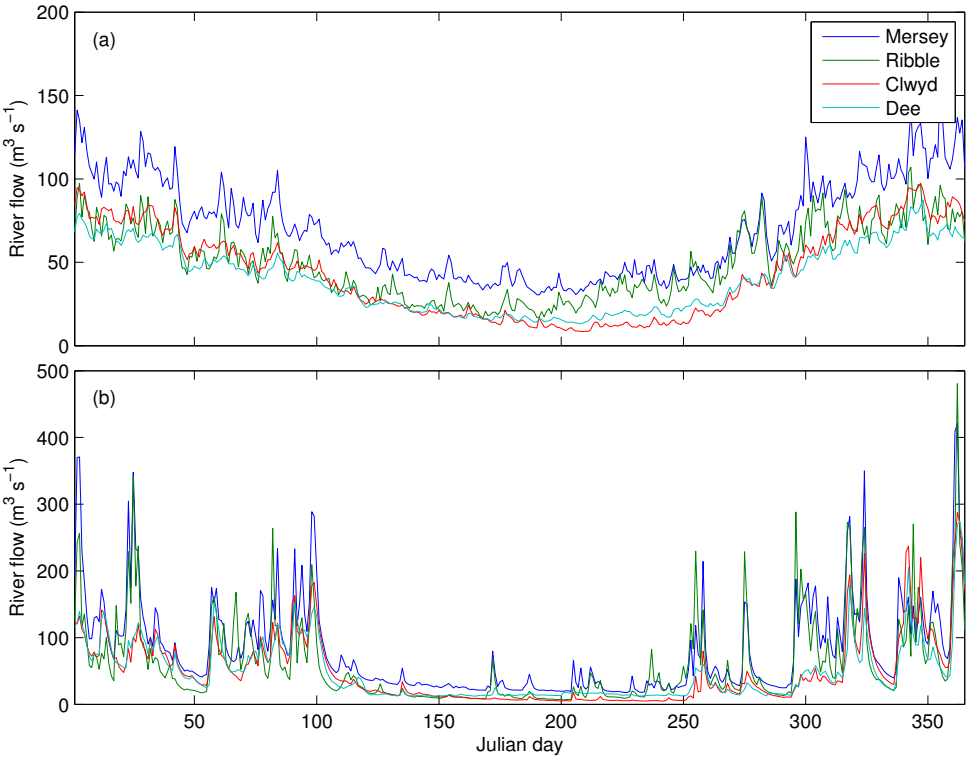

Figure 2.4: Volumetric river flow rates into Liverpool Bay. (a) Climatological mean river flow data showing the daily average rate between 1950 and 2005. (b) River flow data in example year 1994.

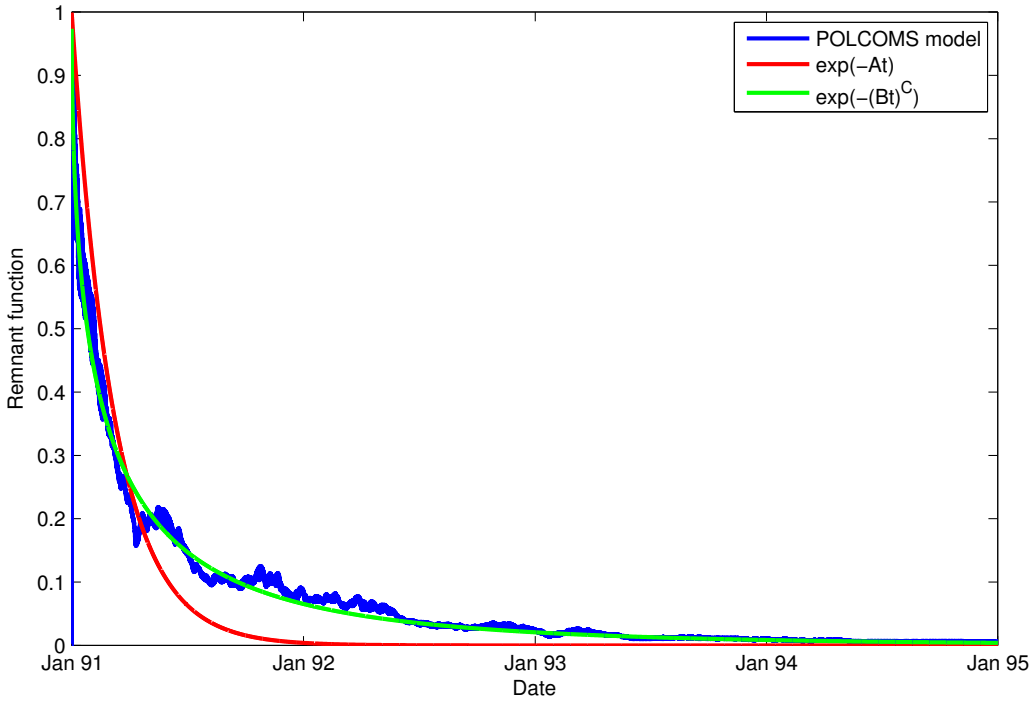

Figure 2.5: Spatially averaged remnant function in Liverpool Bay and fitted curves, with $A = 0.0151$ days^{-1}, $B = 0.0196$ days^{-1}, $C = 0.509$.

that the former equation does not capture the temporal variability of the remnant function in this scenario, it significantly underestimates the mean residence time and it is simply not a suitable model for the remnant function within this region. The latter equation meanwhile fits the POLCOMS output remarkably well. Both curves are displayed in figure 2.5.

2.4.3 Age

Once again the POLCOMS model was initiated on the 1st January 1991 and run for a full decade in order to ensure that Liverpool Bay waters have been entirely renewed and that the age distribution may be regarded as fully developed within the region of interest.

The model output showed a tendency for the mean age in Liverpool Bay

to increase over the initial period of the simulation. This may be due to a combination of recirculation and tidal mixing, facilitating the local retention of freshwater in small concentrations over multiple years and drawing much older seawater into the region. This older seawater will continue to contribute to the mass weighted mean age (and increase it) until the region is entirely flushed. This view is supported by the fact that the remnant function took several years to decay to zero (figure 2.5), indicating that complete basin replenishment takes a considerable length of time and an increase in age over this spin-up period should be expected. It is also possible that undesirable numerical diffusion also contributes to this continuous increase in mean age.

The fully developed year 2000 annual mean surface age distribution is shown in figure 2.6. Despite the regularity of strain induced periodic stratification in Liverpool Bay, the water column resorted to a vertically mixed state on most flood tides. As a result there was little difference between surface and bottom age distributions, and figure 2.6 is representative of the mean age throughout the entire water column. The basin-wide average offshore age gradient was found to be approximately 6 days km^{-1}.

It should be noted that the age exceeds 50 days even in the vicinity of the estuaries in the year 2000 average distribution, as Liverpool Bay draws much older water of Atlantic origin into the region. A similar effect was reported in Deleersnijder et al. (2001).

Over short timescales ($\sim$ 1 day) variability in age is dominated by an oscillation at the semi-diurnal frequency, with younger coastal waters advancing further offshore on the ebb tide, only to return every flood. The average daily oscillation in spatially averaged age according to the POLCOMS model output was 40 days. During spring tides the tidal excursion at the surface can exceed 10 km in Liverpool Bay. Based upon the average horizontal age gradient of approximately 6 days km^{-1} one would anticipate daily fluctuations as large as 60 days during springs at any given location in Liverpool Bay.

Freshwater forcing would appear to be the dominant control upon long term variability in mean age, as dramatic sudden drops in the average age

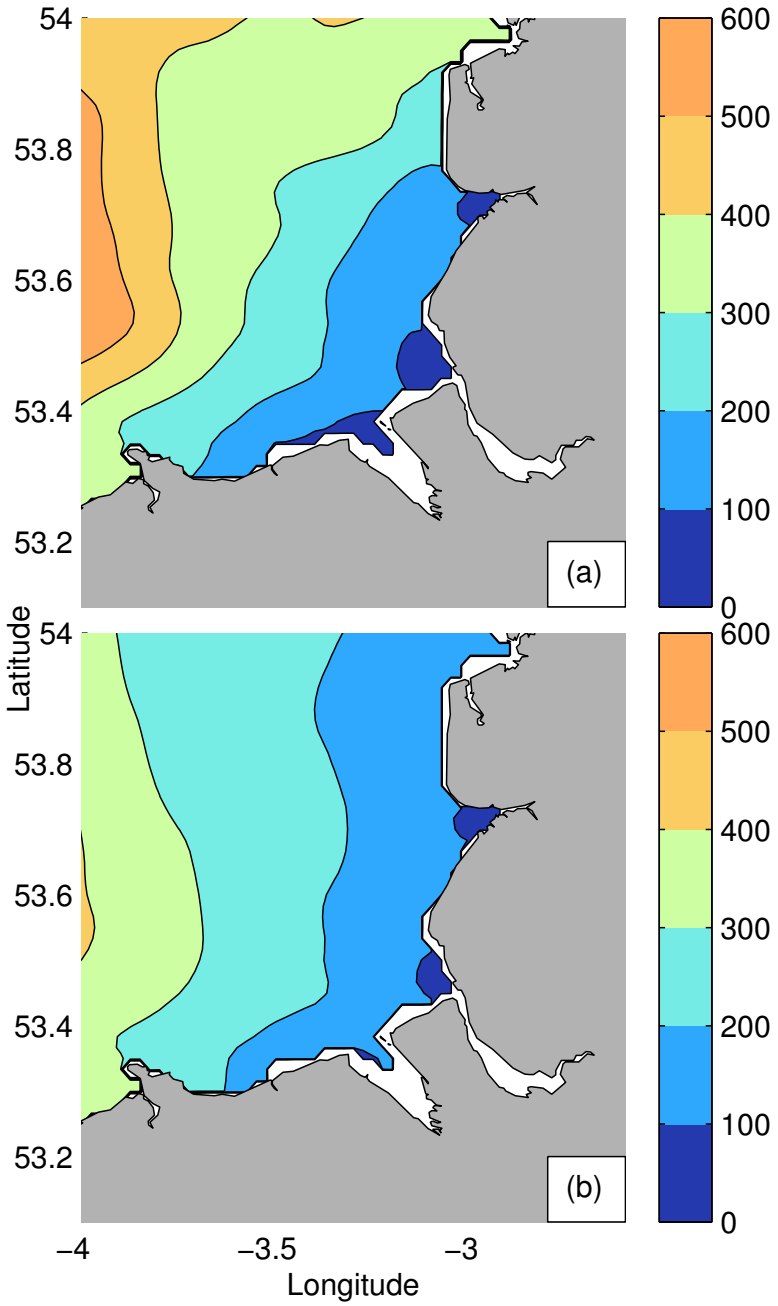

Figure 2.6: (a) Annual mean surface age distribution in the year 2000, given in days. (b) Age calculated from the annual mean surface salinity distribution in the year 2000 using equation 2.22, given in days.

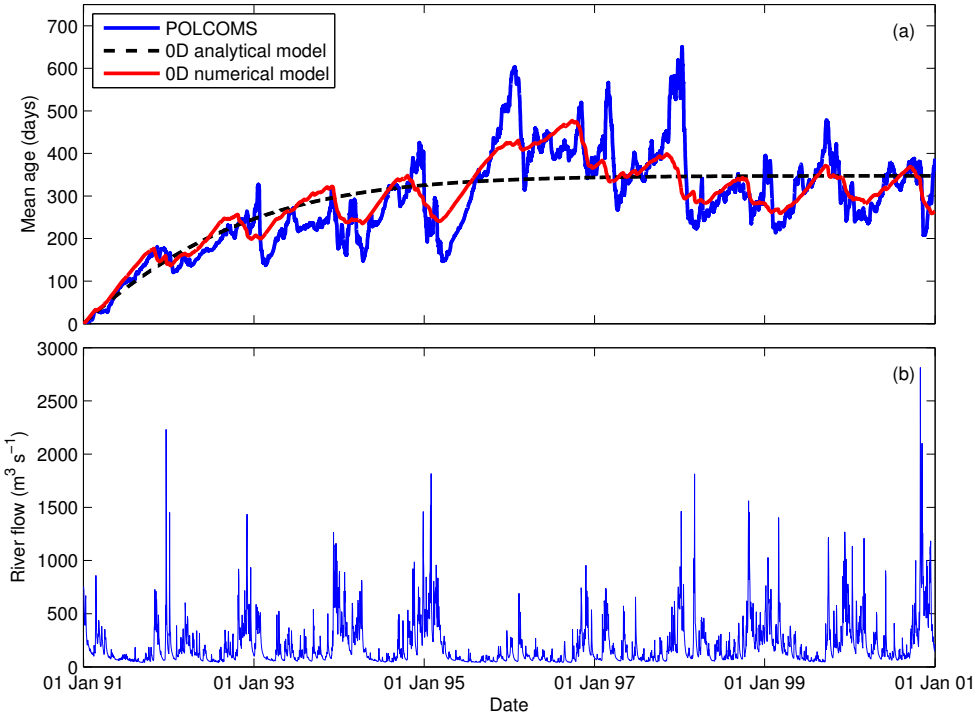

Figure 2.7: (a) Time series of spatially averaged age in Liverpool Bay (given in days), along with the analytical fitted model described by equation 2.18 and the numerical fitted model described by equations 2.13 and 2.15, with $k = 3.33 \times 10^{-8}$ s^{-1}. (b) Total volumetric freshwater input rates into Liverpool Bay from the Mersey, Ribble, Clwyd, Dee and various associated tributaries.

appear to coincide with peak river flows (figure 2.7). This is somewhat intuitive as the introduction of large volumes of young water will act to reduce the mean age. An attempt is now made to explain the way river flow variability can be expected to influence the mean age in a tidally mixed regime using a simplified model.

Consider the scenario where freshwater enters a tidally-stirred domain with age zero at a rate of $Q(t)$ m^3 s^{-1} and is instantly mixed. Suppose also that the mixed freshwater leaves the region at the offshore boundary at a rate proportional to the freshwater content of the bay, then equations 2.11

and 2.12 reduce to,

$$\frac{\mathrm{d}C}{\mathrm{d}t} = Q - kC, \tag{2.13}$$

$$\frac{\mathrm{d}\alpha}{\mathrm{d}t} = C\,(1 - ka) = C - k\alpha, \tag{2.14}$$

where k is a constant to be determined, representing the advection and diffusion terms, and has units s^{-1}. Note that as Q is now taken as a volumetric flux rather than a concentration flux, C now represents a freshwater volume with units m^3 (rather than a tracer concentration) and α now has units m^3 s. Solving for age a,

$$\frac{\mathrm{d}a}{\mathrm{d}t} = 1 - \frac{Qa}{C}. \tag{2.15}$$

Equations 2.13 and 2.15 form a system of ordinary differential equations that may be solved numerically. As river gauge data is already available all that remains is to determine an appropriate value for k.

In order to determine an appropriate value for k, freshwater flow is temporarily treated as a constant by equating the source term to the mean river flow rate $Q(t) = \overline{Q}$, allowing equations 2.13, 2.14 and 2.15 to be solved analytically for $t > 0$,

$$C(t) = \frac{\overline{Q}}{k}\left(1 - e^{-kt}\right), \tag{2.16}$$

$$\alpha(t) = \frac{\overline{Q}}{k^2}\left(1 - e^{-kt} - kte^{-kt}\right), \tag{2.17}$$

$$a(t) = \frac{e^{kt} - kt - 1}{k\,(e^{kt} - 1)}. \tag{2.18}$$

As time develops the freshwater content C will tend towards a maximum capacity of $\overline{Q}/k$, whilst the mean age a will tend towards an upper bound of $1/k$. Supposing the maximum capacity of freshwater in the region is known to be $C_{\max}$, one may take $k = \overline{Q}/C_{\max}$. It was previously shown that the freshwater content in Liverpool Bay is not constant, however by taking the freshwater content of $C_{\max} = 2.4$ km^3, k simply reduces to the inverse of the flushing time,

$$k = \frac{1}{T_F} = 8.51 \times 10^{-8}\mathrm{s}^{-1}. \tag{2.19}$$

Age was determined from equations 2.13 and 2.15 using Runge-Kutta fourth order integration (see appendix for full equations and further details). Obtaining k from the inverse of this flushing time (equation 2.19) and substituting this value into the simplified numerical model results in a dramatic underestimation in the mean age in Liverpool Bay by an average of 151 days, with a root mean squared error of 180 days. A range of different values for k were therefore used, and an optimum fit was found with a value of $k = 3.33 \times 10^{-8}\ s^{-1}$, which approximated the POLCOMS output with a root mean squared error of 56 days and a coefficient of determination of $R^2 = 0.77$ (depicted in figure 2.7a). This value of k corresponds to a maximum freshwater capacity of $C_{\max} = 6.1$ km^3 and a flushing time of 348 days. This is significantly greater than the freshwater content of Liverpool Bay and the flushing time of 136 days predicted earlier. This discrepancy reveals the limitation of such idealised models in complex regions such as Liverpool Bay where freshwater is not mixed uniformly.

It should be highlighted that the intention here was not to predict a spatially averaged age value based upon freshwater budgets, but simply to demonstrate that the strong fluctuations in mean age predicted by the POLCOMS model can largely be explained by volatile river flow rates. In reality Liverpool Bay cannot be regarded as entirely mixed, and the age of water lost at the offshore boundary will certainly exceed the average age due to the offshore age gradient. This is not accounted for in the idealised models, which may be more suitable for ROFIs with weaker horizontal age gradients.

It is also worth highlighting that if age is to develop according to equation 2.18 it will continue to increase over time indefinitely, converging towards an upper bound. It is therefore difficult to determine when the age distribution may be regarded as "fully developed". Ideally one would choose some appropriate value, say $\theta = 0.99$, and regard age as "close enough to the limit" from a time t_0 when $a(t_0) \geq \theta \lim_{t\to\infty} a(t)$. The annual mean age distribution is depicted in figure 2.6 for the year 2000, after 9 continuous years of tracer input. Based upon the optimum value found for k this criterion is met for $\theta = 0.9993$.

Although the age distribution was found to be volatile due to semi-diurnal tidal advection and river flow variability, it is clearly strongly correlated with the salinity distribution. It is therefore perhaps more appropriate to describe age as a function of salinity, rather than provide a mean age distribution in a highly variable environment. Although the concept of fresher water indicating younger age is intuitive, there is no obvious relationship between the two properties. Once again we temporarily neglect the complex physical processes that determine both salinity and age, and turn to a simplistic model to explain this relationship.

Suppose a small water parcel with initial salinity s_0 enters a larger domain at time $t = 0$ with an assigned age of a_0. Results suggest that the salinity of the water parcel $s(t)$ will gradually increase towards that of the background ambient water s_b, at a rate that slows as it approaches the background value. Age meanwhile will increase at a constant rate over time $a(t) = t + a_0$. Here the key assumption is now made that the rate of increase in salinity is proportional to the salinity difference,

$$\frac{\mathrm{d}s}{\mathrm{d}t} = l(s_b - s), \tag{2.20}$$

for some positive constant l. Solving this equation for age as a function of salinity,

$$a(s) = a_0 + \frac{1}{l} \ln \left(\frac{s_b - s_0}{s_b - s} \right). \tag{2.21}$$

Note that in an ideal scenario one would use $a_0 = 0$, however as mentioned previously, the minimum modelled age was found to exceed 0 due to tracer retention and the model resolution. According to POLCOMS hourly output from the year 2000, salinity in Liverpool Bay ranged from approximately 20 to 34, whilst the minimum mass-weighted mean age was 17 days. Taking $s_0 = 20$, $s_b = 34$, $a_0 = 17$ and optimising for l one finds $l = 0.0091$, giving

$$a(s) = 307 - 110 \ln (34 - s) \,\text{days}, \tag{2.22}$$

which fits the model output with a coefficient of determination of $R^2 = 0.925$ based upon a total of 6.3×10^6 data points. This curve captures the trend

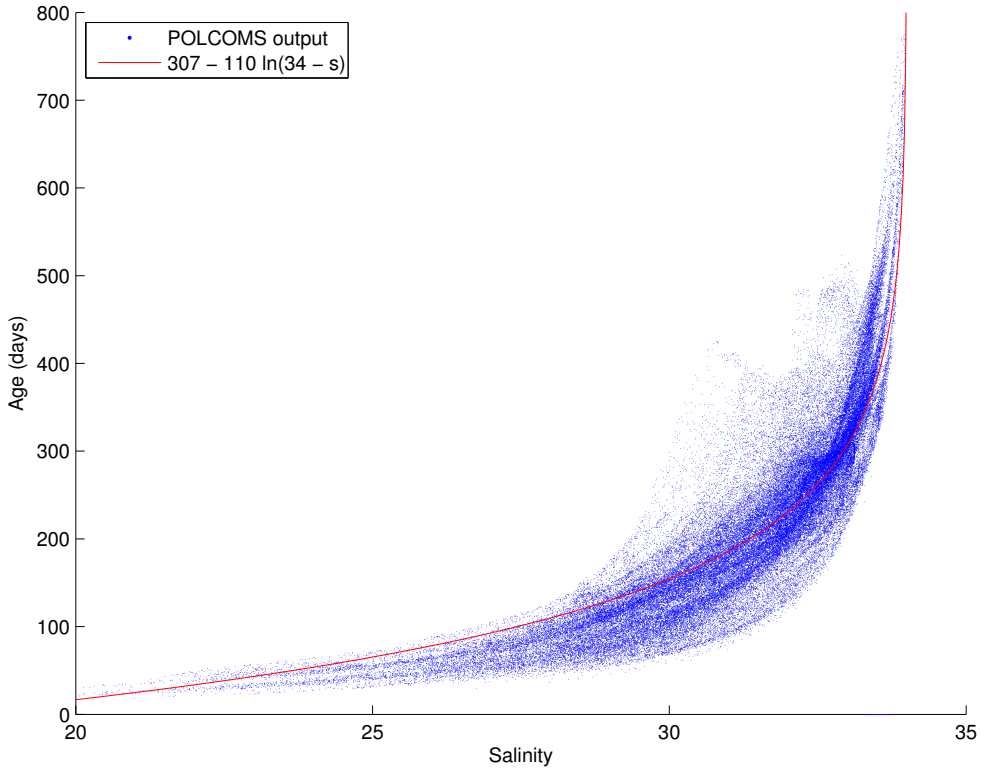

Figure 2.8: A random sample of 10^5 bivariate data points depicting the relationship between salinity and age in Liverpool Bay. Data points were taken from Liverpool Bay during the year 2000 (after 9 years of continuous tracer input).

between salinity and age rather well, however it does not explain the spread (figure 2.8).

2.5 Discussion

Considerable effort has been made in recent years to ensure that standard definitions are applied whenever researching hydrodynamic transport timescales (e.g. Monsen et al., 2002). These values are now fully verifiable and are no longer open to interpretation. Since recent breakthroughs in age and residence time theory (Delhez et al., 1999; Deleersnijder et al., 2001; Delhez

et al., 2004; Mercier and Delhez, 2010) these temporal properties have found application in diverse research areas including freshwater transport (Zhang et al., 2010), anthropogenic carbon monitoring (Waugh et al., 2004) and long term trends in retentive seasonal gyres (Olbert et al., 2011). Here these ideas have been applied to a vigorously mixed, hyper-tidal ROFI with multiple freshwater sources.

Perhaps the first investigation of hydrodynamic timescales in the Irish Sea comes from Bowden (1955) who analysed salinity anomalies to deduce a weak northwards basin-wide flow and predicted transit times between different stations. Since then the distribution of radioactive isotopes have been analysed by Jefferies et al. (1982) to deduce a residence time of 530 days for the northern Irish Sea. More recently Dabrowski et al. (2010) conducted a modelling investigation and found considerable seasonable variability in the residence time of the Irish Sea, which was found to range from 386 days in the summer to 444 days in the winter. Some studies have considered the residence time of the eastern Irish Sea separately and found values ranging from 208 days (Dabrowski and Hartnett, 2008) to 290 days (Jefferies et al., 1982).

By utilising the POLCOMS Irish Sea model it has been possible to estimate a mean residence time of 103 days for Liverpool Bay. Although Liverpool Bay is a distinct sub-region of the eastern Irish Sea and direct comparisons to studies of larger domains cannot be made, the results presented in the current study do appear reasonable and consistent with previous work. The total volume of Liverpool Bay is approximately 55 km^3, whereas the eastern Irish Sea has a volume of roughly 440 km^3. The volume of the eastern Irish Sea is therefore a factor of 8 greater than that of Liverpool Bay, however the residence time would appear to be a factor of only 2 to 3 times longer. Liverpool Bay would therefore appear to be considerably more retentive than other regions of the Irish Sea. This claim is supported by the numerical study of Dabrowski and Hartnett (2008) that found a backwater to form in Liverpool Bay in the case of a hypothetical spill at the Sellafield nuclear reprocessing plant.

It has been necessary to neglect the spatial variability of residence time here in favour of computational efficiency. Intuitively one would anticipate the residence time to decrease in the proximity of the offshore boundaries, reaching a maximum value at the coastal areas. As the coastal zone coincides with the primary local sources of deleterious anthropogenic inputs, the mean residence time presented here may actually underestimate the typical exposure of Liverpool Bay to anthropogenic disturbances. Assessing this spatial variability in the distribution of residence time remains an important challenge for future research.

The flushing time within Liverpool Bay was found to be 136 days based upon climatological river flow data and a background salinity of 34, typical of the central Irish Sea. Whilst residence time and flushing time both serve to assign a timescale to the retention of a water body, it is important to highlight the difference between what each calculation actually approximates. The mean residence time is an estimation of the average length of time that a water parcel will remain within the vicinity before advancing further offshore, whilst flushing time is an approximation of the length of time taken to entirely replenish a freshwater volume equal to that contained within the bay. The fact that the flushing time exceeds the residence time therefore agrees with intuition.

The mean age within Liverpool Bay was found to increase over the first few years of the model simulation due to retention of small concentrations of freshwater over multiple years. This is consistent with the length of time taken for the remnant function to fully diminish. Recent investigations into Liverpool Bay have found the salinity structure to be highly mobile and this study shows that the age distribution also fluctuates according to tidal advection and freshwater forcing. A mean age distribution has been provided, however due to the temporal variability it may be more appropriate to estimate age from salinity. This equation is restricted to salinities between 25 and 34, however this comfortably covers the values that are typically observed in Liverpool Bay. It should be noted that despite a strong coefficient of determination, error margins are potentially quite large when estimating

age from salinity due to the considerable scatter (figure 2.8). Similarly large scatters have been reported in other freshwater plumes (e.g. Zhang et al., 2010).

Concentrations of nitrogen and phosphorous typically build up each year from September until the following spring, and are then depleted by phytoplankton (Greenwood et al., 2011). Therefore any freshwater older than a year is likely to be of limited importance to anyone concerned with nutrient enrichment, and the age distribution provided here will typically overestimate the transit time of nutrients from the rivers to offshore locations. It may be possible however to calculate the age of nutrients using a biophysical model with appropriate sink terms in equations 2.11 and 2.12. As linear relationships are widely observed between nutrient concentrations and salinity (Greenwood et al., 2011), and this study provides a method to estimate age from salinity, the ideas presented here could potentially be used alongside such a biophysical model to allow the age of nutrients to be predicted from salinity alone. This presents an exciting area for future research that would be tremendously beneficial for marine management.

This study has highlighted some of the problems that are encountered when attempting to evaluate age and residence time in a tidally mixed hydrographical regime. Our understanding of freshwater transport time and retention has been enhanced through this research, however the spatial variability of residence time in Liverpool Bay remains to be identified. Age is particularly difficult to interpret, as the age increases significantly over the first few years of tracer input due to local retention and mixing. From the results presented here it is clear that no single timescale can simultaneously characterise every temporal property of transport and replenishment in a hyper-tidal region of freshwater influence.

2.6 Appendix: Numerical Methods

A zero-dimensional model of average freshwater age in a tidally mixed regime is given by the system of ordinary differential equations 2.13 and 2.15. In

an attempt to demonstrate that much of the variability in age predicted by the POLCOMS model run can be explained by fluctuations in river flow, these equations were integrated numerically with Runge-Kutta fourth order integration. The freshwater content C^{n+1} and age a^{n+1} on day $n+1$ were calculated using daily mean river flow rates Q^n $\mathrm{m^3 s^{-1}}$ and a freshwater loss rate k as the only input data. Linear interpolation was used to provide intermediate values of Q. The equations determining mean age are as follows,

$$C^{n+1} = C^n + \frac{1\,\mathrm{day}}{6}\left(f_1 + 2f_2 + 2f_3 + f_4\right) \tag{2.23}$$

$$a^{n+1} = a^n + \frac{1\,\mathrm{day}}{6}\left(g_1 + 2g_2 + 2g_3 + g_4\right) \tag{2.24}$$

where

$$f_1 = Q^n - kC^n \tag{2.25}$$

$$f_2 = 0.5\left(Q^n + Q^{n+1}\right) - k\left(C^n + 0.5f_1\right) \tag{2.26}$$

$$f_3 = 0.5\left(Q^n + Q^{n+1}\right) - k\left(C^n + 0.5f_2\right) \tag{2.27}$$

$$f_4 = Q^{n+1} - k\left(C^n + f_3\right) \tag{2.28}$$

$$g_1 = 1 - a^n Q^n / C^n \tag{2.29}$$

$$g_2 = 1 - 0.5\left(a^n + 0.5g_1\right)\left(Q^n + Q^{n+1}\right) / \left(C^n + 0.5f_1\right) \tag{2.30}$$

$$g_3 = 1 - 0.5\left(a^n + 0.5g_2\right)\left(Q^n + Q^{n+1}\right) / \left(C^n + 0.5f_2\right) \tag{2.31}$$

$$g_4 = 1 - \left(a^n + g_3\right) Q^{n+1} / \left(C^n + f_3\right). \tag{2.32}$$

Initial conditions of $C^0 = a^0 = 0$ are assumed, and $a^0/C^0 = 0$ is taken to avoid division by zero in the calculation of g_1 on the first time step.

Chapter 3

The Influence of Behaviour on Larval Dispersal in Shelf Sea Gyres: *Nephrops norvegicus* in the Irish Sea

This chapter is based upon Phelps, J. J. C., Polton, J. A., Souza, A. J. and Robinson, L. A. The influence of behaviour on larval dispersal in shelf sea gyres: Nephrops norvegicus in the Irish Sea. *Marine Ecology Progress Series*, 518: 177-191, 2015.

Abstract

The western Irish Sea seasonal gyre is widely believed to play an important role in the local retention of resident larvae. This mechanism could be particularly crucial for the larvae of the heavily fished crustacean *Nephrops norvegicus* (L.), as their sediment requirements highly restrict where they are able to settle. As recent research suggests that the gyre may be becoming less retentive due to changes in atmospheric forcing, it is now crucial to understand how the gyre influences dispersal. This investigation addresses the hypothesis that shelf sea gyres reinforce larval retention using a biophysical model with vertical migration, habitat selection and temperature-dependent pelagic

larval duration (PLD) configured to match the behaviour of *N. norvegicus* larvae.

The results of this study suggest that the gyre does increase the likelihood that passive larvae remain within the western Irish Sea, on the condition that the larvae remain fixed at the depth of peak gyral flow. Retention rates are significantly lower when vertical migration is introduced, and there is no evidence that the gyre promotes larval retention amongst either vertically migrating larvae, or larvae that require muddy sediments for successful settlement. By contrast, vertical migration is shown to be favourable for retention in the eastern Irish Sea. PLD varies by a factor of two according to release date and location; such variations are shown to affect dispersal. The simulations suggest that whilst some highly limited and almost entirely unidirectional larval exchange may occur, the distinct sites largely rely upon local recruitment. The ecological implications of these findings are discussed.

3.1 Introduction

Nephrops norvegicus (L.) is a heavily fished, benthic decapod-crustacean that inhabits muddy sublittoral sediments throughout European continental shelf seas (Farmer, 1975). The meroplanktonic larval phase of *N. norvegicus* in the western Irish Sea has been of considerable interest since the discovery of a strong seasonal baroclinic gyre that encircles a region inhabited by the adult population (Hill et al., 1994). The larvae generally hatch during April and May every year (Dickey-Collas et al., 2000a), pass through three distinct zoeal larval stages (Farmer, 1975), and have a temperature-dependant pelagic larval duration (PLD) that ranges from approximately 72 days at 8 °C to 26 days at 15 °C (Dickey-Collas et al., 2000b; Smith, 1987). Adult *N. norvegicus* require muddy sediments in order to construct their burrows, and the spatial distribution of these sediments places a major constraint on where the larvae are able to settle. Any larvae that are unable to find a suitable habitat at the end of their larval phase are assumed to fall to mortality. After noting that drifting buoys were retained in the gyral system, Hill et al. (1996) proposed

that the seasonal gyre may act to retain the larvae within the waters overlying these muddy sediments, ultimately promoting self recruitment.

The western Irish Sea gyre has since been a focal point of numerous observational (Hill et al., 1997; Horsburgh et al., 2000), theoretical (Hill, 1996) and numerical (Xing and Davies, 2001; Horsburgh and Hill, 2003) investigations, and the timing, strength and drivers of the gyre are now relatively well established. A dense cold water pool forms early each spring, trapped beneath a sharp seasonal thermocline and isolated from adjacent bottom waters by abrupt bottom density fronts. This density field is stable due to strong surface heat fluxes and weak tidal energy (Simpson and Hunter, 1974). As a result of geostrophy, the bottom density gradients induce a cyclonic velocity field, with peak flows at the thermocline approximately 24 m below the surface. Cyclonic circulation is observed as early in the year as April, then the strength of the gyre develops gradually as bottom density gradients sharpen, reaching peak velocities of 0.2 m s^{-1} during August, and the gyre finally breaks down during October (Horsburgh et al., 2000). A recent modelling investigation found evidence to suggest that there is a long-term trend in the dynamics of the gyre due to changes in atmospheric conditions, resulting in a stronger, but less retentive gyre (Olbert et al., 2011). The long-term mean flow through the Irish Sea is considered to be weak (< 0.01 m s^{-1}) and northwards (Bowden, 1950; Wilson, 1974).

Although the physical environment in the western Irish Sea may be well understood, many of our assumptions about larval transport in the region are derived either from passive fixed-depth drifting buoys, or directly from the mean circulation. There is now a substantial body of evidence to demonstrate that the meroplanktonic larvae of marine invertebrates are able to control their depth within the water column (e.g. Cushing, 1951; Cronin and Forward, 1979; Forward et al., 1984; Lindley et al., 1994; Knights et al., 2006), and that this mechanism may influence their trajectory (Hill, 1991; Smith and Stoner, 1993; North et al., 2008; Sundelof and Jonsson, 2012), therefore larvae should not be regarded as entirely passive. In regions with a strong vertical velocity shear, swimming vertically just a few metres may result in

vastly different dispersion scenarios (Vikebo et al., 2005). *N. norvegicus* larvae are believed to migrate vertically according to time of day (diel vertical migration or DVM) and larval stage (ontogenetic migration) (Hillis, 1974; Lindley et al., 1994), therefore caution should be taken when drawing conclusions from passive, fixed-depth drifters. Furthermore the gyre has been described as "leaky" as not all drifting buoys are entrained within the gyre (Hill et al., 1994, 1997). Horsburgh et al. (2000) reported that loss from the gyral system is particularly likely during the early stages of the heating season, in May and early June, however this period actually corresponds to the latest stages of the *N. norvegicus* hatching window (Dickey-Collas et al., 2000a), therefore one may anticipate some loss of larvae from the system. This is supported by larval surveys that each show the occurrence of larvae outside the muddy sediment regions inhabited by adult *N. norvegicus* (Hillis, 1974; White et al., 1988).

Whilst each of these studies have contributed to our understanding of larval dispersion in this region, evidence that the gyre acts as an effective retention mechanism for planktonic larvae with complex behaviour remains inconclusive, and it is clear that there are still numerous questions regarding the migration of western Irish Sea *N. norvegicus* larvae, and more generally, the relationship between planktonic larvae and shelf sea gyres. We are able to draw some insight from larval surveys (Hillis, 1974; Nichols et al., 1987; White et al., 1988; Horsburgh et al., 2000) and other modelling studies (e.g. Emsley et al., 2005; Fox et al., 2006, 2009; van der Molen et al., 2007; Robins et al., 2013) that address larval transport in the Irish Sea, and some of these studies are discussed in greater detail later, however this is the first investigation to utilise a three dimensional hydrodynamic model coupled to an individual based model (IBM) where the vertical migration behaviour, temperature-dependant PLD and habitat are each parametrised specifically to match the behaviour of *N. norvegicus* larvae. As the influence of the western Irish Sea gyre upon *N. norvegicus* transport is one of the most frequently cited examples of a biophysical interaction between planktonic larvae and local density-driven flow, there is clearly a great need for a detailed and focused

investigation on the subject.

The principal objective here is to examine spatial and temporal variability of larval dispersal distance and retention rates in two regions in the Irish Sea inhabited by *N. norvegicus* (figure 3.1), and to determine how these factors are affected by larval behaviour. The results are then scrutinised to establish whether they support the larval retention hypothesis of Hill et al. (1996). Additionally, the extent of particle exchange between the distinct regions is assessed in order to identify whether the simulations are consistent with a collection of metapopulations connected through larval exchange, or isolated *N. norvegicus* populations where self-recruitment dominates.

This investigation also presents an opportunity to study the PLD of *N. norvegicus*. Larval culture studies (e.g. Thompson and Ayers, 1989; Dickey-Collas et al., 2000b) provide excellent ways to determine PLD from temperature, however temperature is not uniform in reality. As the larvae migrate vertically through a sharp thermocline, they may be subject to daily temperature changes of several degrees Celsius, making it very difficult to estimate PLD in the field. In this investigation larval growth rates are determined from these temperature relations, allowing us to estimate spatial and temporal variability to PLD. As sea surface temperature increases gradually over the heating season, the PLD of larvae can be expected to decrease. As a shorter PLD is generally associated with a shorter dispersion distance (Shanks et al., 2003; Cowen and Sponaugle, 2009), this could lead to greater retention rates amongst larvae that hatch later in the season, and perhaps reinforce a seasonal asymmetry caused by the strengthening gyre.

Whilst this investigation focuses upon the Irish Sea, Horsburgh et al. (2000) highlights that isolated cold water pools have been identified across the world, and notes that numerical models suggest cyclonic flow fields in some cases. Additionally, the co-occurrence of the gyre and the muddy sediment is not coincidental, both are consequences of weak local tidal energy. As many benthic species are selective about habitat, retention of *N. norvegicus* larvae in the western Irish Sea could be a particular case of a more general problem.

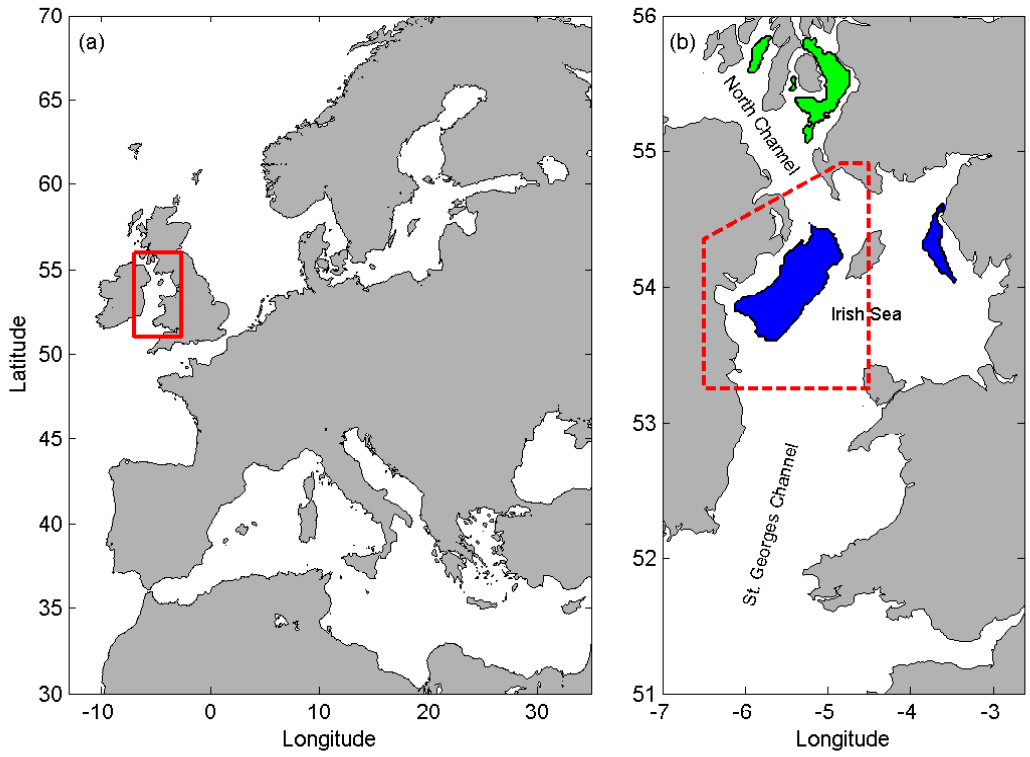

Figure 3.1: POLCOMS Irish Sea model domain with (a) shown within the European continental shelf; (b) with the Irish Sea muddy sediments (where particles are initialised) shown in blue, the additional North Channel muddy sediments shown in green, and the bounded western Irish Sea region highlighted by dashed red lines.

3.2 Methods

3.2.1 Hydrodynamic Model

The Proudman Oceanographic Laboratory Coastal Ocean Modelling System (POLCOMS) hydrodynamic model is used to provide sea surface elevation and three dimensional fields of velocity, temperature and vertical diffusivity to an IBM. POLCOMS operates upon a staggered Arakawa B-grid (Arakawa and Lamb, 1977) in the horizontal, and terrain following $\sigma-$coordinates in the vertical. The model adopts the piecewise parabolic method (PPM) (Colella

and Woodward, 1984), which allows for artificial steepening of gradients, and is highly regarded by shelf sea modellers for its relatively low numerical diffusivity (James, 1996). The combination of the PPM advection scheme and the Arakawa B-grid ensure that sharp gradients such as tidal mixing fronts are not eroded in the advection process, making the model particularly suitable for modelling the western Irish Sea gyre. Atmospheric forcing is calculated with COARE 3 bulk formulae (Fairall et al., 2003) using 1 ° and six hourly ECMWF wind and surface flux data. Tidal velocities and elevations are fully resolved, and are forced at the open boundaries.

The POLCOMS Irish Sea set-up is used for the current study, a high resolution ($\sim$ 1.8 km horizontal resolution, 32 σ-coordinate layers) model of a shelf sea region containing the whole Irish Sea, St George's Channel and the North Channel (7 ° to 2.6 ° W, 51 ° to 56 ° N, see figure 3.1). The Irish Sea set-up is well documented and has been utilised to study shelf sea processes within numerous recent modelling investigations (e.g. Polton et al., 2011; O'Neill et al., 2012; Phelps et al., 2013). Further technical details of POLCOMS are provided by Holt and James (2001).

POLCOMS is coupled to the General Ocean Turbulence Model (GOTM) (Umlauf and Burchard, 2003) which allows the user to choose from a selection of turbulence closure schemes. The $k-\epsilon$ closure scheme (Canuto et al., 2001) is used throughout this investigation.

3.2.2 Particle Tracking Model

The IBM is an offline three-dimensional Lagrangian particle tracking model with additional subroutines to parametrise vertical migration behaviour, settlement and a temperature-dependant PLD, and was developed from scratch specifically for this investigation following the guidelines provided by North et al. (2009) and Willis (2011). Sea surface elevation and velocity are updated every 300 seconds, and are interpolated linearly in time and bilinearly in space to give values at the location of each particle. Particle advection is calculated using Runge-Kutta fourth order integration (RK4) with advection time step of 60 seconds. RK4 is a stable and reliable multi-step method

for numerical integration, and is known to calculate particle displacement with much greater accuracy than simpler integration schemes such as Euler or second-order Runge-Kutta methods (RK2) (North et al., 2009; Qiu et al., 2011; Willis, 2011). This improved accuracy is particularly important in circular flows such as eddies and gyres, as Euler methods and RK2 typically lead to significant non-physical divergence away from the centre of the circular flow.

Temperature and vertical diffusivity are updated once every 600 seconds, and a cubic smoothing spline is fitted vertically to the discrete diffusivity values, ensuring that both diffusivity and its first derivative are smooth, and that the second derivative is continuous throughout the water column. Vertical diffusion is calculated using a random walk model described by Hunter et al. (1993); Visser (1997); Ross and Sharples (2004) which includes additional terms to prevent artificial particle accumulation in regions of low diffusivity. The diffusion sub-model uses a time step of 6 seconds. Further details of the diffusion model, and verification that it satisfies the well mixed condition are reserved for the appendix. Horizontal diffusion is neglected. Reflective boundary conditions are placed at the sea surface, bottom and land boundaries to prevent particles leaving the water column. Any particles that are advected beyond the model domain through the open boundaries are removed from the system.

3.2.3 Larval Behaviour Sub-model

The vertical migration component of the larval behaviour sub-model is based upon the correlated random walk model described by North et al. (2008). As there is little direct evidence of the swimming capabilities of *N. norvegicus* larvae, parameters were determined using a one-dimensional model to ensure that vertical density profiles were qualitatively similar to those recorded by Hillis (1974) and Lindley et al. (1994).

The maximum swimming speed of each particle increases from 1 mm s^{-1} during the first larval stage to 3 mm s^{-1} in the final stage. This swimming speed is then multiplied by a random number taken from the continuous uni-

form distribution $U[0,1]$, reflecting the variability of larval swimming speed. Whilst it is possible that the larvae may be able to swim at greater speeds in reality, it is the vertical profiles that will influence horizontal trajectories rather than swimming velocity itself. Finally the direction of particle movement is determined using a stochastic scheme, whereby swimming velocity is directed upwards if a second random number taken from $U[0,1]$ exceeds a weighted parameter λ, and downwards otherwise. The weighted parameter λ is a function of larval stage, time of day and depth in the water column, and is used to control the mean characteristics of particle swimming. The precise mathematical calculation of λ is reserved for the appendix.

Particles are forced to ascend towards the surface shortly after hatching, and then they migrate vertically about a mean position each day, reaching their highest point in the water column each midnight, and descending to their deepest point at midday (figure 3.2). The particles continue this DVM pattern throughout their PLD, but they are gradually permitted to descend into slightly deeper waters, until the second half of their final larval stage when they begin to swim directly towards the seabed.

The PLD of many marine species are highly dependent upon water temperature (O'Connor et al., 2007). Several larval culture studies have aimed to establish the precise relationship between *N. norvegicus* PLD and temperature, and these are summarised in Powell and Eriksson (2013). For this investigation we adopt the parameters of Dickey-Collas et al. (2000b) for larval stages 1 and 2, Smith (1987) for stage 3 following Dickey-Collas et al. (2000a) (figure 3.3). The duration θ_i (given in days) of larval stage i can be approximated by the following function of seawater temperature T ($^{\circ}C$).

$$\theta_i = \begin{cases} \exp\left(4.265 - 0.161\,T\right) & \text{if } i = 1 \\ \exp\left(4.646 - 0.175\,T\right) & \text{if } i = 2 \\ \exp\left(4.188 - 0.113\,T\right) & \text{if } i = 3 \end{cases} \tag{3.1}$$

This function assumes that temperature is constant throughout each larval stage, however in practice the spatial and temporal variability in temperature coastal regions is often too great to be ignored (see figure 3.4). The

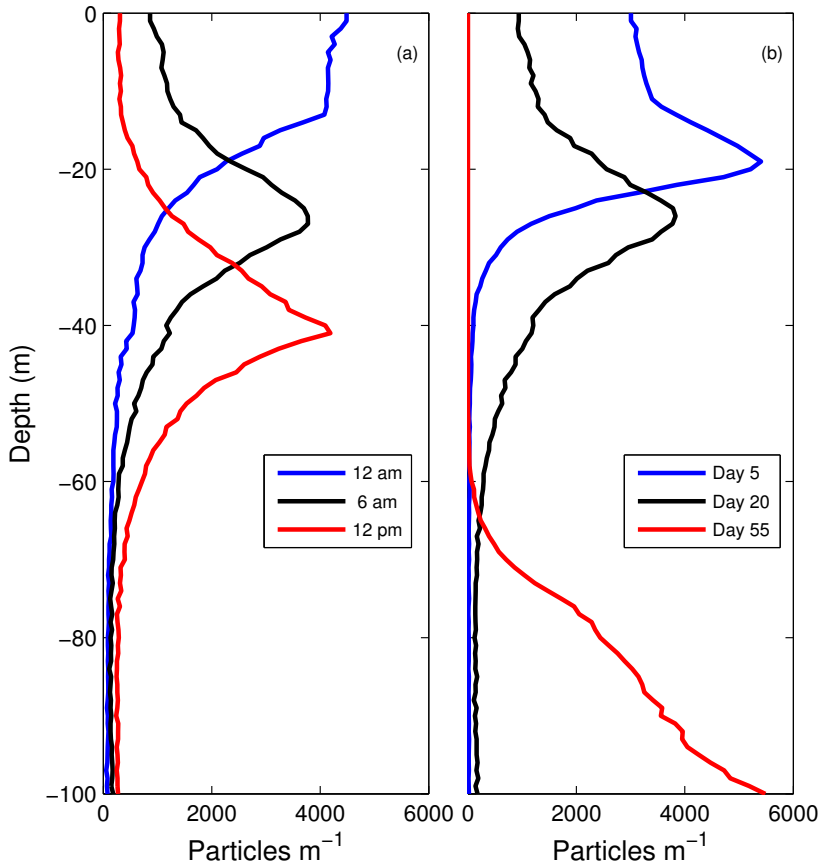

Figure 3.2: Results of a one-dimensional model simulation where 10,000 particles are released and tracked for 60 days. Depths are governed by vertical diffusion and swimming behaviour. (a) Particle density profile at three different times on day 20, showing DVM. (b) Particle density profile at three different stages of the pelagic phase, each at 6 a.m., showing ontogenetic migration. Note that particles are released in unison, whereas larval density profiles in field observations show larvae with a range of ages.

seawater temperature surrounding a moving particle will vary according to time t and particle location $\mathbf{x}$, which in turn can also be regarded as a function of time $\mathbf{x} = \mathbf{x}(t)$. As such the duration of larval stage i for a particle

can be rewritten as a function of time

$$\theta_i(t) = \exp\left(a_i + b_i T(t)\right) \tag{3.2}$$

where the coefficients a_i and b_i are as in equation 3.1. To account for this variability in temperature, each particle is allocated a normalised stage duration τ_i that increases according to

$$\frac{\mathrm{d}\tau_i}{\mathrm{d}t} = \frac{1}{\theta_i(t)}, \tag{3.3}$$

where a particle enters larval stage i at time t_i such that $\tau_i(t_i) = 0$, and enters the following larval stage $i+1$ at a time t_{i+1} such that $\tau_i(t_{i+1}) = 1$. Note that t_1 corresponds to the particle release time and if the particles pass through n distinct larval stages ($n = 3$ for *N. norvegicus*), t_{n+1} represents the settlement time. The total PLD of each particle is therefore equal to $t_{n+1} - t_1$. Also note that in the special case of uniform temperature, the stage durations of Dickey-Collas et al. (2000a) and Smith (1987) still apply. It should be highlighted that the temperature relations derive from larval culture studies where the larvae are typically held at a constant temperature, therefore it is not entirely clear how a variable temperature would affect the PLD in reality. The method used here is a practical way to incorporate these relations in a variable environment. Similar methods have been used previously to simulate the larvae of other species (e.g. Nicolle et al., 2013). Whilst this study focuses upon the temperature dependant PLD of *N. norvegicus*, this approach could easily be adapted to model larvae of another species with a PLD that varies according to salinity or other properties.

At the end of the final larval stage, particles remain pelagic for up to one additional day and settle upon muddy sediments upon impact. Particles are not able to settle prior to this period, and any particles that have not encountered suitable substrate by the end of this period are removed from the system.

Mortality of *N. norvegicus* larvae is highly complex due to predation and parasites (Farmer, 1975). Although estimates of daily larval mortality

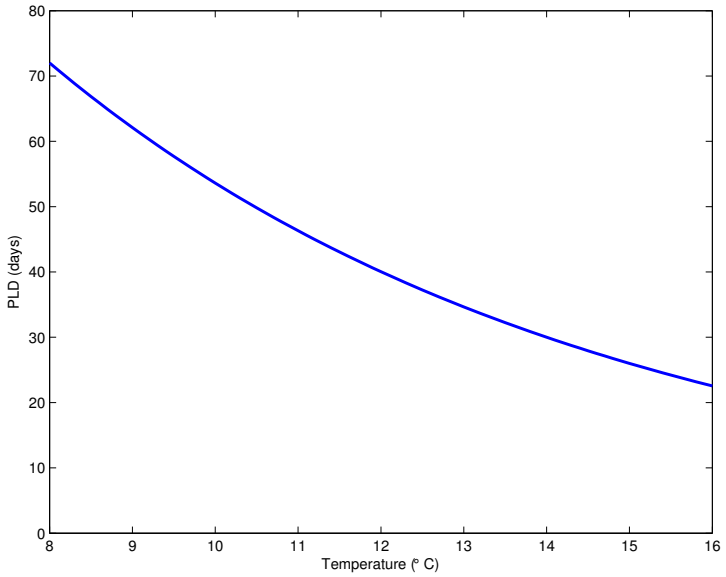

Figure 3.3: Variation of *N. norvegicus* PLD according to water temperature according to Dickey-Collas et al. (2000b) (stages 1 and 2) and Smith (1987) (stage 3).

rates are available (Nichols et al., 1987; Dickey-Collas et al., 2000a; Briggs et al., 2002), little is known about how mortality varies spatially and temporally. Mortality is therefore neglected entirely in this investigation. This also ensures that a far greater number of particles are available for statistical analysis. It should be highlighted that in reality mortality will diminish recruitment rates considerably, and it is likely that mortality will not have a uniform effect and this would influence results. This is not a problem here as this investigation is chiefly concerned with the influence of the physical environment upon dispersal.

3.2.4 Model Set-ups and Analysis Techniques

Particles are initially distributed uniformly across both the western and eastern Irish Sea muddy sediment regions (figure 3.1, blue regions), with over $170,000$ particles in total over both regions for each simulation. This is re-

peated for six different release dates, with three different model set-ups. The number of particles was confirmed to be sufficient in a sensitivity analysis, (repeated simulations had median dispersal distances that differed by less than 0.1 km, and connectivity statistics differed by less than 0.1 %). In a similar study, Robins et al. (2013) deemed that $10,000$ particles per site were sufficient for modelling larval dispersal in the Irish Sea. It should be noted that some observations strongly indicate that the western Irish Sea *N. norvegicus* population is spatially inhomogeneous in reality, with peak values in the centre of the region (Hillis, 1974; White et al., 1988), however the lack of available quantitative data on the distribution of adult *N. norvegicus* makes it very difficult to accurately replicate the true hatching pattern in the model. This is not a problem as this investigation is primarily concerned with spatial and seasonal variability of larval dispersion, rather than providing population mean values.

The particles are initially released on 15^{th} April, and then every ten days until 4^{th} June, using meteorological data from 2005. These dates span the hatching season of *N. norvegicus* larvae (Dickey-Collas et al., 2000a). Each particle is introduced into the water column at a random time on the allocated release date to minimise the influence of initial tidal state on the overall results.

No particles are released from the additional muddy sediments in the Scottish coastal waters, adjacent to the North Channel (figure 3.1, green regions) as they are in close proximity to the model boundary, and large numbers of particles would almost certainly leave the model domain. The model runs are therefore able to investigate larval exchange in both directions between the eastern and western Irish Sea, but only one-way connectivity to the North Channel. As the mean circulation through the North Channel is predominantly northwards (aside from a narrow and relatively weak southward current in the west) (Brown and Gmitrowicz, 1995), one would assume that larval transport from the North Channel into the Irish Sea is rather unlikely.

In order to investigate the influence of larval behaviour, three model set-

ups are used, and elements of the larval behaviour sub-model are introduced in stages. In the first set-up (fixed-depth), particles are fixed at 24 m depth in the vertical (the depth of the fixed drifting buoys in Horsburgh et al. (2000), and the approximate depth of thermocline), or fractionally above the seabed where depths are shallower than 24 m, and each particle is tracked for 60 days. In the second model set-up (active-depth) particles are released from the seabed, and their depth is subsequently governed by stochastic diffusion and vertical migration, and particles are again tracked for 60 days. The third and final set-up (full-model) is equivalent to the active-depth set-up, except that PLD is determined by water temperature using equations 3.2 and 3.3.

Finally the fixed-depth and active-depth simulations are repeated with one additional release date on 1st November in order to investigate how retention rates would be affected if the larvae emerged after the gyre had fully broken down. This is not repeated for the full-model set-up as cold winter temperatures would lead to an unrealistically high PLD. It should be stressed that no larvae are believed to hatch at this time in reality, and the extra release date is included only to study the influence of the gyre on dispersal.

The results are presented by summarising the particle retention rates, dispersal distances and connectivity statistics for each individual model run. The 'local retention rate is defined here as the percent of particles that settled upon the same muddy sediment region from which they were released. The 'bounded retention rate is defined here as the percent of particles that remained within the bounded western Irish Sea region (figure 3.1) at the end of their PLD, but did not necessarily settle upon the muddy sediments. This value is only presented for particles seeded in the western Irish Sea. The bounded retention rate is therefore perhaps a better measure of retention in a more general context, but the local retention rate is more relevant to *N. norvegicus*. Particle transport distances are calculated as the great-circle distance between the initial location and settlement sites.

3.3 Results

3.3.1 Hydrodynamic Model Output

Simulated peak surface temperatures in the western Irish Sea in 2005 rose from approximately 8 °C in early April to 14.5 °C in August (figures 3.4, 3.5, 3.6). Thermal stratification gradually developed over this period, and surface to bottom temperature differences reached 5 °C in July. The water column returned to a vertically mixed state in mid-October.

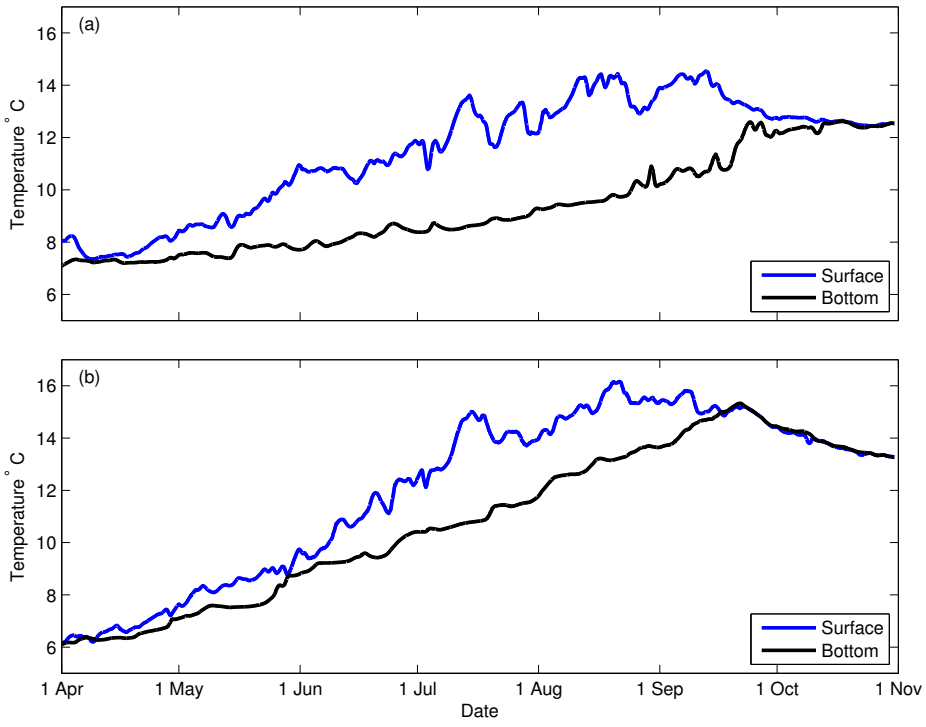

Figure 3.4: Temperature (°C) time series from POLCOMS output; (a) western Irish Sea (54 ° N, −5.4 ° E); (b) eastern Irish Sea (54.3 ° N, −3.75 ° E). Temperatures have been passed through a central moving average filter to reduce the signal from semi-diurnal tidal advection

Residual sub-surface circulation was cyclonic in the western Irish Sea during April, however mean velocities were slow at this point, generally below

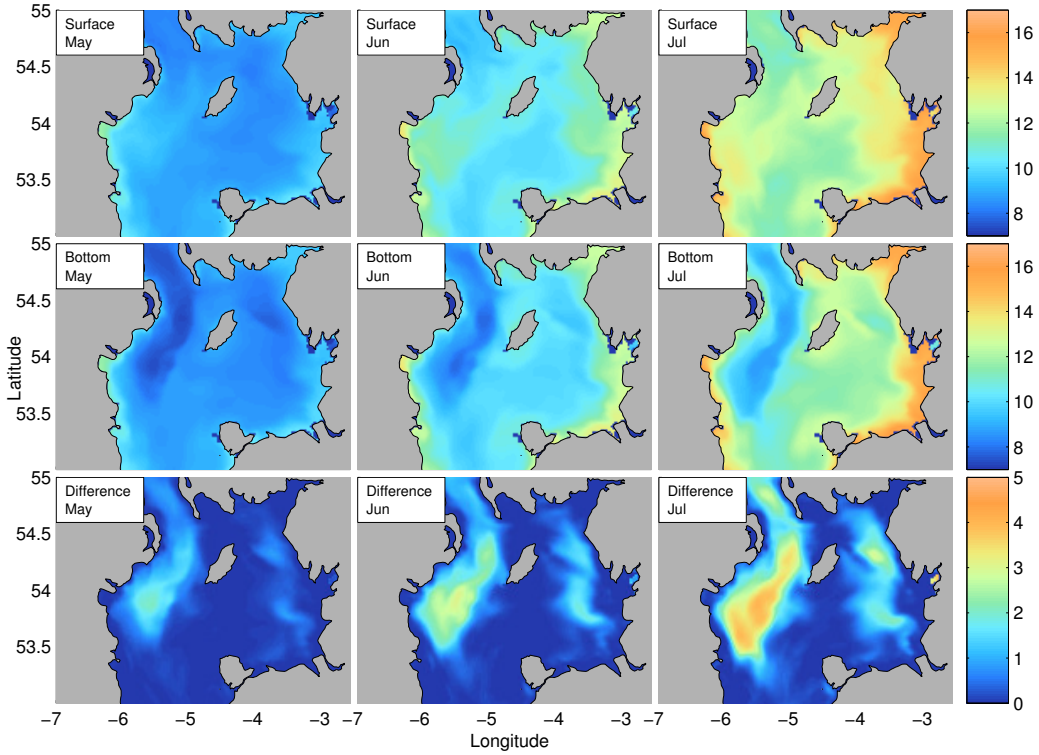

Figure 3.5: Monthly mean surface and bottom temperature (°C), and vertical temperature difference (surface minus bottom temperature) in the Irish Sea during May, June and July 2005.

0.05 m s^{-1} (figures 3.7, 3.8). The northward component of the gyre on the eastern flank of the muddy sediment region developed first, with peak flows reaching 0.1 m s^{-1} in May, whilst the southward return flow on the western flank remained considerably slower until June. Mean velocities reached their peak of approximately 0.2 m s^{-1} during August, then the gyre was almost entirely broken down by late October. There was a strong and persistent north-westward current located at the entrance to the North Channel, flowing along the Scottish coastline at velocities of the order of 0.2 m s^{-1}. This strong coastal flow has been observed in ADCP and HF radar data (Knight and Howarth, 1999), and as POLCOMS suggests that the mean current intersects the far northern part of the cyclonic gyre, this could potentially be

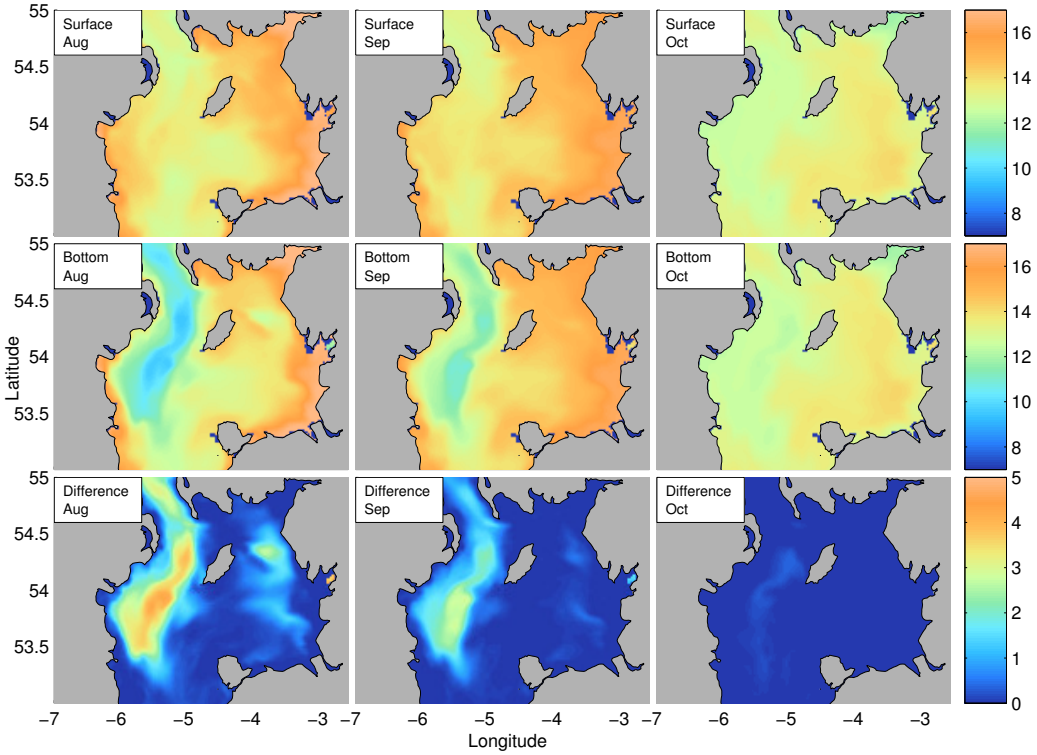

Figure 3.6: Monthly mean surface and bottom temperature (°C), and vertical temperature difference (surface minus bottom temperature) in the Irish Sea during August, September and October 2005.

an important mechanism for transporting larvae from the Irish Sea into the North Channel.

The simulated temperature and velocity fields were in good general agreement with the observations of Horsburgh et al. (2000). POLCOMS captures the two distinct maxima in thermal stratification, however the model predicts lower peak surface temperatures than those reported in 1995, and slightly weaker stratification. It is not clear whether these minor differences are due to inter-annual variability or model performance.

Greater seasonal variability was found in the eastern Irish Sea, where surface temperatures ranged from approximately 6 to 16 °C, however thermal stratification was somewhat weaker than in the western Irish Sea. Bot-

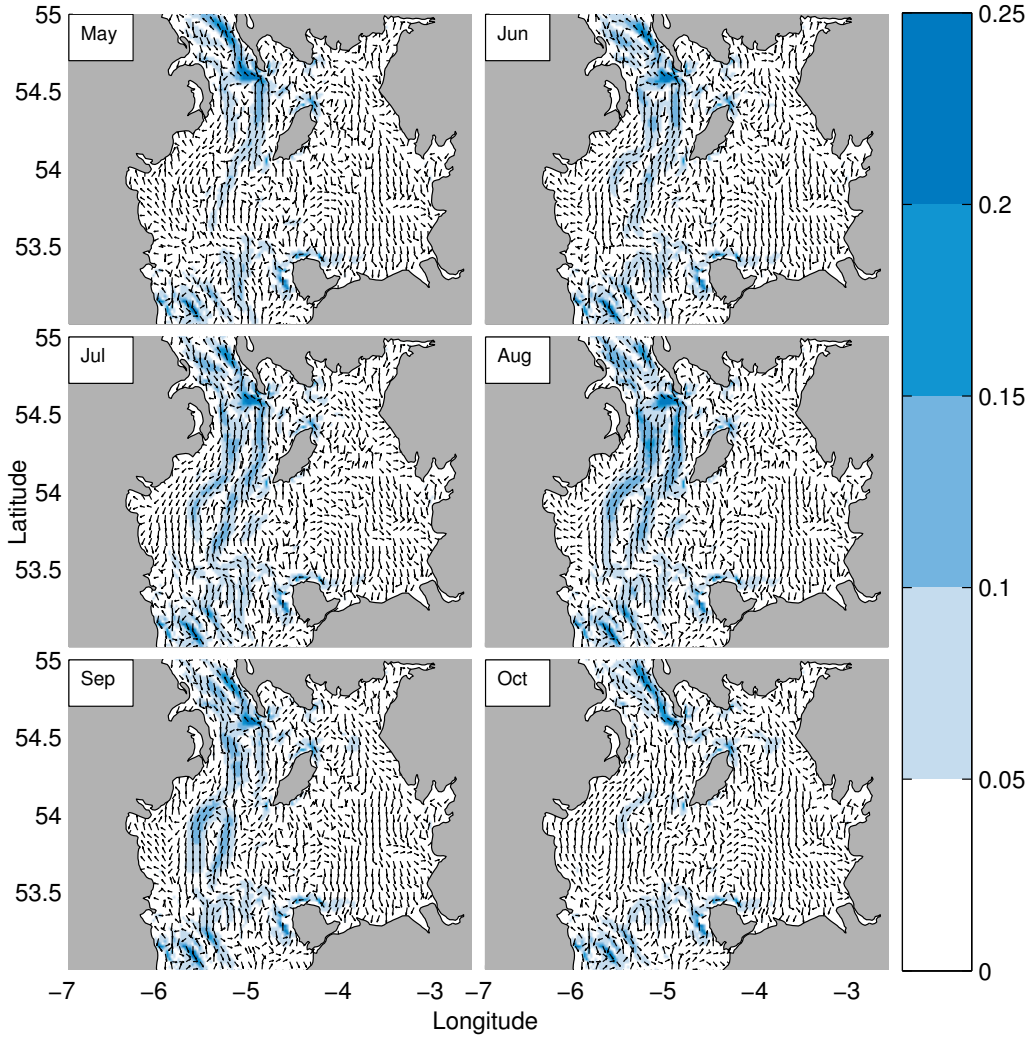

Figure 3.7: Monthly mean velocity (m s^{-1}) at 24 m depth in the Irish Sea during 2005. Magnitude is denoted by colour, direction is denoted by arrows shown at every 9^{th} model grid cell.

tom flow in this region was generally southward and weak ($\sim$ 0.01 m s^{-1}), whereas surface circulation appeared to be highly variable, both spatially and temporally. However the long-term average surface flow was predominantly northwards over the eastern *N. norvegicus* group. This is broadly consistent with the characterisation of eastern Irish Sea circulation by Howarth (1984).

3.3.2 Fixed-depth Particles

Dispersal distance distributions were positively skewed for all model set-ups, release dates and sites (figure 3.9), and were bimodal in some cases. As these distributions were highly non-normal, median dispersal distances are presented (table 3.1) rather than mean values, and non-parametric Kruskal-Wallis tests were conducted rather than ANOVA to confirm differences between distributions.

The gyre was clearly the dominant influence upon long-term fixed-depth particle transport in the western Irish Sea and cyclonic trajectories were clearly visible (figure 3.8), even amongst particles released on the earliest release date. Across all six spring release dates an average of 93 % of all fixed-depth particles were retained within the bounded western Irish Sea region (table 3.2). The overwhelming majority of the remaining particles were advected into the North Channel (6.3 % of the total), although in the last two spring release dates these were outnumbered by particles advected into the eastern Irish Sea. There was a product-moment correlation coefficient of 0.90 between bounded retention rate and Julian release date during this period, indicating a clear increase in retention with gyre strength. Furthermore, the November bounded retention rate was lower than that of all but the first spring release date. These simulations are therefore in good general agreement with the drifting buoy observations of Horsburgh et al. (2000), and they support the hypothesis that the seasonal gyre increases the likelihood that a passive object fixed at the depth of the thermocline will remain within the western Irish Sea, and this effect is more pronounced as the gyre strength develops.

The average local retention rate in the western Irish Sea was 42 % (table 3.3), therefore fewer than half of the particles that remained within the western Irish Sea actually returned to the muddy sediments. There is a clear spatial variability in local retention rates (figure 3.10), particles released from the centre of the region had almost a 100 % retention rate, whereas particles released from the edges of the muddy sediments were far less likely to return. Although the November local retention rate was somewhat lower at 37 %,

there was no linear correlation between release date (gyre strength) and local retention rates over the six spring release dates. The results suggest that the gyre does not have a spatially uniform effect upon local retention rates, as the spring releases generally had greater local retention rates in the central and eastern parts of the western Irish Sea site, but lower retention rates on the northern and western flanks. On average 1.0 % of particles released from the western Irish Sea over the first half of the spring release period settled upon the North Channel muddy sediments (table 3.3), however this rate was strongly diminished over the following releases, and a negligible amount reached the eastern Irish Sea muddy sediment site on any date.

The overall median particle transport distance in the western Irish Sea during spring was 39 km, although 4.9 % of particles were dispersed 100 km or greater (figure 3.9), and the greatest recorded distances exceeded 270 km. Whilst there was no clear trend in dispersal distance as the gyre developed (table 3.1), the median distance of the November release was considerably greater than that of all six spring releases. A Kruskal-Wallis test confirmed that the differences between the dispersal distances of different release dates were significant ($\chi^2 = 1.3e + 3$, df $= 5$, p-value < 0.001).

In the eastern Irish Sea the overall median transport distance was slightly shorter at 34 km due to the weaker mean circulation, however only 2.4 % of particles were locally retained, reflecting the smaller size of the muddy sediment region. Local retention rates were much more variable in the eastern Irish Sea (table 3.3), for example particles released on the 5^{th} of May were almost four times more likely to be retained than those released on 25^{th} April. Some particle exchange from the eastern Irish Sea to the North Channel muddy sediments occurred over the first two release dates (< 1 %), but all other exchange from the eastern Irish Sea was highly limited (≤ 0.1 %).

3.3.3 Active-depth Particles

In the active-depth simulations 82 % of particles seeded in the western Irish Sea during spring were retained within the bounded region (table 3.2), however only 32 % settled upon the western Irish Sea muddy sediments (table

Population	set-up	15 Apr	25 Apr	5 May	15 May	25 May	4 Jun	1 Nov
Western Irish Sea	fixed-depth	38.7	37.8	39.0	38.2	38.0	42.2	48.0
	active-depth	45.0	43.4	34.5	45.5	50.5	59.9	49.2
	full-model	46.7	47.0	38.0	49.5	54.9	59.4	n/a
Eastern Irish Sea	fixed-depth	39.0	40.1	29.1	35.7	33.1	29.3	n/a
	active-depth	26.4	24.7	26.1	30.6	22.6	21.7	n/a
	full-model	31.9	25.5	25.4	28.9	20.7	22.1	n/a

Table 3.1: Median horizontal distance (km) between initial and final particle locations, separated according to release site, set-up and release date.

Set-up	15 Apr	25 Apr	5 May	15 May	25 May	4 Jun	1 Nov
fixed-depth	82.8	91.3	93.5	95.6	95.4	97.9	83.5
active-depth	70.2	82.7	88.6	86.8	85.6	80.7	84.0
full-model	73.6	79.8	86.7	85.0	81.5	83.3	n/a

Table 3.2: Percent of particles seeded in the western Irish Sea that remained within the bounded region at the end of their PLD (bounded retention rate), separated according to release date and model set-up.

Set-up	Initial site	Settle site	15 Apr	25 Apr	5 May	15 May	25 May	4 Jun
fixed-depth	WIRS	WIRS	43.99	40.48	43.76	36.02	49.00	41.37
		EIRS	0.00	0.00	0.00	0.01	0.01	0.00
		NC	0.87	1.09	1.01	0.33	0.08	0.07
	EIRS	WIRS	0.10	0.02	0.00	0.03	0.08	0.02
		EIRS	1.51	0.79	3.15	3.14	2.64	3.38
		NC	0.69	0.70	0.00	0.06	0.03	0.00
active-depth	WIRS	WIRS	27.19	32.74	39.98	34.28	33.14	24.38
		EIRS	0.00	0.01	0.00	0.00	0.00	0.00
		NC	0.72	0.65	0.14	0.24	0.09	0.14
	EIRS	WIRS	0.28	0.30	0.82	0.66	0.30	0.15
		EIRS	1.91	7.51	4.12	2.42	0.77	2.28
		NC	0.07	0.02	0.01	0.02	0.02	0.00
full-model	WIRS	WIRS	23.34	27.65	34.16	33.11	25.82	23.30
		EIRS	0.00	0.00	0.00	0.00	0.00	0.00
		NC	1.41	0.41	0.17	0.31	0.12	0.11
	EIRS	WIRS	0.99	0.49	0.76	0.65	0.26	0.06
		EIRS	1.86	10.64	3.51	3.19	1.80	1.38
		NC	0.25	0.00	0.03	0.02	0.01	0.00

Table 3.3: Connectivity table detailing the percentage of particles released from a particular region that landed on each muddy sediment region. Particles are separated according to model set-up, initial site and release date. Abbreviations are WIRS, western Irish Sea; EIRS, eastern Irish Sea; NC, North Channel.

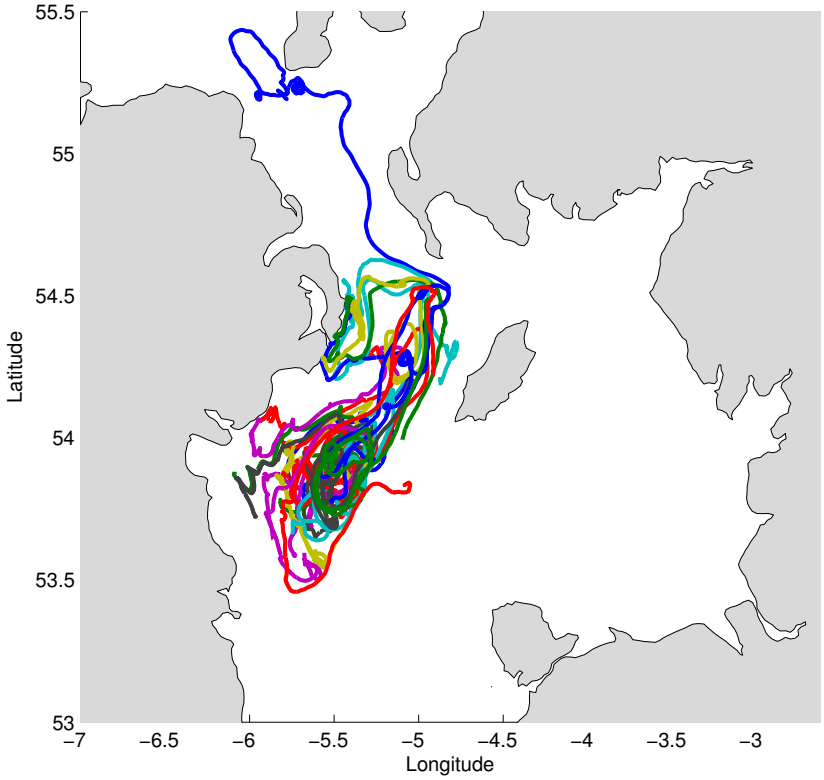

Figure 3.8: Trajectories of a random sample of 24 particles released from the Irish Sea in the fixed-depth simulations (4 particles from each spring release date). Trajectories have been passed through a central moving average filter to reduce the signal from semi-diurnal tidal advection. Colours are for visual identification of individual trajectories and do not denote any property.

3.3). Therefore vertical migration led to a considerable reduction to both the bounded and local retention rates in this region. Dispersal distances were also much greater with this model set-up, with a median value of 47 km across all six spring releases. There was no evidence that the gyre promotes retention of vertically migrating particles, as both the bounded and local retention rates were greatest amongst particles that were released during the middle of the hatching period (tables 3.2 and 3.3, figure 3.11), and this coincided with shorter dispersal distances (table 3.1). Differences in dispersal distances between release dates were significant in a Kruskal-Wallis test

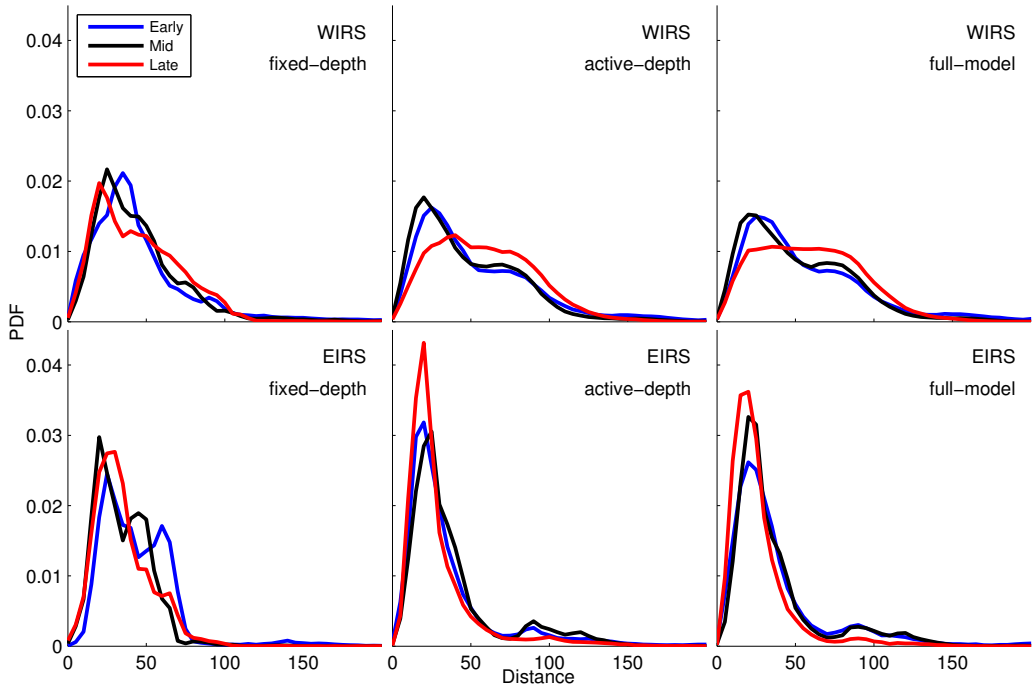

Figure 3.9: Probability density function of transport distance from early (15$^{\text{th}}$ and 25$^{\text{th}}$ April), mid (5$^{\text{th}}$ and 15$^{\text{th}}$ May) and late (25$^{\text{th}}$ May and 4$^{\text{th}}$ June) *N. norvegicus* spawning dates. Particle transport distance data are placed into 5 km bins and pooled according to release date. Distances greater than 200 km were extremely rare and are not shown. Abbreviations are WIRS, western Irish Sea; EIRS, eastern Irish Sea.

($\chi^2 = 2.8e{+}4$, df $= 5$, p-value < 0.001). Furthermore the local retention rate during the November release scenario was 39 %, which is considerably greater than the average value during spring. There were some similarities with the fixed-depth particles however, as the greatest local retention rates were found amongst particles released from the centre of the muddy sediments (figure 3.11), and the majority of particles that left the bounded western Irish Sea region altogether were advected into the North Channel (17 % of the total during spring).

By contrast, active-depth particles released during spring in the eastern Irish Sea had an overall median dispersal distance of 25 km, which is 9 km

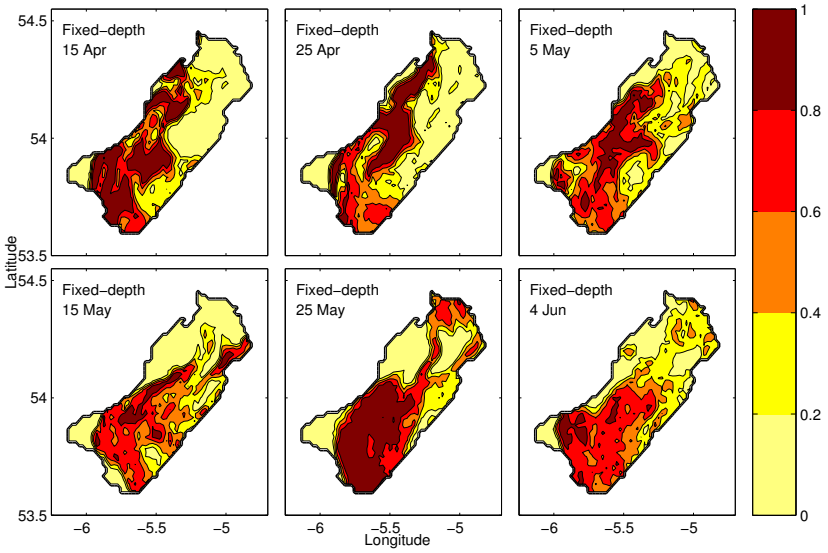

Figure 3.10: Fixed-depth particle local retention rates in the western Irish Sea, mapped onto the POLCOMS Irish Sea grid according to particle release site.

shorter than the distance amongst fixed-depth particles, and the average local retention rate was somewhat greater at 3.2 %. Once again the results showed a high degree of temporal variability in the eastern Irish Sea. Connectivity between distinct regions was highly limited. Perhaps the most notable distinction between the model set-ups was the greater number of particles from the eastern Irish Sea settling upon the western Irish Sea muddy sediments in the active-depth set-up, peaking at 0.8 % on the 5$^{\text{th}}$ May release.

3.3.4 Full-model Particles

In the full-model simulations the average bounded and local retention rates in the western Irish Sea were 82 % and 28 % respectively (tables 3.2 and 3.3, figure 3.11), and the overall median dispersal distance was 50 km (table 3.1, figure 3.9). Therefore the inclusion of a temperature-dependent PLD did not affect the proportion of particles that remained within the wider western Irish Sea, but it did lead to a small reduction in the proportion of particles

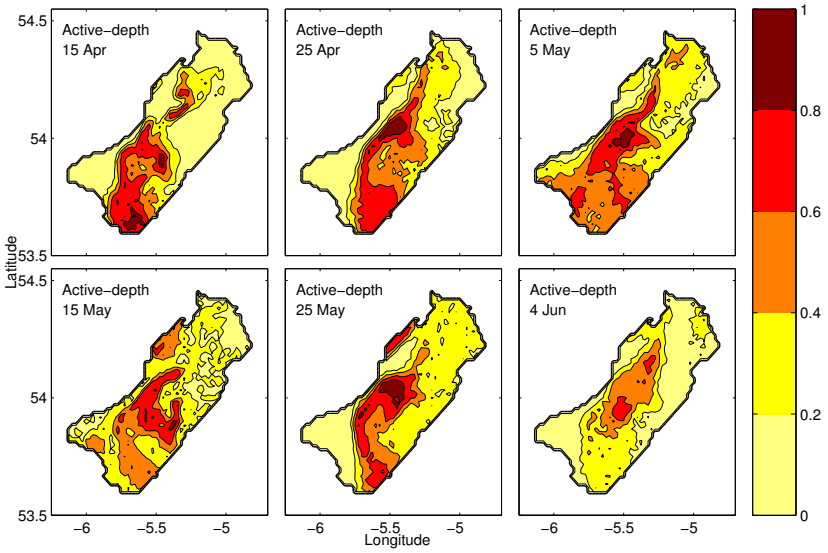

Figure 3.11: Active-depth particle local retention rates in the western Irish Sea, mapped onto the POLCOMS Irish Sea grid according to particle release site.

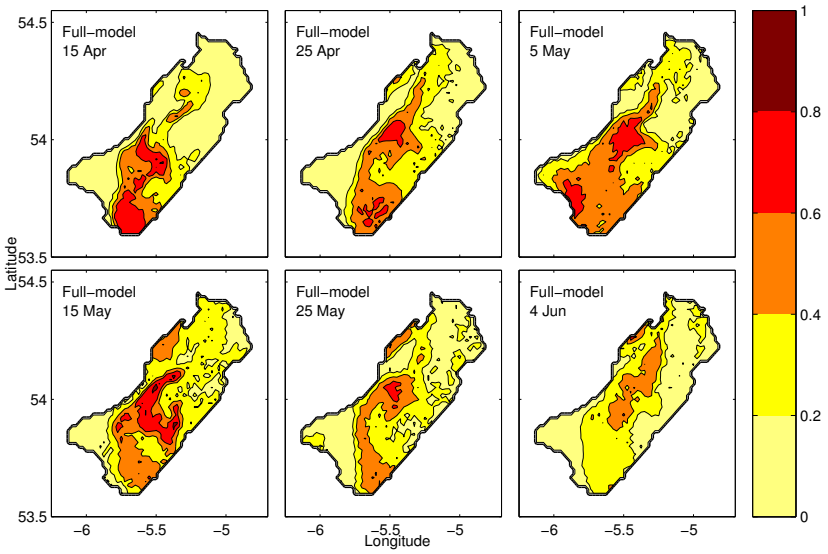

Figure 3.12: Full-model particle local retention rates in the western Irish Sea, mapped onto the POLCOMS Irish Sea grid according to particle release site.

that were able to settle upon the muddy sediments, and a slight increase in dispersal distances. Seasonal and spatial trends in retention rates remained the same as in the previous set-up, with the greatest local retention amongst particles released from the centre of the western Irish Sea population, and in the middle of the hatching period (figure 3.12). Differences between the dispersal distances of different release dates were significant in a Kruskal-Wallis test ($\chi^2 = 1.6e + 4$, df = 5, p-value < 0.001). On average 3.7 % of particles were retained locally in the eastern Irish Sea, which is somewhat greater than the rate in the active-depth simulations, although the overall median dispersal distance was almost unchanged.

Full-model particle exchange rates were generally similar to those in the previous set-up however there was a slightly greater mean rate of transport from the eastern Irish Sea to the western population (table 3.3). Once again this limited connectivity was greatest in the initial part of the hatching period, and transport in the reverse direction remained negligible.

The mean PLD of western Irish Sea particles reduced from 70 days on 15$^{\text{th}}$ April to 59 days on 4$^{\text{th}}$ June. The eastern Irish Sea displayed even greater seasonal variability, with the mean PLD reducing from 67 to 44 days over the hatching period due to the wider range in water temperature. The PLD of particles that were released closer to the warmer Irish coastal waters on the western flank of the population was typically around 20 days shorter than the PLD in the central and eastern regions of the population (figure 3.13). There was also a small zonal PLD gradient in the eastern Irish Sea, particles that were released closer to the English coastline typically had a PLD of around 5 days shorter than those that hatched further offshore (figure 3.14).

3.4 Discussion

The dispersal of marine larvae by ambient circulation is fundamental to population dynamics, and it is an important consideration in the effective design of marine protected areas (Cowen and Sponaugle, 2009). This is particularly true for benthic invertebrate species such as *N. norvegicus*, as they typically

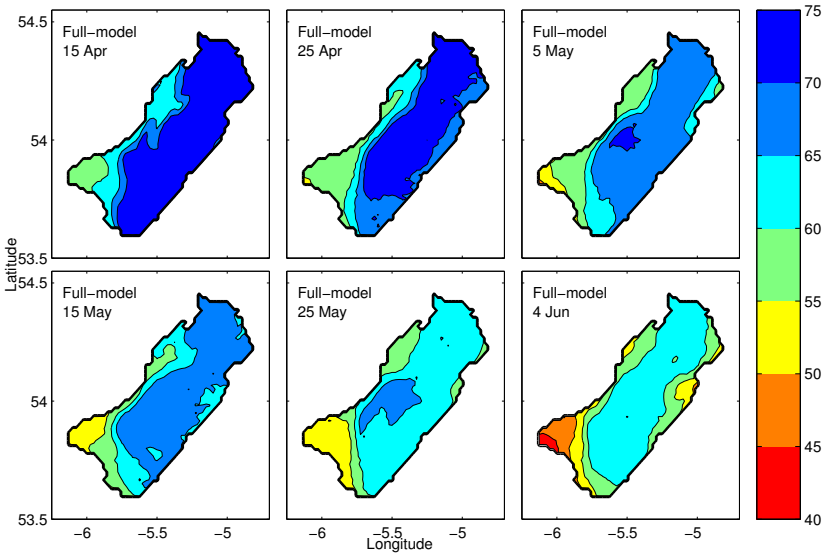

Figure 3.13: Mean pelagic larval duration (in days) of particles in the western Irish Sea. Particles are mapped onto the POLCOMS Irish Sea grid according to initial particle location, and separated according to the release date.

remain sessile or sedentary throughout their adult life. Understanding the drivers of larval dispersal and the factors that influence population connectivity is therefore an important challenge for marine ecologists.

The western Irish Sea seasonal gyre is a widely cited example of a regional dynamical system that affects larval dispersal (e.g. Hill et al., 1996; Dickey-Collas et al., 1997; Hill et al., 1997). The influence of the gyre upon *N. norvegicus* is particularly important from an ecological perspective due to the intense trawling efforts and the spatial distribution of the requisite muddy sediments in relation to the gyre. Despite this, previous studies have largely neglected certain aspects of *N. norvegicus* larval behaviour, such as sediment requirements, vertical swimming or appropriate PLD. As recent modelling work suggests that the dynamical characteristics of the gyre may be changing (Olbert et al., 2011), it is now imperative that the effect of the gyre on *N. norvegicus* larval dispersal is properly understood. This investigation has thoroughly tested the validity of the hypothesis that the gyre acts as an

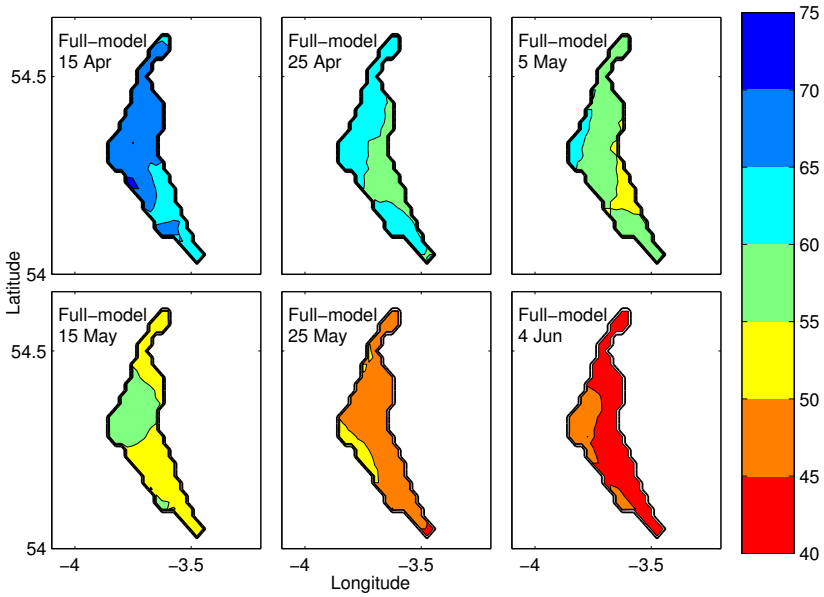

Figure 3.14: Mean pelagic larval duration (in days) of particles in the eastern Irish Sea. Particles are mapped onto the POLCOMS Irish Sea grid according to initial particle location, and separated according to the release date.

effective retention mechanism for *N. norvegicus* larvae.

The results of this investigation suggest that the seasonal gyre does reinforce retention of larvae within the wider western Irish Sea region, on the condition that the larvae remain fixed at the depth of peak gyral flow. Approximately half of these larvae will fall outside of the muddy sediments at the end of their larval phase however (assuming a PLD of around 60 days), and the local retention rate does not appear to increase with gyre strength. There is therefore little evidence that the gyral circulation promotes local recruitment amongst fixed-depth larvae that require muddy sediments for successful settlement.

The influence of the gyre is not spatially uniform across the western Irish Sea. The results suggest that the gyral system reinforces local retention amongst larvae that originate from the central part of the muddy sediments, and diminishes retention rates around the periphery (figure 3.15). In reality

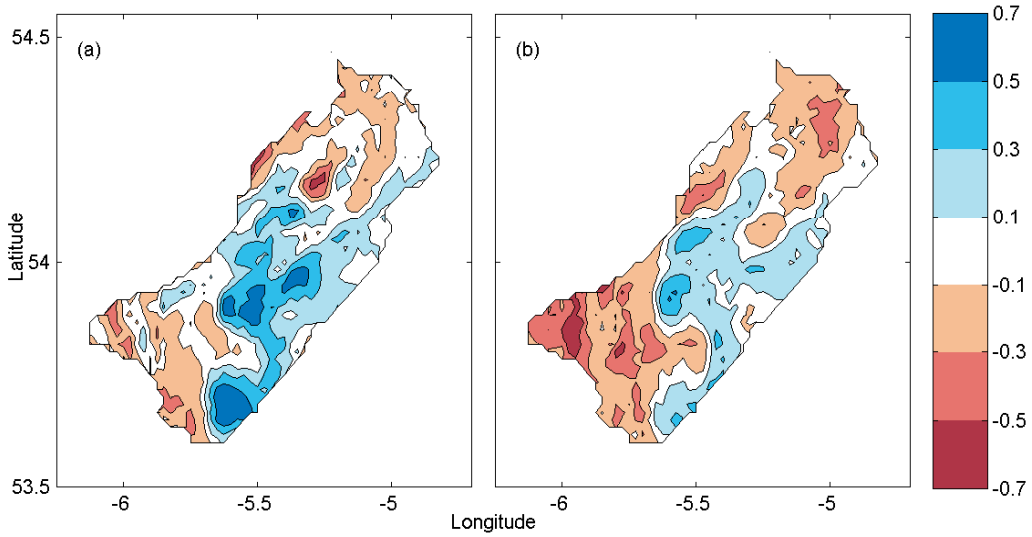

Figure 3.15: Average spring local retention rate minus the November local retention rate in the western Irish Sea. Particles are mapped onto the POL-COMS grid according to initial location. Positive values indicate that the seasonal gyre aids particle retention in that region, whilst negative values indicate the gyre inhibits local retention. (a) fixed-depth model set-up. (b) active-depth model set-up.

larval densities are greatest in the centre of the region, therefore the results of this investigation may be consistent with the gyre retention hypothesis of Hill et al. (1996) after accounting for this spatial variability. Future modelling investigations should aim to utilise a non-uniform initial particle distribution to confirm whether this is the case.

On average, vertically migrating particles were dispersed 10 km further, and were approximately 25 % less likely to be locally retained, relative to fixed-depth retention rates. This can be explained by the fact that the gyre is vertically confined to a relatively narrow band around the thermocline, and vertical migration will increase the likelihood of escaping this circulation. Shear diffusion and vertically sheared tidal currents may introduce further net transport away from the adult grounds. Furthermore, retention rates amongst vertically migrating particles were greater in May than June

despite the weaker gyral flow. Vertical migration is clearly a significant influence upon larval dispersal in shelf sea gyres, and this investigation finds no evidence that gyral circulation promotes local retention of vertically migrating larvae. Diel vertical migration is common amongst many meroplanktonic larvae and holoplanktonic organisms such as copepods, and there are several proposed explanations for the adaptive significance of this behaviour, including evasion of visually dependent predators (Zaret and Suffern, 1976; Gliwicz, 1986), metabolic benefits (McLaren, 1963) and decreasing exposure to damaging solar radiation (Leech and Williamson, 2001). It is certainly possible that one of these explanations could hold for *N. norvegicus* larvae. Whilst this investigation cannot determine the reason for vertical migration of *N. norvegicus* larvae, the results do suggest that larvae in the western Irish Sea do not migrate for the purpose of local retention.

By contrast, in the eastern Irish Sea vertical migration appears to reduce dispersal distance and increase retention rates. This can be explained by the fact that migrations between a northward surface mean flow and a southward bottom flow will ultimately reduce net advection. *N. norvegicus* larvae released from the eastern Irish Sea are typically advected much shorter distances, however larval retention rates are considerably lower due to the smaller habitat area. Retention rates in the eastern Irish Sea display considerable short-term variability, which suggests that wind may play a significant role in determining local retention. A small minority of larvae from both sites can be expected to be dispersed over hundreds of kilometres. Peak dispersal distances are slightly lower than those reported for fish eggs and larvae in the Irish Sea by van der Molen et al. (2007), however this is explained by the fact that *N. norvegicus* have a shorter PLD.

N. norvegicus PLD varies considerably both spatially and temporally due to changes in water temperature. Larvae that hatch in the central and western parts of the western Irish Sea population during April typically spend twice as long in the plankton as larvae that hatch from the coastal areas during July. In the western Irish Sea the mean PLD was generally greater than the 60 days assumed for the first two model set-ups, and this resulted

in an increase in dispersal distances and a reduction in retention rates.

Whilst investigating the influence of vertical migration strategy on larval retention in the Irish Sea, Emsley et al. (2005) concluded that DVM supported particle retention by increasing the probability of larvae becoming entrained within the gyre. The results of the current study would initially appear to directly oppose this conclusion, despite also using POLCOMS. The discrepancy between the findings could be for a number of reasons. Firstly the computational advances of the past decade allowed the use of more advanced numerical methods in the current investigation (notably RK4 particle advection, significantly greater number of particles, shorter time steps and the introduction of stochastic vertical diffusion). Furthermore the current study is focused upon *N. norvegicus*, therefore a more realistic PLD is adopted (rather than 30 or 90 days), and a particle is considered to be "retained" if it returns to the muddy sediments, rather than if it remains within the model boundaries. Vertical swimming behaviour is also parametrised differently, and the passive particle depths are not equal, therefore the findings of the two investigations are perhaps not mutually exclusive. Several other modelling studies report that vertical migration has a significant effect on larval (or fish egg) transport in the Irish Sea (e.g. Fox et al., 2006; van der Molen et al., 2007; Robins et al., 2013), however these studies largely focus upon species with coastal or estuarine hatching sites and nursery grounds, so it is more difficult to make direct comparisons to an offshore benthic species such as *N. norvegicus*.

In all simulations, local retention rates were significantly greater amongst particles released from the central part of the gyre, whereas those released from the periphery were highly likely to be lost from the system. This suggests that the adult *N. norvegicus* that inhabit the central part of the muddy sediments may play the most important role in sustaining the population. Therefore if a marine protected area was considered for a gyral system such as the western Irish Sea, the results of this investigation suggest that it may be more ecologically effective if the centre of the gyre was prioritised.

Olbert et al. (2011) proposed that changing atmospheric conditions are re-

sulting in stronger cyclonic circulation in the western Irish Sea, but a shorter gyre duration and a delay in the peak flow, coupled with a decrease in the residence time. It is difficult to determine exactly how such changes would affect resident larvae and speculation should be avoided, however it is worth noting that the current investigation finds that the greatest local retention rates are found during early May, and this period corresponds with the peak hatching time of *N. norvegicus* larvae (Dickey-Collas et al., 2000a). Any delay in the onset of the gyre could upset this synchronisation, unless it is matched by a similar delay in hatching time. The decrease in residence time in the region suggests that the region is becoming less retentive, and this could lead to greater losses of larvae from the system. Further work should aim to investigate how the long-term inter-annual variability of the gyre will affect larval retention.

Overall this investigation is in agreement with the conclusion of van der Molen et al. (2007), that the capability of the western Irish Sea gyre to retain larvae appears to be relatively weak. This conclusion is supported further by larval surveys (Hillis, 1974; White et al., 1988) that clearly show *N. norvegicus* larvae outside the muddy sediment regions, suggesting some loss from the system due to mean advection, although Nichols et al. (1987) proposed that this could potentially be due to adults living outside the muddy substrate that is recognised as the boundary of the *N. norvegicus* population. It appears that whilst Horsburgh et al. (2000) provides an excellent and thorough assessment of the physical and dynamical properties of the western Irish Sea gyre, the fixed-depth drifters neglect too many factors for their trajectories to be representative of *N. norvegicus* larvae. This should serve as a warning for marine ecologists to exercise extreme caution whenever attempting to deduce information about larval dispersal from passive drifter observations. Although it is also important to take care when attempting to assess population connectivity from numerical simulations alone, these simulations suggest that the distinct *N. norvegicus* sites largely rely upon local recruitment of larvae, despite some evidence of highly limited one-way connectivity in a pattern that broadly reflects the mean circulation in the

Irish Sea.

3.5 Appendix A: Vertical migration parametrisation

The weighted parameter λ is calculated using the following function of larval stage, time of day and depth in the water column. Here z denotes depth (given in metres, positive z is directed upwards in the water column, reaching 0 at the surface), P is the period of DVM (i.e. one day), t denotes time in days and τ represents the normalised stage duration.

$$\lambda = \begin{cases} \tau\left(1+\sin(2\pi t/P)-0.2\alpha\right) & \text{if stage } = 1, \tau \leq 0.5 \\ 0.5\left(1+\sin(2\pi t/P)-0.2\alpha\right) & \text{if stage } = 1 \\ 0.5\left(1+\sin(2\pi t/P)-0.2\alpha\right) & \text{if stage } = 2 \\ 0.5\left(1+\sin(2\pi t/P)\right) & \text{if stage } = 3, \tau \leq 0.5 \\ (1-\tau)\left(1+\sin(2\pi t/P)\right)+2\tau-1 & \text{if stage } = 3, \tau > 0.5 \end{cases} \tag{3.4}$$

where α is introduced to prevent particles accumulating in the bottom waters during the first two larval stages, given by

$$\alpha = \begin{cases} 1 & \text{if } z \leq -40 \text{ m} \\ 0 & \text{if } z > -40 \text{ m}. \end{cases} \tag{3.5}$$

Note that in the active-depth simulations, τ is calculated by assuming a uniform temperature of 9.23 °C, therefore permitting vertical migration using this sub-model whilst still forcing a PLD of 60 days.

3.6 Appendix B: The Well Mixed Condition

Hunter et al. (1993), Visser (1997) and Ross and Sharples (2004) have each highlighted the fact that it is necessary to exercise caution when attempting to simulate diffusion in an environment where diffusivity is spatially variable, as the "naive model" may lead to artificial accumulation of particles in regions of low diffusivity. Additional care must be paid to the time step selection and

boundary conditions. In this investigation, vertical diffusion was calculated using the following equation (see e.g. Ross and Sharples, 2004), where K represents vertical diffusivity, z_n represents the depth of a particle at time t_n, Δt is the diffusion time step (6 seconds) and R is a random variable taken from a normal distribution with mean 0 and standard deviation r,

$$z_{n+1} = z_n + \Delta t \frac{\partial K}{\partial z}(z_n) + R \left[\frac{2\Delta t}{r} K \left(z_n + \frac{\Delta t}{2} \frac{\partial K}{\partial z}(z_n) \right) \right]^{\frac{1}{2}}. \tag{3.6}$$

A one-dimensional idealised simulation was conducted in order to verify that this vertical diffusion scheme, along with the selected time step and reflective boundary conditions, satisfied the well mixed condition. I.e. if particles are initially uniformly distributed throughout the water column, then they will remain uniformly distributed as long as there are no external factors such as vertical migration, variable bathymetry or vertical advection. An inhomogeneous vertical diffusivity profile was extracted from the POLCOMS output, and $10,000$ particles were initialised uniformly over depth, and diffused vertically for a PLD of 60 days. At the end of the 60 day PLD the particles were binned into 1 m intervals and a χ^2 goodness-of-fit test was conducted to test the hypothesis that the particles were uniformly distributed at the 5 % level.

H_0 : The distribution of particles fits a uniform distribution.

H_A : The distribution of particles does not fit a uniform distribution.

The final distribution of particles appeared approximately uniform (figure 3.16) and the null hypothesis could not be rejected at the 5 % level ($\chi^2 = 42.7$, df $= 39$).

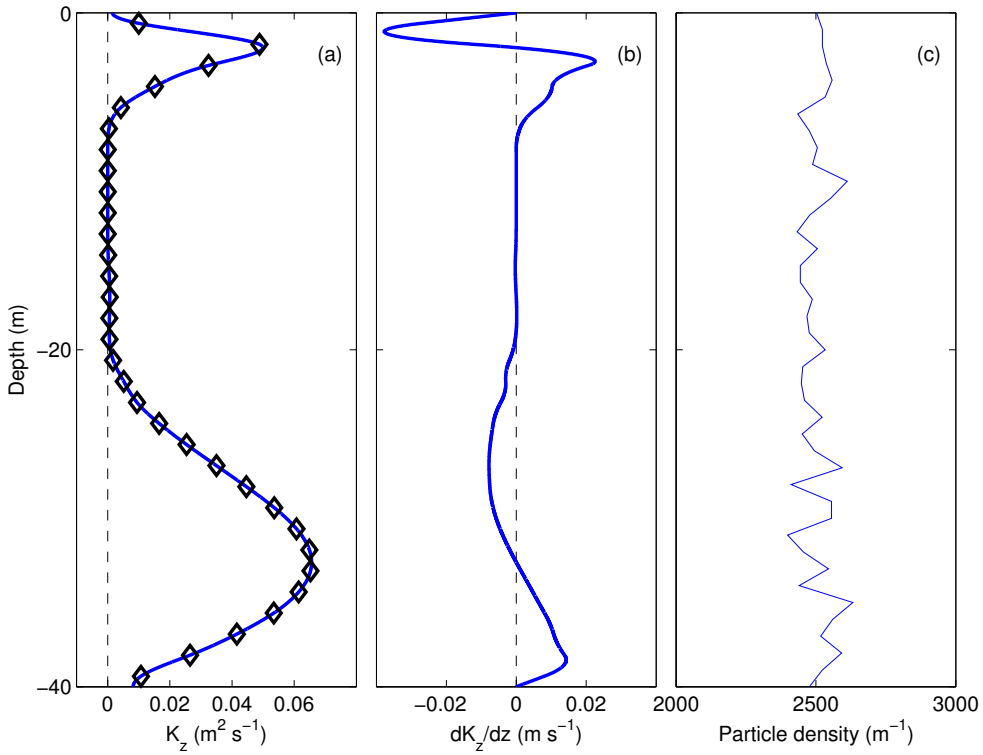

Figure 3.16: (a) Cubic smoothing spline (blue line) fitted to discrete values of vertical diffusivity K (m^2 s^{-1}) taken from POLCOMS output (black diamonds). (b) First derivative of vertical diffusivity (m s^{-1}). (c) Final particle distribution. Particles are binned into 1 metre intervals.

Chapter 4

A Cautionary Note on the Parametrisation of Passive Particles in Larval Dispersal Modelling Studies

Abstract

Larval behaviour is widely recognised as an important influence upon larval transport, however passive particles are still an effective tool for marine modellers when utilised in conjunction with active particles (with parametrised larval behaviour) in order to determine how behaviour affects dispersal. In this context the term "passive" is broadly understood to indicate an absence of biological behaviour, however it is not used consistently, and is often not precisely defined. This numerical investigation demonstrates that different parametrisations of passive particles may lead to opposing conclusions about the influence of vertical migration.

The problem is initially highlighted using an idealised one-dimensional example of estuarine and tidal flow in an open channel. The same scenarios are then investigated using a three dimensional hydrodynamic model with a coupled particle tracking model in Liverpool Bay, a shallow hyper-tidal coastal embayment with a density driven circulation.

Simulations indicate that diel vertical migration (DVM) promotes coastal retention in Liverpool Bay when compared to passive particles that are fixed at either surface or random depths, however the same results can be used to conclude that DVM facilitates offshore transport when compared to passive particles that are advected with bottom or depth-mean currents, or particles that are diffused throughout the water column. Such dependence upon passive particle parametrisation is unsatisfactory and it leaves the influence of larval behaviour upon transport open to some interpretation. It is argued here that the most appropriate parameterisation depends on the particular investigation being undertaken, but it is emphasised that this selection should be clearly specified in the methodology.

4.1 Introduction

The dispersal of meroplanktonic larvae in marine environments is crucial for population connectivity, particularly amongst benthic invertebrate species that are either sessile or sedentary throughout their adult lives (Cowen and Sponaugle, 2009). As larval dispersal is difficult to observe directly, marine ecologists routinely utilise numerical models to determine the dynamics of a population. This typically involves using a hydrodynamic model to supply physical data (velocity, elevation, diffusivity etc.) to an offline Lagrangian particle tracking model. Particles (representing larvae) are then initialised at a known spawning site, and advected for a period of time corresponding to the pelagic larval duration (PLD) of the particular species under investigation. Such techniques have found numerous applications, for example the design of effective marine protected area (MPA) networks (Jones et al., 2009), the spread of invasive species (McQuaid and Phillips, 2000) and the role of offshore renewable energy devices as artificial reefs (Adams et al., 2014).

Early larval dispersal studies generally simulated passive particles in two-dimensional models, however there have been significant developments in recent years. It is now widely recognised that larval behaviour can dramatically influence larval trajectory (Paris et al., 2005; Cowen et al., 2006), and it has

become standard practice for larval modelling studies to incorporate biological processes such as vertical migration (North et al., 2008), directed horizontal swimming (Staaterman and Paris, 2014) or a temperature-dependant pelagic larval duration (PLD) (Phelps et al., 2015a).

Although the use of passive particles alone is now generally discouraged, they are still regularly utilised effectively in conjunction with active particles with parametrised larval behaviour. This may be either to investigate a range of possible dispersal scenarios, or to determine how the behaviour affects larval transport (e.g. Emsley et al., 2005; Paris et al., 2005; Fox et al., 2006; Paris et al., 2007; Brochier et al., 2008; Butler et al., 2011; Phelps et al., 2015a; Robins et al., 2013). Other studies choose to adopt passive particles to simulate pelagic fish eggs before introducing behaviour during the later larval stages (Bolle et al., 2009).

The term "passive" is generally understood to imply a lack of active larval behaviour, however the parametrisation of passive particles is inconsistent in the literature. Particles described as passive are variously dispersed throughout the water column (Bolle et al., 2009, stages 1 and 2), fixed at a constant pre-determined depth (Phelps et al., 2015a), restricted to remain with a particular vertical layer (Emsley et al., 2005), advected using vertically averaged two-dimensional models (Davidson and deYoung, 1995), or a combination of the above (Puckett et al., 2014). Further variability can be introduced by the inclusion of horizontal or vertical diffusion. Furthermore some publications simply describe particles as passive and provide little further explanation about what is meant by this. The choice of passive particle parametrisation will affect transport, and this could ultimately influence the conclusion drawn about the effect of vertical migration upon larval dispersal. This problem is now highlighted with an idealised example of one dimensional flow in an open channel.

4.2 Idealised Scenario

Consider an open channel along the x-axis (where positive x is directed offshore), with depth z ranging from $z = -h$ at the bottom to $z = 0$ at the fixed surface. Horizontal velocity u is split between two components, a tidal velocity $u'(t, z)$ that varies with depth and time t, and a residual estuarine component $\overline{u}(z)$ that varies with depth alone. For simplicity we follow Simpson et al. (1990) for both velocity terms, adopting a steady-state estuarine flow profile (e.g. Officer, 1976, p. 118)

$$\overline{u}(z) = \frac{gh^3}{48N_z}\frac{1}{\rho}\frac{\partial \rho}{\partial x}\left(1 - 9\sigma^2 - 8\sigma^3\right) \quad \text{m s}^{-1} \tag{4.1}$$

where $\sigma = z/h$ and g, N_z and ρ represent gravitational acceleration, eddy viscosity and density respectively. The tidal component is allowed to vary in the vertical using the profile of Bowden and Fairbairn (1952),

$$u'(t, z) = \hat{u}\left(1.15 - 0.425\sigma^2\right) \quad \text{m s}^{-1} \tag{4.2}$$

where $\hat{u}$ is a time-varying depth-mean tidal current. For this example we use approximate values in Liverpool Bay (see section 4.3), with $h = 20$ m, and take $N_z = 0.0129$ m^{2}s^{-1} and $\frac{\partial \rho}{\partial x} = 1.2 \times 10^{-4}$ kg m^{-4} following Verspecht et al. (2009b), and force $\hat{u}$ with the principal tidal constituents in Liverpool Bay.

Five different passive scenarios are considered here (referred to as the surface, bottom, random-fixed, depth-mean and diffused scenarios), followed by an active diel vertical migration (DVM) example. In each simulation $100,000$ particles are released in a normal distribution centred upon $x = 0$ km with a standard deviation of 10 km, and are advected for a PLD of 30 days before settling. In the surface and bottom scenarios particles are vertically fixed to the surface ($z = -1$ m) and bottom ($z = -h + 1$ m) respectively. In the depth-mean scenario particles are advected with the vertically averaged velocity. In the random-fixed scenario particles are uniformly distributed throughout the water column, and each particle remains fixed at its initial depth throughout the PLD. In the diffused scenario, particles spawn at the

bottom ($z = -h$ m) and are constantly diffused in the vertical using the following numerical stochastic scheme

$$z_{n+1} = z_n + R\sqrt{2r^{-1}K\Delta t} \quad \text{m} \tag{4.3}$$

where z_n represents the depth of a particle at time step n, R is a random number taken from the uniform distribution $U[-1, 1]$ with variance $r = 1/3$, the time step is $\Delta t = 5$ s and vertical diffusivity is taken as a constant $K = 0.001$ m^{2}s^{-1}. Note that whilst this "naive model" (equation 4.3) can lead to artificial particle accumulation in regions of low diffusivity (Hunter et al., 1993; Visser, 1997; Ross and Sharples, 2004), there are no such problems in this example because of the uniform diffusivity. Finally, in the active DVM scenario particles are released from the bottom ($z = -h$ m), and swim vertically with a constant speed of 3 mm/s, directed towards the surface between 6 p.m. and 6 a.m., and towards the seabed during the remaining hours. The DVM particles are also subject to stochastic vertical diffusion. The results of the idealised model are summarised in figure 4.1.

As one would expect, each parametrisation leads to a different final particle distribution, but more importantly it is possible to draw opposing conclusions about the effect of diel vertical migration upon dispersal depending upon which of the five passive simulations is regarded as the "base scenario". The DVM particles are advected a mean distance of 14.7 km offshore, whereas the surface and bottom passive particles are advected 36.7 km offshore and 10.8 km onshore respectively. The final particle distributions of remaining three passive scenarios (random-fixed, depth-mean and diffused) are all centred within 1 km of the origin (slightly off-centre due to the tidal state at the end time), however they each have a vastly different spread, with standard deviations of 23, 5 and 8 km respectively. DVM can therefore be regarded as promoting coastal retention in relation to the passive surface particles, but one could equally conclude that it facilitates offshore transport in relation to all other passive scenarios. Similarly if the random-fixed or the diffused particles are taken as the base scenario, the results show that DVM forces particles to be more spatially confined. One could interpret this to mean

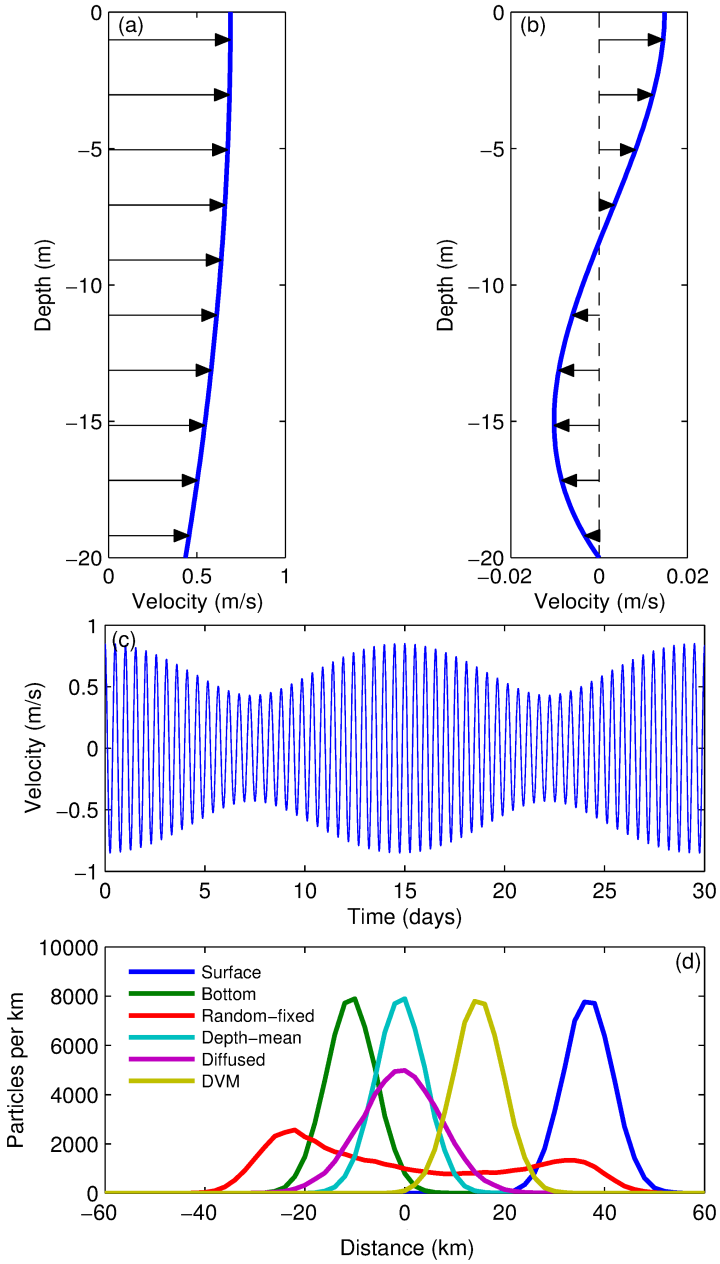

Figure 4.1: (a) Example vertical profile of tidal velocity u'. (b) Vertical profile of estuarine velocity $\overline{u}$. (c) Time series of depth-mean tidal velocity $\hat{u}$. (d) Final distribution of particles (binned into 2 km intervals).

that DVM reduces dispersal and connectivity, making it more likely for a population to be ecologically closed.

Each of these idealised simulations are now repeated in Liverpool Bay using a three-dimensional hydrodynamic model and an offline Lagrangian particle tracking model, in order to determine whether passive particle parametrisation remains important in a complex coastal environment.

4.3 Liverpool Bay

4.3.1 Study Region

Liverpool Bay is a shallow, hyper-tidal region of freshwater influence (ROFI) (Simpson, 1997), located in the eastern Irish Sea (figure 4.2). The region has a strong offshore salinity-controlled density gradient that drives a sheared residual circulation that rotates with depth (Heaps, 1972). The mean surface flow is directed offshore (northwards) and of the order of 0.04 m s^{-1}, and bottom flow is directed onshore (southwards) and is of a similar magnitude (figure 4.3). The tidal range can be as large as 10 m, and spring tidal currents are of the order of 0.75 m s^{-1} (Polton et al., 2011). Unlike in the idealised scenario of section 4.2, the rectilinear east-west tidal flow is approximately perpendicular to both the surface and bottom components of the local mean circulation. Despite the strong tidal mixing, numerical studies reveal that Liverpool Bay is somewhat retentive due to the onshore bottom flow, with a mean residence time of over 100 days (Phelps et al., 2013).

4.3.2 Methods

For this investigation we use POLCOMS (Proudman Oceanographic Laboratory Coastal Ocean Modelling System), a three-dimensional hydrodynamic model (Holt and James, 2001), using the Irish Sea set-up (figure 4.2) with approximately 1.8 km horizontal resolution and 32 vertical σ-coordinate layers. POLCOMS is forced by ECMWF meteorological data at the surface, tidal elevation and velocity at the open boundaries, and has lateral freshwa-

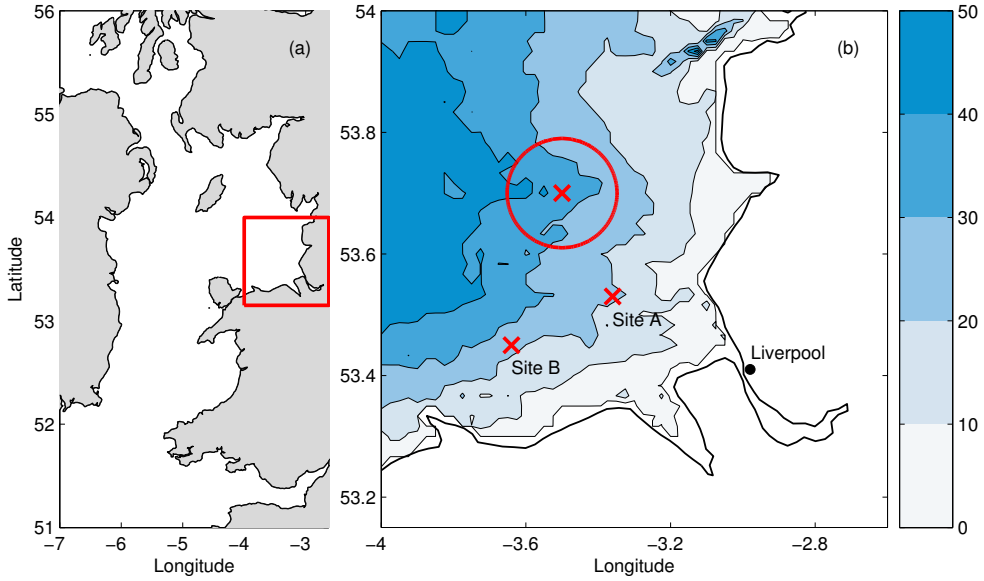

Figure 4.2: (a) Full domain of the hydrodynamic and particle tracking models, with Liverpool Bay highlighted in red. (b) Bathymetry (m) in Liverpool Bay with isobaths marked every 10 m. Particles are initialised uniformly at sea points within the red circle of 10 km radius centred upon the 3.5 ° W, 53.7 ° N. The location of the site A and site B permanent moorings are also shown.

ter input at the river locations. The $k-\epsilon$ turbulence closure scheme (Canuto et al., 2001) is selected for this study. For further information regarding the performance of the POLCOMS Irish Sea set-up in Liverpool Bay the reader is referred to Polton et al. (2011).

POLCOMS provides dynamical and physical data (sea surface elevation, and three dimensional fields of velocity and diffusivity) for an offline Lagrangian particle tracking model. The particle tracking model is described in detail in Phelps et al. (2015a), but briefly, the model uses bilinear interpolation of velocity and Runge-Kutta 4^{th} order integration for advection. Stochastic vertical diffusion is calculated by fitting a cubic smoothing spline to POLCOMS diffusivity output, and using the numerical scheme described by Visser (1997) and Ross and Sharples (2004) to ensure that the model sat-

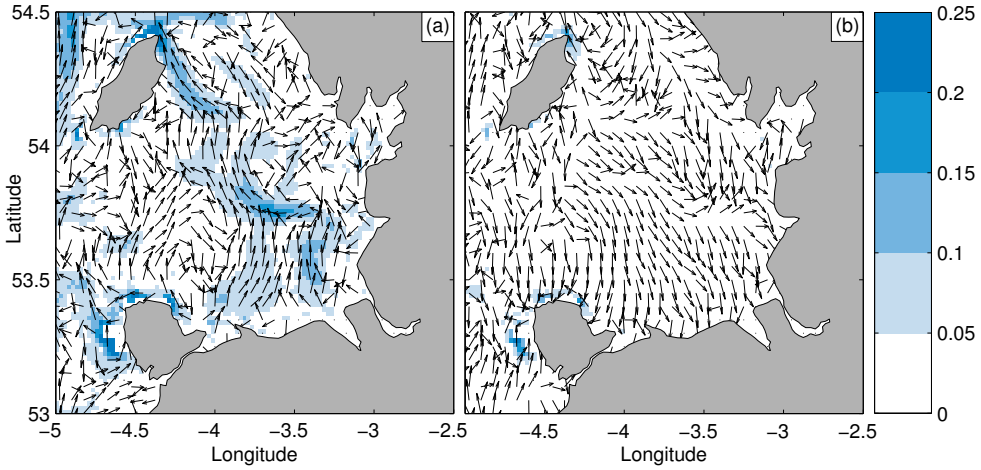

Figure 4.3: Mean circulation in Liverpool Bay and the eastern Irish Sea in June 2005 according to POLCOMS output. Velocity magnitude (m s^{-1}) is indicated by colour, velocity direction is indicated by arrows given at every third grid cell in both directions. (a) Surface flow. (b) Bottom flow.

isfies the well-mixed condition. Reflective boundaries are placed at the sea surface, bottom and lateral land boundaries.

Once again, five passive simulations are conducted (surface, bottom, random-fixed, depth-mean and diffused) followed by an active DVM simulation. Particle depths are identical to those described in section 4.2, except that maximum depth h is taken from the local bathymetry. Particles are initialised at every two seconds of a degree (longitude and latitude) within a circular area of radius 10 km in Liverpool Bay (figure 4.2), giving over 139,000 particles per simulation. All particles are initially released at a random time on the 1st of June 2005 and are advected for 30 days before settling.

4.3.3 Results

Model output data are presented here by outlining the dispersal direction and great-circle distances between the initial and final location of each particle. These results are depicted in figures 4.4, 4.5 and 4.6. Dispersal distances are

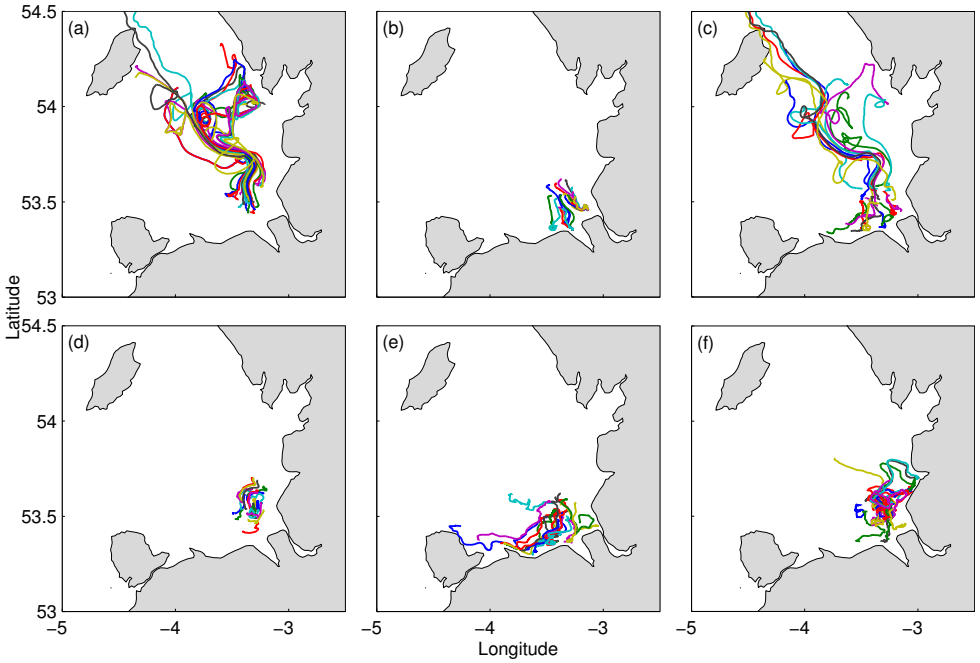

Figure 4.4: Random sample of 20 particle trajectories from each simulation. (a) surface; (b) bottom; (c) random-fixed; (d) depth-mean; (e) diffused; (f) DVM. Trajectories are passed through a moving average filter to remove semi-diurnal tidal advection (hence the apparent transport over land in panels a and c).

highly asymmetrical in most cases (figure 4.5), therefore median values are presented rather than means.

The surface particles were dispersed further than any other passive scenario, with a median dispersal distance of 79.9 km. Over 99.9 % of these particles were advected northwards by the mean surface flow. In contrast the median dispersal distance of all bottom particles was 33.8 km, and 90.5 % of particles were advected southwards. There was a clear dichotomy in the random-fixed scenario where dispersal was determined by particle depth. Particles that were trapped in the surface layer were advected offshore by the northward surface current, whereas particles fixed closer to the seabed were advected onshore by the southward bottom flow (figure 4.6). The overall

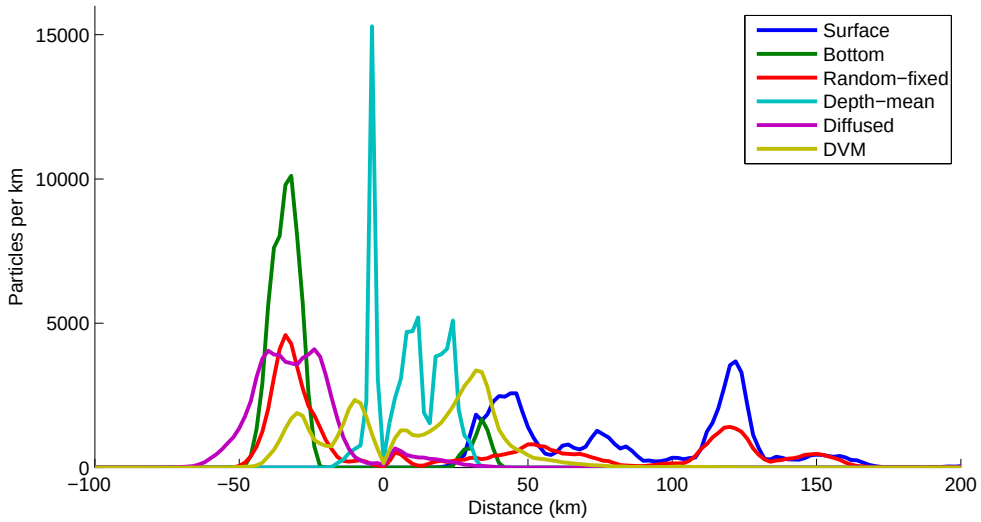

Figure 4.5: Distribution of dispersal distances for each model scenario. Particles are binned into 2 km intervals. Here negative distances indicate that the particle is dispersed south of its initial site.

median dispersal distance was 38.2 km, and the proportion of particles that were advected to the north and south were approximately equal (48.9 % and 51.1 % respectively).

In the depth-mean simulation, dispersal distances were considerably shorter than in any other scenario, with a median distance of 9.5 km. This is clearly due to the fact that the depth-averaged velocity is far weaker than either the surface or bottom components of the mean circulation. In total 66.8 % of these particles were advected north of their origin. The spread of dispersal distances was also far shorter than in previous simulations (figure 4.5). Indeed depth-mean dispersal distance has a standard deviation of 11.3 km, compared to the equivalent standard deviations of 40.0, 20.2 and 68.2 km for the surface, bottom and random-fixed scenarios respectively.

The most striking aspect of the diffused scenario results was the significant transport to the south west (figure 4.6). There are two separate physical processes in Liverpool Bay that could contribute to this westward transport. Firstly the combination of vertical diffusion and a vertically-sheared oscil-

lating current can introduce an effective horizontal diffusion parallel to the direction of the oscillatin flow due to a process referred to as shear dispersion (Bowden, 1965). In Liverpool Bay the tidal flow is almost entirely rectilinear, flowing east-west, therefore shear dispersion would lead to particle diffusion along the zonal axis. Secondly there is a small but significant zonal component of the residual flow in the mid-depths in Liverpool Bay. This component is spatially variable, flowing eastward at site A (eastern Liverpool Bay, figure 4.2) at velocities reaching approximately 1 cm s^{-1}, and westward at site B (western Liverpool Bay, figure 4.2) at a similar velocity, and this is captured by the POLCOMS model (see Polton et al., 2011, for further details). This zonal component of the mean velocity in Liverpool Bay would also affect the fixed-depth particles, however the shear dispersion mechanism would not. The median dispersal distance amongst vertically diffused particles was 31.4 km and 92.8 % of these particles were dispersed south of their initial site. Again dispersal distances are relatively homogeneous, with a standard deviation of only 16.3 km.

Finally, in the DVM simulation the majority of particles were advected northwards (62 %), with a median dispersal distance of 26.6 km. Once again it is possible to draw different conclusions about the influence of vertical migration upon larval dispersal in Liverpool Bay depending which passive particle parametrisation is chosen. If absolute dispersal distances are considered, one can conclude that vertical migration is conducive for local larval retention when compared to either surface, bottom, random-fixed or vertically diffused particles. Conversely if the depth-mean particles are taken as the base scenario, it is equally possible to conclude that vertical migration is not favourable for local larval retention. If dispersal direction is considered, it could be argued that vertical migration also hampers coastal retention in contrast to the bottom passive particles, which were predominantly advected southwards (onshore).

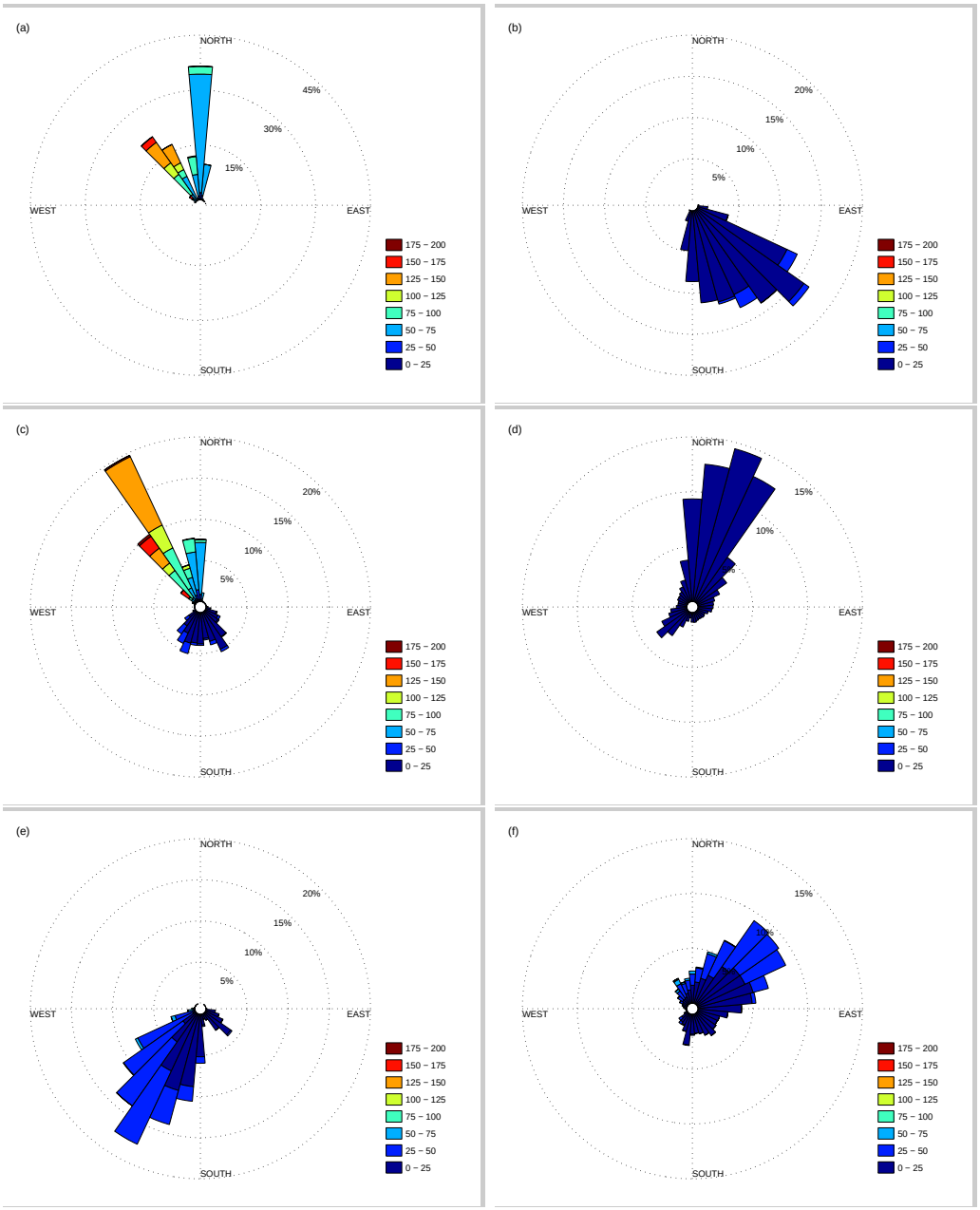

Figure 4.6: Frequency of dispersal distances in each direction according to model run. (a) Surface. (b) Bottom. (c) Random fixed. (d) Depth-mean. (e) Diffused. (f) Diel vertical migration.

4.4 Discussion

Passive particle models have largely been superseded by complex biophysical models that incorporate active behaviour, such as vertical migration and settlement cues, however numerous recent investigations utilise both passive particles and active particles with complex larval behaviour, and draw comparisons between the results to determine the effect that behaviour has upon dispersal. Although passive particles are frequently used in this manner, they are not parametrised consistently. This article highlights the fact that this lack of consistency becomes problematic when attempting to draw conclusions about larval behaviour, because different passive particle parametrisations can lead to directly opposing conclusions about the effect that larval behaviour has on transport. For example, vertical migration may promote local retention when compared to passive particles in the surface layer, but without contradiction it may appear detrimental to retention when compared to passive particles that are distributed throughout the water column.

The intention of this investigation was to illustrate the importance of an aspect of larval dispersal modelling that is regularly overlooked using idealised examples, however it certainly does not provide an exhaustive account of either passive particle parametrisations or larval behaviour. It is important to recognise that in reality larval swimming activity is highly complex and species dependent, and the swimming behaviour implemented in this model is certainly a major oversimplification, which does not represent any particular species. Many larger larvae are also capable of directed horizontal swimming at considerable velocities (Leis et al., 1996; Leis and Carson-Ewart, 1997; Fisher et al., 2005). Some larvae are also known to adapt their behaviour according to physical cues such as habitat availability or the presence of adults, and other factors such as mortality may affect dispersal patterns. These aspects of larval behaviour are neglected in this study, however they would certainly lead to greater variability in the results.

Liverpool Bay was chosen as the study region due to complex nature of the local circulation, with strong vertically sheared tidal currents, and a

highly variable density-driven mean flow. Souza and Lane (2013) used the POLCOMS online Lagrangian particle tracking model with a fine resolution ($\sim$ 180 m, 10 vertical σ-coordinates) set-up to investigate the fate of dredged sediment in Liverpool Bay, and showed that the density-driven residual circulation leads to onshore transport of sediments, that are ultimately advected into the Mersey estuary. As these suspended sediments are subject to a settling velocity, the results correspond most closely with the bottom passive particles in the current study, and the onshore transport of bottom particles is consistent in both investigations. Although it may initially appear that the high resolution Liverpool Bay set-up would be more appropriate for the current study, there is an important trade-off between resolution and model domain size. The resolution of the current study may not be sufficiently fine to resolve transport up the Mersey estuary, however the model domain size of Souza and Lane (2013) would not be sufficiently large enough to contain many of the surface and random-fixed particles over a thirty day PLD.

To conclude this investigation we make two closely related recommendations for future investigations that seek to draw comparisons between passive and active particles. Firstly one should carefully consider the most appropriate passive particle parametrisation, and this selection should be clearly stated in the methodology rather than loosely declaring that the particles are dispersed passively. Evidently there is no single parametrisation that is universally suitable. For example Phelps et al. (2015a) investigated the role of the western Irish Sea gyre on larval dispersal, and fixed passive particles at the depth of peak gyral flow (24 m) to permit direct comparisons with fixed-depth drifter observations, however this clearly would not be an appropriate default choice for the vast majority of modelling investigations. Secondly one should avoid vague decelarations such as "vertical migration enhances local retention", and instead offer more specific concrete conclusions, such as "local retention rates are greater amongst vertically migrating larvae than larvae that remain within the surface mixed layer".

Chapter 5

Larval Dispersal in the North Sea and Connectivity Between Offshore Installations

Abstract

Offshore oil and gas platforms often function as artificial reefs that benefit local marine biota, however they may also facilitate the spread of nonindigenous invasive species which threaten biodiversity. It is therefore imperative to determine whether such installations are connected via larval dispersal. This investigation uses an individual based model to assess larval dispersal and connectivity between artificial installations in the North Sea.

Approximately 5 % of all particles successfully settled upon an offshore installation, and connectivity occured over distances of the order of 100 km. Dispersal was found to be strongly dependent upon the vertical distribution of particles. On average particles trapped within the surface layer were advected 95 km over 30 days, whereas particles in the bottom layer were advected an average distance of 52 km over the same period, and had a slightly greater successful settlement rate. In terms of dispersal distance and settlement rates, vertically migrating particles fell between the surface and bottom scenarios, however vertically migrating particles settled upon a greater number of distinct installations. Averaged over the three scenarios,

particles settled upon 72 % of the installations in the southern North Sea, but only 40 % of the installations in the northern North Sea, confirming previous findings that connectivity is greater in the southern North Sea.

5.1 Introduction

Artificial installations in the marine environment such as oil and gas platforms and offshore wind turbines can serve as artificial reefs, providing additional habitat space for sessile marine invertebrates including mussels and barnacles (Svane and Petersen, 2001; Wilhelmsson and Malm, 2008; Langhamer et al., 2009; Boehlert and Gill, 2010). These installations may be highly beneficial to the local benthic marine assemblage, which in turn may attract pelagic organisms and potentially enhance fisheries. Although artificial reefs are widely regarded as an effective way of strengthening marine biodiversity, caution must be exercised because it is also possible for such structures to act as "stepping stones", enabling the spread of non-indigenous invasive species into new environments via larval dispersal (Glasby et al., 2007; Adams et al., 2014).

Invasive species have been identified as a significant threat to marine biodiversity (Carlton and Geller, 1993; Mack et al., 2000; Ruiz et al., 2000; Branch and Steffani, 2004), as they increase competition for finite resources, leading to changes in community structure and potentially local extinctions. Although the majority of successful invasions have been attributed to fouling upon the hulls of ships and planktonic organisms inhabiting ballast water (Ruiz et al., 2000), invasive species are generally able to thrive in a diverse range of environments, and they may be particularly well suited to settling upon certain artificial substrates (Glasby et al., 2007). It is therefore imperative that the role of artificial offshore installations upon connectivity is properly understood.

In this investigation we explore larval dispersal and connectivity between offshore stations in the North Sea listed in the OSPAR inventory of offshore installations (OSPAR Commission, 2013). Whilst these stations vary

in nature, the inventory predominantly consists of operational oil and gas platforms. After excluding stations that were either located either outside the model boundary, outside the region of interest (e.g. in the Irish Sea) or for which there was no available data on the location, a total of 1113 offshore installations remained (displayed in figure 5.1).

Biofouling has been recorded on a wide range of artificial installations within the North Sea and adjacent seas including offshore wind turbines (Degraer and Brabant, 2009) wave power foundations and buoys (Langhamer et al., 2009) and oil platforms (Forteath et al., 1982). Such installations are numerous in this marine region, and many lie within close proximity to one another, indeed 80 % of the 1113 installations investigated here (figure 5.1) are located within 5 km of another neighbouring station. Whilst larval dispersal distances vary greatly according behaviour, pelagic larval duration (PLD), local hydrodynamics and other factors, some species are capable of dispersing larvae 100 km and greater, therefore migration between the North Sea offshore installations is certainly a plausible prospect.

Thorpe (2012) investigated connectivity of oil and gas platforms in the North Sea by analysing tidal ellipses and streamlines in the mean flow field, and concluded that connectivity between these platforms was probable, but spatially variable. In the southern UK sector of the North Sea 60 % of offshore installations were found to be connected by tidal flows, whereas only 23 % were connected in the northern UK sector. The aim of the current study is to build upon the work of Thorpe (2012) by utilising a high-performance, three-dimensional Lagrangian particle tracking model with spatially and temporally variable velocity fields, resolving both tides and residual currents. Three contrasting vertical swimming behaviour parameterisations are also incorporated into the model in order to determine whether vertical swimming affects connectivity in this environment.

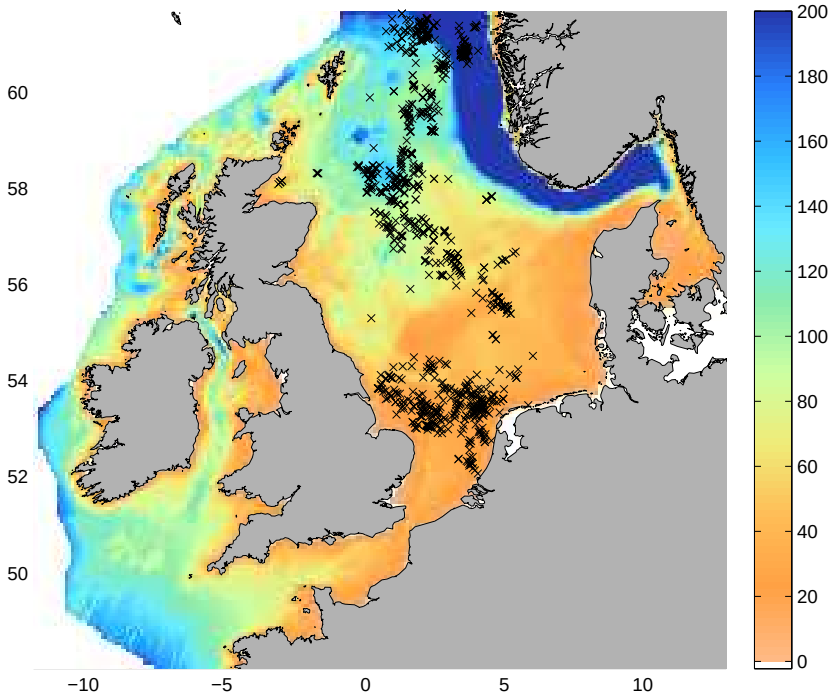

Figure 5.1: POLCOMS MRCS bathymetry (m, capped at 200 m to show greater detail in region of interest). White regions lie outside the model domain. Black crosses denote the 1113 locations from the OSPAR inventory of offshore installations that are considered in this investigation.

5.2 Methods

This investigation was conducted using the POLCOMS hydrodynamic model with the Medium Resolution Continental Shelf (MRCS) setup (described in Holt et al., 2005), with a horizontal grid resolution of approximately 7 km. Whilst the original MRCS setup used 20 s-coordinate vertical layers, the current study used 32 $\sigma-$coordinate vertical layers. This hydrodynamic model was used to provide sea surface elevation and three dimensional fields of velocity and diffusivity for an offline particle tracking model described by Phelps et al. (2015a).

POLCOMS output of sea surface elevation and velocity were read by the partcle tracking model every 300 s, and diffusivity was read every 600 s. This

POLCOMS output was then interpolated linearly in time to update the fields for every internal time step (advection time step of 60 s, vertical diffusion time step of 6 s). The particle tracking model uses Runge-Kutta 4^{th} order integration for particle advection and vertical diffusion is calculated using a stochastic numerical scheme (Visser, 1997; Ross and Sharples, 2004). Reflective boundaries at the sea surface, seabed and horizontal land boundaries prevent particles leaving the water column. Any particles that are advected outside the model domain through the open boundaries are removed from the system and are not included in the following analyses. Further technical details of the particle tracking model are found in Phelps et al. (2015a).

Particles were initially distributed at the 1113 locations shown in figure 5.1. Unfortunately there was no available data for the size and shape of each individual station, therefore each installation was assumed to take the form of a column with a 50 m by 50 m square cross section, extending from the seabed to the sea surface. Particles were initially distributed uniformly around the perimeter of each column, with 1000 particles per installation. Particles were each released at a random time on 1^{st} January 2002, and were subsequently advected for a PLD of 30 days, typical of many marine invertebrates and fish (Shanks, 2009). The POLCOMS model was run from 1^{st} January 2001, providing a full year model spin-up prior to particle introduction. Each particle was assumed to be capable of settling after 20 days in the plankton upon direct contact with any offshore installation. Any particle that had failed to find a suitable artificial substrate at the end of the 30 day PLD was removed from the system.

Three model setups were used, each with different larval behaviour parameterisations, and are henceforth referred to as the surface, bottom and diel vertical migration (DVM) setups. In the surface setup particles were initially distributed throughout the uppermost 10 m of the water column. After release these particles were subsequently subject to turbulent diffusion throughout their PLD, however they were retained in the surface waters by placing a reflective boundary condition at 10 m depth. Similarly bottom particles were initially distrbuted throughout the bottom 10 m, and a

reflective boundary condition was placed 10 m above the seabed to ensure particles were retained in the bottom waters. In the DVM scenario particles remained within the surface 10 m between midnight and 06.00, descended towards the seabed at a constant velocity of 3 mm s^{-1} between 06.00 and midday, remained within the bottom 10 m between midday and 18.00, and ascended towards the surface at a constant velocity of 3 mm s^{-1} between 18.00 and midnight. This vertical swimming strategy represents the most common form of DVM behaviour amongst planktonic organisms including marine larvae, referred to as nocturnal (or normal) DVM, whereby larvae inhabit the surface waters during the night and descend to deeper darker waters during the day.

5.3 Results

The mean circulation in the North Sea was generally anticlockwise. Whilst bottom flow was relatively weak, surface flow was considerably stronger, exceeding 0.1 m s^{-1} throughout much of the domain, and reaching 0.25 m s^{-1} in some coastal regions such as the Skagerrak (figure 5.2). Well established dynamic features such as the Dooley Current and the Norwegian Coastal Current (Svendsen et al., 1991) are easily identifiable in the mean flow. Further details about the physical and dynamical oceanography of the North Sea, and POLCOMS MRCS model verification can be found in Holt et al. (2005).

In order to present the results, particles were binned onto a 2° longitude by 1° latitude grid, stretching from 52° to 62° N. and −4° to 8° E (figure 5.3) according to their origin. Altogether 19.9 %, 3.9 % and 16.5 % of particles were advected beyond the model domain through an open boundary in the surface, bottom and DVM model set-ups respectively. All of these particles originated from the 6 most northern grid cells (from rows A and B in figure 5.3), and they all left the model through the northern boundary. Little can be said about the dispersal of these particles, and it is difficult to determine the likelihood of re-entry into the model domain, therefore these

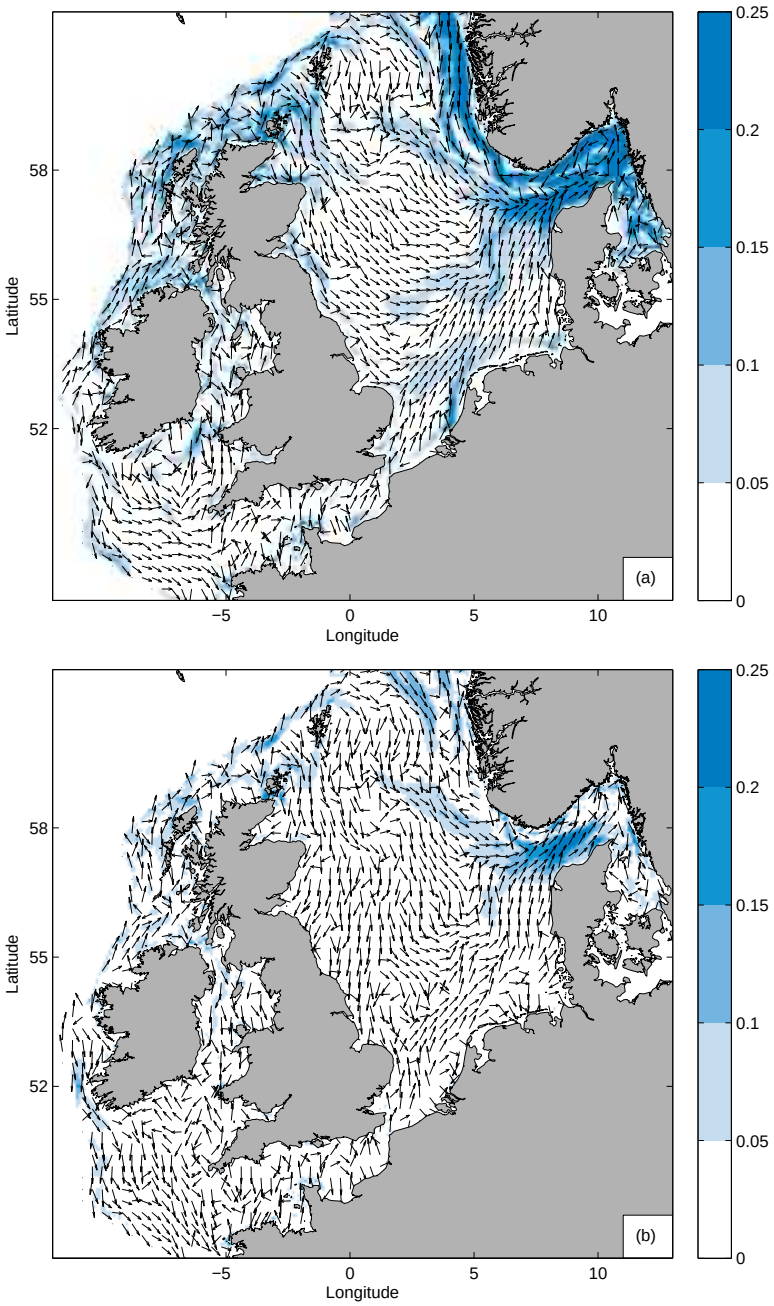

Figure 5.2: Monthly mean circulation in the North-east Atlantic continental shelf during January 2002 from the POLCOMS MRCS model output. Arrows (shown at every fourth grid cell in both directions) indicate direction, the colour axis indicates magnitude (m s^{-1}). (a) surface velocity. (b) bottom velocity.

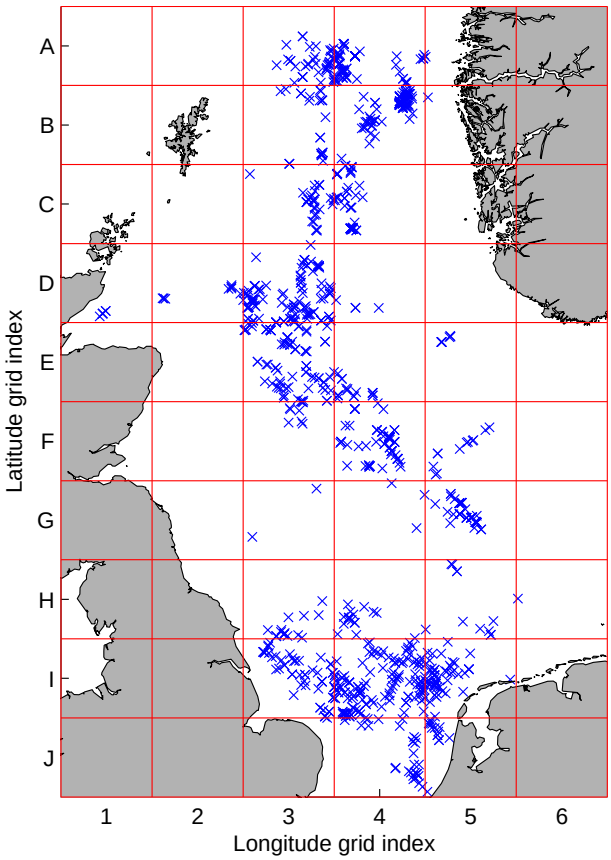

Figure 5.3: Location of the offshore installations shown on a 2° longitude by 1° latitude grid. Each particle is assigned to a particular grid cell (e.g. D3) according to its initial location. Note that this does not indicate the horizontal resolution of the model, this grid is only used for the presentation of results.

particles were removed prior to all further analyses, and the following dispersal distances and connectivity statistics are representative of the remaining particles. Dispersal distance distributions were highly asymmetrical (figure 5.4), therefore we present median rather than mean values.

In the surface scenario 3.9 % of the particles successfully settled upon an offshore installation. The results suggest that larval exchange may be possible over relatively large spatial scales (figure 5.5). Only 68 particles (< 0.01 %)

settled upon the same installation that they were released from, and only 27.9 % of particles that did settle remained within their original 2° longitude by 1° latitude grid cell. The median dispersal distance amongst particles that settled upon an installation was 77.9 km, and the greatest distance amongst settled particles was 221.2 km. The median dispersal distance of all particles (including those that did not settle, but excluding those that left the model boundaries) was 94.5 km, and the greatest distance was 400.9 km (figure 5.4). In total surface particles settled upon 46.5 % of all the offshore installations, however this value varied considerably according to location. In the southern North Sea (south of 55 ° N, grid rows H, I and J in figure 5.3) 63.3 % of stations were settled upon, whereas in the northern North Sea (north of 55 ° N) only 38.7 % were settled upon.

In the bottom scenario 5.5 % of the particles settled upon an offshore installation. This time 827 particles (0.07 %) settled upon the same installation that they were released from, and 65.7 % of particles that did settle remained within their original 2° longitude by 1° latitude grid cell (figure 5.6). Amongst particles that successfully settled the median dispersal distance was 32.0 km, and the maximum dispersal distance was 170.3 km. The median dispersal distance of all particles was 51.7 km, and the greatest distance was 341.2 km. Bottom particles settled upon 50.0 % of all offshore installations, including 38.9 % of the northern North Sea stations, and 74.2 % of the southern North Sea stations.

In the DVM scenario 4.1 % of the particles successfully settled. Only 209 particles (0.02 %) settled upon the same installation that they were released from, and 51.5 % of particles that did settle remained within their original 2° longitude by 1° latitude grid cell (figure 5.7). The median dispersal distance amongst particles that settled upon an installation was 47.2 km, and the greatest distance amongst settled particles was 198.4 km. The median dispersal distance of all particles was 66.5 km, and the greatest distance was 401.9 km. DVM particles settled upon 54.0 % of all offshore installations, including 43.1 % of the northern North Sea stations, and 77.9 % of the southern North Sea stations (figure 5.8).

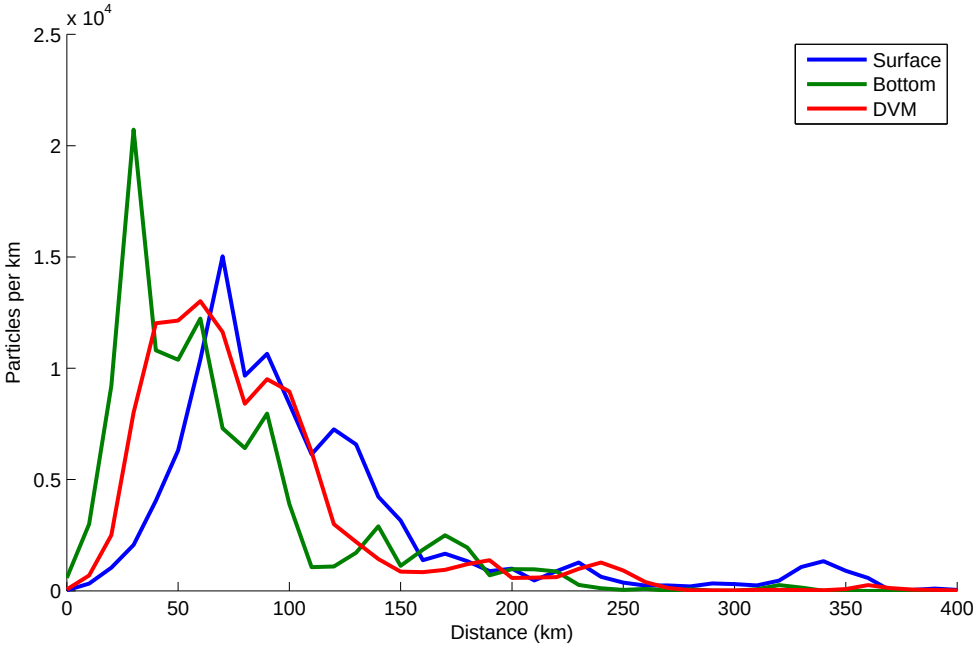

Figure 5.4: Distribution of dispersal distances for each model set-up (after excluding particles that were advected beyond the model boundaries). Particles were binned into 10 km intervals.

5.4 Discussion

This investigation found that larval exchange may be possible over scales of the order of 100 km, but connectivity between offshore installations is both spatially variable and strongly dependent upon the vertical distribution of larvae. Larvae that reside within the surface layer were typically advected around twice as far as those that remained in the bottom waters, however bottom dwelling larvae had a greater probability of settling upon an artificial installation. This was due to the fact that the mean surface circulation is considerably stronger than the flow at the seabed (figure 5.2). Both dispersal distances and settlement rates amongst vertically migrating larvae were found to be between the corresponding values for surface and bottom dwelling larvae.

Whilst successful settlement rates were greatest in the bottom scenario,

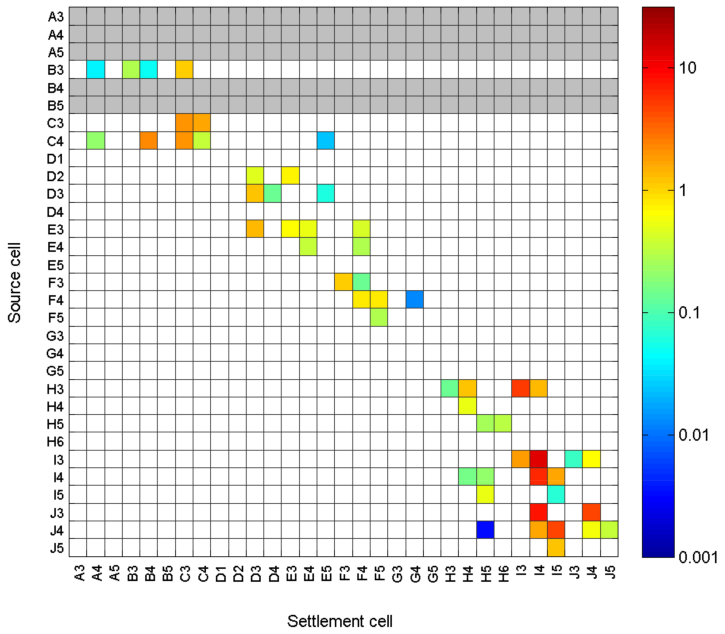

Figure 5.5: Connectivity matrix for the surface set-up, depicting the percentage of particles released from a particular 2° longitude by 1° latitude grid cell that settled upon an offshore installation in each grid cell. Cells that contain no offshore installations (e.g. B2) are omitted from this matrix. The connectivity percentage is denoted by the colour axis (on a log scale). White cells indicate a complete absence of connectivity. Rows of grey cells indicate that over 50 % of particles originating from these cells were advected beyond the model domain due to the close proximity to the northern boundary, therefore connectivity statistics could not be properly evaluated.

vertically migrating particles settled upon the greatest proportion of distinct offshore installations. This fact suggests that, at least in the North Sea, vertically migrating larvae may be more successful biological invaders than larvae that remain fixed within a particular layer.

Averaged accross the three scenarios, particles settled upon approximately 72 % of the installations south of 55° N, but only 40 % of installations north of 55° N. These results therefore appear to confirm the conclusion of Thorpe (2012) that connectivity is greater between offshore installations in

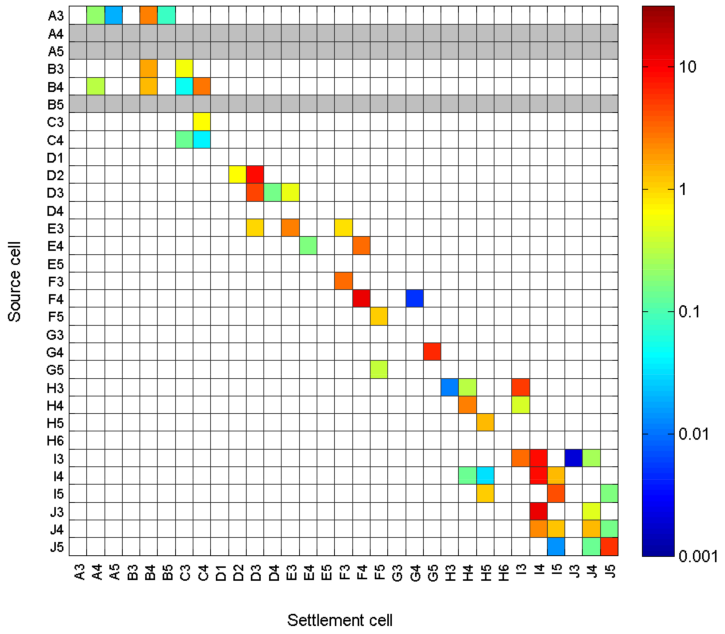

Figure 5.6: As figure 5.5 but for the bottom set-up.

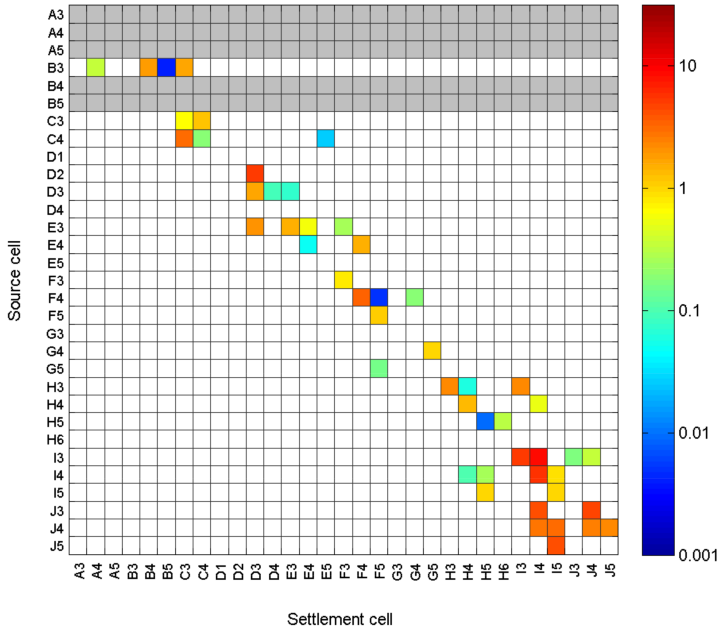

Figure 5.7: As figure 5.5 but for the DVM set-up.

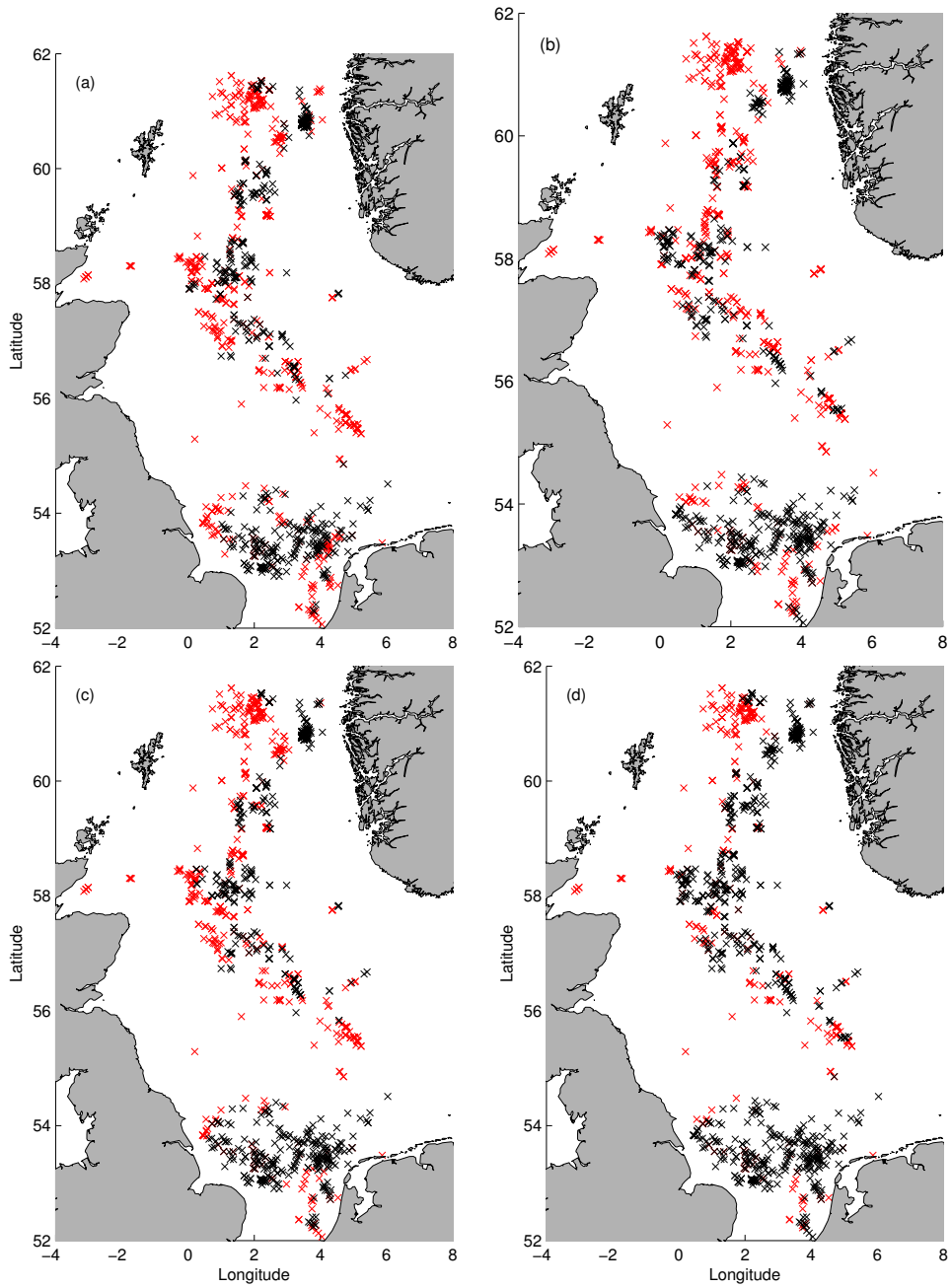

Figure 5.8: Offshore installations that were settled upon are depicted by black crosses, all others are represented by red crosses. (a): Surface particles, (b): Bottom particles, (c): DVM particles, (d): All particles (union of all three setups).

the southern North Sea than those in the northern North Sea. Furthermore not a single particle released from the northern North Sea successfully settled with the southern North Sea or vice versa (see figures 5.6 to 5.7, A to G corresponds to the northern North Sea, H to J corresponds to the southern North Sea). This suggests that, at least for species with a 30 day PLD, the artificial offshore installations of the northern North Sea are not biologically connected to those of the southern North Sea via larval exchange.

It should be highlighted that this study only considers dispersal of larvae with a PLD of 30 days. Whilst this duration is a perfectly reasonable starting point, PLDs amongst marine invertebrates can range from less than a day to several months (Shanks, 2009), therefore a value of 30 days would not be a realistic estimate for many species. This PLD selection will almost certainly affect dispersal, and longer PLDs are generally associated with greater dispersal distances (Shanks et al., 2003). In the North Sea one would anticipate an increase in PLD to lead to greater connectivity between distant offshore installations. Further work should aim to determine how larval dispersal and connectivity are affected by PLD in the North Sea.

Chapter 6

Summary

This thesis presents several shelf sea modelling investigations that cover a wide range of topics including hydrodynamic transport timescales, larval dispersal in seasonal gyres and biological connectivity between artificial offshore installations. Each study demonstrates that high performance numerical models are invaluable tools for shelf sea oceanography research. Although the diversity of this material makes it difficult to consolidate the results of the distinct investigations, some common outcomes did emerge. The primary results of each chapter are now briefly revisited before discussing general conclusions.

Chapter 2 utilised hydrodynamic transport timescale theory developed by Delhez et al. (1999); Deleersnijder et al. (2001); Delhez and Deleersnijder (2002) and others to assess age, residence time and flushing time in Liverpool Bay. Although concrete timescales were successfully deduced, the simulations demonstrated the complexity of the subject, and it is incorrect to assume that any significant volume of seawater will have a uniform age, or will be advected offshore at a uniform rate. The residence time of 103 days and the age distribution depicted in figure 2.6 are potentially misleading if taken in isolation.

Tracers were strongly mixed throughout Liverpool Bay due to a combination of the strong turbulent mixing, vertically sheared velocity field and multiple freshwater sources, therefore mean age and residence time contin-

ued to increase for several years after the initial tracer input. It was necessary to extend the tracer input duration in order to ensure that the age and residence time had stabilised, however this requirement does imply that these timescales are not appropriate for all purposes. For example, nutrient concentrations are partially depleted during spring and summer every year (Greenwood et al., 2011), therefore tracer masses that are multiple years old may not be relevant if one is concerned nutrient enrichment. Accurate calculation of the age of nutrients would require the use of an ecosystem model, and this is beyond the scope of this study. The age distribution derived here would be more suitable for assessing more persistant dissolved pollutants. The ability to estimate age from salinity is an exciting development as age is not directly observable, however equation 2.22 should be used with care, as it describes the long-term mean age rather than short-term transit times.

Chapter 3 examined the hypothesis of Hill et al. (1996) that shelf sea gyres facilitate local retention of planktonic larvae using an individual based model. Some limited evidence was found to support the gyre retention hypothesis provided that the larvae remain fixed at the depth of peak gyral flow, however this assumption is unrealistic, and when larval behaviour was introduced the gyre appeared to inhibit local retention. This shows that larval dispersal cannot be reliably deduced from passive drifting buoys in vertically sheared currents. Another key development in this investigation was the use of a temperature-dependent PLD. Using temperature relations derived from larval culture studies it was shown that PLD can vary significantly within a single local population according to hatching time and location.

In chapter 4 the focus returned to Liverpool Bay. The primary purpose of this study was to highlight the fact that passive particles are not defined consistently, and different parameterisations can lead to directly opposing conclusions about the influence of larval behaviour. The author first noted this problem whilst attempting to contrast the conclusion of chapter 3, i.e. that vertical migration leads to a reduction in local retention rates in shelf sea gyres, with the conflicting conclusion of Emsley et al. (2005). As the two studies use different passive baseline scenarios, it is entirely possible that

both contrasting sets of findings are correct, without contradiction. Such ambiguity would be rather unhelpful for anyone attempting to utilise the research to make marine spatial planning decisions. It is therefore argued that the passive particle parameterisation should be carefully considered for any investigation, and it should be explicitly declared.

The original intention was to build upon this work by simulating larval dispersal from the local rivers, and to combine this with the timescale analysis in chapter 2 to determine whether larval dispersal patterns could be predicted by the mean age distribution. For example, would larvae with a PLD of 30 days settle in the region with an equivalent mean age of 30 days? There were however two major obstacles to this approach. Firstly, many particles were retained along the reflective coastal boundary, therefore some of the scenarios were virtually indistinguishable from one another. This coastal retention is realistic as estuaries can be sinks rather than sources of material. Secondly, and more importantly, the tracer mixing issue identified previously meant that for most sensible PLD values, the mass-weighted mean age exceeded the PLD everywhere. This demonstrates that Eulerian tracers are highly unsuitable for investigating larval dispersal, and a Lagrangian formulation of age and residence time would be far more relevant. An Eulerian approach may be appropriate in a less turbulent environment without a strong vertical shear, where age increases linearly with distance from a single source, and doesn't continue to increase for several years. If this technique was successful it would permit the creation of a single map that could simultaneously depict possible settlement locations for any given PLD, however this is arguably highly optimistic as it would still neglect larval behaviour.

Finally chapter 5 modelled larval dispersal between artificial offshore installations in the North Sea. Typically around 5 % of all simulated particles successfully reached an offshore installation, and as many as 63 % of the distinct installations were settled upon. These results suggest that larval migration between these artificial sites may be prevalent. Once again the results were strongly dependent upon vertical swimming behaviour; surface dwelling larvae will typically be advected twice as far as deep water larvae,

but have lower settlement rates, whilst vertically migrating larvae settled upon the highest proportion of distinct nodes. The study also confirmed previous findings (Thorpe, 2012) that connectivity between sites is significantly greater in the southern North Sea than in the northern North Sea, and found that the distinct regions were not connected via larval exchange over a 60 day PLD.

Overall this thesis demonstrates that whilst the concept of larval dispersal modelling is relatively straightforward in theory, results are highly sensitive to an overwhelming array of biological (vertical swimming behaviour, PLD, habitat preferences, mortality, settlement cues), physical (residual circulation, shear dispersion, temperature) and numerical (turbulence closure model, stochastic diffusion scheme, advection scheme, model resolution, time step) factors.

Numerous independent investigations have shown that active larval behaviour can have a significant influence upon dispersal (e.g. Vikebo et al., 2007), and this fact has been repeatedly verified throughout this thesis. One of the most important conclusions that can be derived from this work is that not only does larval behaviour alter dispersal, but the same behaviour pattern can affect dispersal in completely different ways depending upon the local dynamical regime. Indeed in the western Irish Sea local retention rates were lower, and dispersal distances were greater amongst vertically migrating larvae than fixed depth larvae. Meanwhile approximately 100 km away in the eastern Irish Sea the opposite relationship was found, with greater retention rates and shorter dispersal distances amongst vertically migrating larvae. Previous studies have suggested that larval behaviour will tend to minimise dispersal and promote local recruitment (e.g. Paris and Cowen, 2004), however there are multiple evolutionary drivers behind each aspect of behaviour, and the tendency of DVM to boost recruitment is clearly not universal.

Shanks et al. (2003) and Shanks (2009) report that dispersal distance is generally positively correlated with PLD, although both studies are careful to stress that there are many exceptions to this rule. This thesis also contains

several notable examples that go against this trend. For example the fixed-depth particles released from the eastern Irish Sea in chapter 3 were advected a median distance of 34 km over a 60 day PLD, whereas the surface particles released in the North Sea in chapter 5 were advected a median dispersal distance of 78 km over a 30 day PLD, i.e. more than double the distance despite half the PLD.

One aspect of larval dispersal modelling that has been a considerable drawback throughout this research is the fact that reports on larval behaviour are overwhelmingly qualitative rather than quantitative. Detailed descriptions of behaviour are highly valuable and interesting from an ecological perspective, however they can be difficult to utilise in a numerical model unless accompanied by reliable quantitative data. This was a significant hindrance when attempting to simulate *N. norvegicus* larval behaviour in chapter 3. Although *N. norvegicus* larvae are known to migrate vertically, sources of information are scarce, and little is known about vertical swimming speeds for example. It was therefore necessary to manipulate parameters to create particle density profiles that resembled those in a single field investigation (Hillis, 1974). In the vast majority of situations it is far more practical to investigate larval dispersal in a more general context, simulating common behaviour patterns such as diel vertical migration as in chapters 4 and 5, rather than focusing upon a particular species. Despite the heavy reliance upon limited biological data, the current work demonstrates that larval dispersal studies remain highly valuable, and with a little care they may be used to provide rigorous solutions to important research questions in the field of marine ecology.

This thesis now concludes with one final numerical investigation into the effect of CO_2 leakages at potential carbon sequestration sites upon the marine carbonate system in the North Sea. Whilst this is clearly a transition from larval dispersal, many of the modelling techniques and analyses will be familiar from the preceding studies.

Appendix A

Modelling Large-Scale CO_2 Leakages in the North Sea

This appendix is based upon Phelps, J. J. C., Blackford, J. C., Holt, J. T. and Polton, J. A. Modelling Large-Scale CO2 Leakages in the North Sea. *International Journal of Greenhouse Gas Control*, 2015, in press. doi: 10.1016/j.ijggc.2014.10.013

Abstract

A three dimensional hydrodynamic model with a coupled carbonate speciation sub-model is used to simulate large additions of CO_2 into the North Sea, representing leakages at potential carbon sequestration sites. A range of leakage scenarios are conducted at two distinct release sites, allowing an analysis of the seasonal, inter-annual and spatial variability of impacts to the marine ecosystem.

Seasonally stratified regions are shown to be more vulnerable to CO_2 release during the summer as the added CO_2 remains trapped beneath the thermocline, preventing outgasing to the atmosphere. On average, CO_2 injected into the northern North Sea is shown to reside within the water column twice as long as an equivalent addition in the southern North Sea before reaching the atmosphere.

Short-term leakages of $5,000$ tonnes CO_2 over a single day result in substantial acidification at the release sites (up to -1.92 pH units), with significant perturbations (> 0.1 pH units) generally confined to a 10 km radius. Long-term CO_2 leakages sustained for a year may result in extensive plumes of acidified seawater, carried by major advective pathways. Whilst such scenarios could be harmful to marine biota over confined spatial scales, continued unmitigated CO_2 emissions from fossil fuels are predicted to result in greater and more long-lived perturbations to the carbonate system over the next few decades.

A.1 Introduction

Carbon dioxide capture and storage (CCS) provides the only methodology able to transform fossil fuel based power generation (and some other industrial processes) to relatively low carbon emissions, consistent with climate change mitigation. However, leakage from storage is possible and it is necessary to understand the outcome of a range of leakage scenarios, to enable both efficient monitoring and to understand the nature of environmental impact that could occur.

With little evidence to draw on, leakage scenarios are somewhat hypothetical, ranging from leakage via abandoned boreholes, leakage through fractures or seismic chimneys and finally catastrophic blowouts. The leakage rate for these scenarios can be estimated as 1, $100 - 1,000$ and $10,000$ tonnes of CO_2 per day (IEA GHG, 2008), although there is much debate, as yet unpublished, regarding the geological mechanisms that would allow the high end-scenarios. A further set of scenarios can be based on failure of pipeline transport and can be more accurately estimated from existent flow capacities (for example 1 Mt/year or 2740 t/day at Sleipner (Statoil, 2013)). Although regulations for CCS pipelines are not finalised, it is industry standard for the oil and gas industry for pipelines to include emergency shutdown valves which can close a pipeline instantaneously once a critical threshold of pressure is reached (National Research Council, 1994). Once shutdown has occurred

rapid depressurisation will occur, depending on the size of the leakage, thus significant leakage can be presumed to be a short term event of the order of a day. Within this work we do not address the likelihood of leakage, except to make the broad statement that effective monitoring and site operation should render the high end reservoir leakage scenarios highly unlikely to occur.

Given the spatial and temporal scales of impact, no one model system is capable of effectively addressing all possible scenarios; the low-end scenarios result in metre scale impacts (Dewar et al., 2013), whilst the higher end scenarios result in kilometre scale impacts (Blackford et al., 2008). In this paper we investigate the high-end leakage scenarios, with a state of the art three dimensional shelf hydrodynamic model POLCOMS (Holt and James, 2001) coupled with a model of CO_2 speciation in seawater (Blackford and Gilbert, 2007). This allows the assessment of CO_2 plume dispersion within a realistic simulation of the mixing processes that operate in the region. Whilst similar to previously published simulations (Blackford et al., 2008) this work includes improvements to the parameterisation of alkalinity (Artioli et al., 2012), includes density effects associated with high concentrations of CO_2 (Song et al., 2002), has improved assumptions regarding the initial shape of the gaseous CO_2 plume and most importantly provides a finer model resolution, such that the length scales of model and impact are more consistent. The leakage scenarios in the two studies also differ, and the current investigation explores inter-annual variability.

Addressing these high end, arguably highly unlikely, scenarios may be seen as unnecessary or alarmist. It is however important to understand the absolute maximum limits on impact that might arise and to underline the need for good operational practice and monitoring. It is also important to understand whether such events are readily detectable.

A.2 Methods

A.2.1 Leakage Sites Selection

Two locations in the North Sea were selected for the simulated release of CO_2, hereby referred to as the north site (57.75 N, 1.0 E) and the south site (54.0 N, 1.0 E), displayed in figure A.1. Both of these locations correspond to potential sites of carbon sequestration but differ markedly in the hydrophysical properties. The north site corresponds to the approximate location of the Forties oil field and is characteristic of the relatively deep northern North Sea with a depth of 98 metres, whilst the south site represents the approximate location of the Viking group of oil fields and is more typical of the shallow southern North Sea with a depth of 43 metres. These locations also correspond with earlier work (Blackford et al., 2008) but with improved estimates of bathymetry.

Both stations experience strong macro-tidal flow, with spring tidal velocities reaching approximately 0.5 m/s and 0.85 m/s at the north and south site respectively. Mean residual circulation at the north site is dominated by the Dooley Current, a broad semi-permanent barotropic current that flows eastwards, following the meandering 100 metre isobath (Svendsen et al., 1991; Holt and Proctor, 2008). Although the Dooley Current reaches speeds of 0.3 m/s, the north site is some distance from these peak flows, and bottom velocities are somewhat weaker. POLCOMS model output suggests that there is a considerable degree of spatial variability to the mean circulation at the south site, and the mean flow is an order of magnitude weaker than the tidal currents. The mean residual circulation in the North Sea is displayed in figure A.2.

Stratification in the North Sea is predominantly controlled by temperature, with the exception of the Norwegian Trench and the southern coastal regions near large continental rivers, where freshwater inputs result in salinity stratification (Holt and Proctor, 2008). Seasonal surface heat fluxes lead to strong stratification in the northern North Sea during the summer, with surface to bottom temperature differences exceeding 10 °C, whilst the shallower

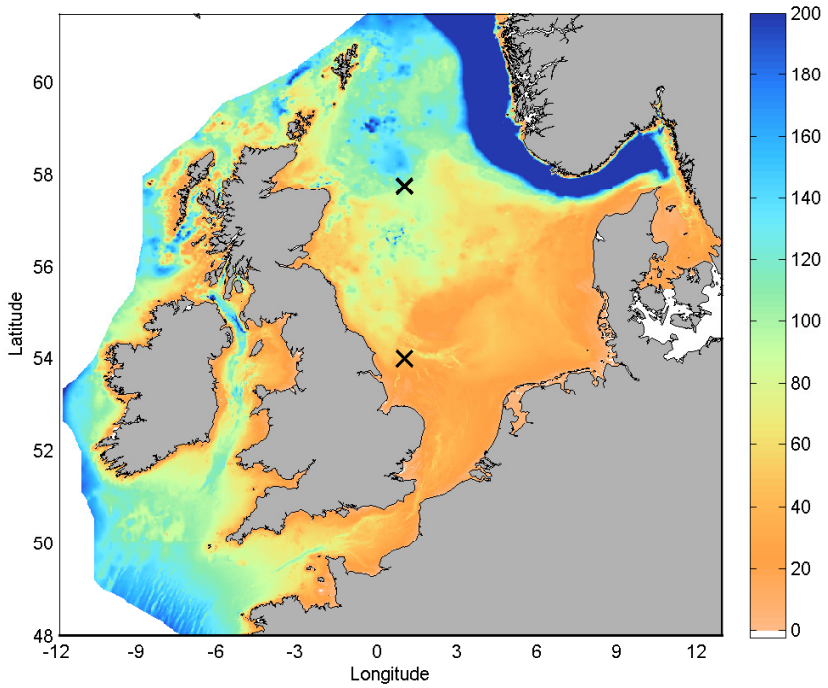

Figure A.1: (a) Bathymetry (m) in the POLCOMS HRCS model domain. The colour axis is capped at 200 m to show greater detail in the region of interest. CO_2 leakage sites are denoted by black crosses.

waters further south remain vertically mixed throughout the year (figure A.3). The vertical temperature structure at the two sites investigated here broadly reflect this pattern, surface to bottom temperature differences at the north site reach 8.7 °C, although the south site actually lies in a transitional region and does experience some weak stratification for short periods of time (figure A.4). For a more thorough account of the physical oceanography of the North Sea the reader is referred to Svendsen et al. (1991).

A.2.2 Model Description

The hydrodynamic component of this modelling study is provided by POLCOMS and is fully described in Holt and James (2001) and Holt and Proctor (2008). POLCOMS is a three dimensional hydrodynamic model formulated

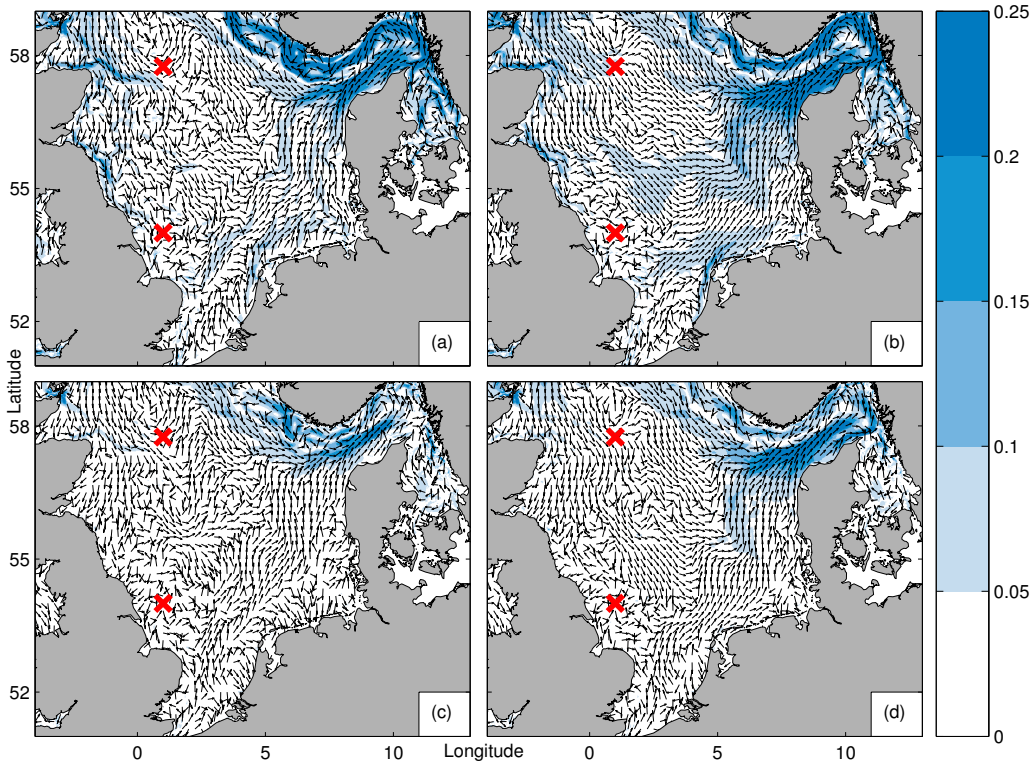

Figure A.2: Mean velocity (m/s) in the North Sea according to POLCOMS output. Black arrows (shown every 144$^{\text{th}}$ grid cell) depict direction, the colour corresponds to the magnitude. (a) summer surface; (b) winter surface; (c) summer bottom; (d) winter bottom. Summer plots give the average velocity between June and August 1999. Winter plots give the average between December 1999 and February 2000. Surface plots show the average between the surface and 10 m depth. Bottom plots show the average velocity between 40 m depth and the sea bed (or bottom grid cell where depths are shallower than 40 m). The colour axis is capped at 0.25 m/s to show greater detail in the region of interest.

upon a staggered Arakawa B-grid (Arakawa and Lamb, 1977) in the horizontal, and terrain following σ-coordinates in the vertical. The model uses the piecewise parabolic method (PPM) advection scheme (Colella and Woodward, 1984), favoured for being highly non-diffusive (James, 1996). The combination of the B-grid and the advection scheme ensure POLCOMS is

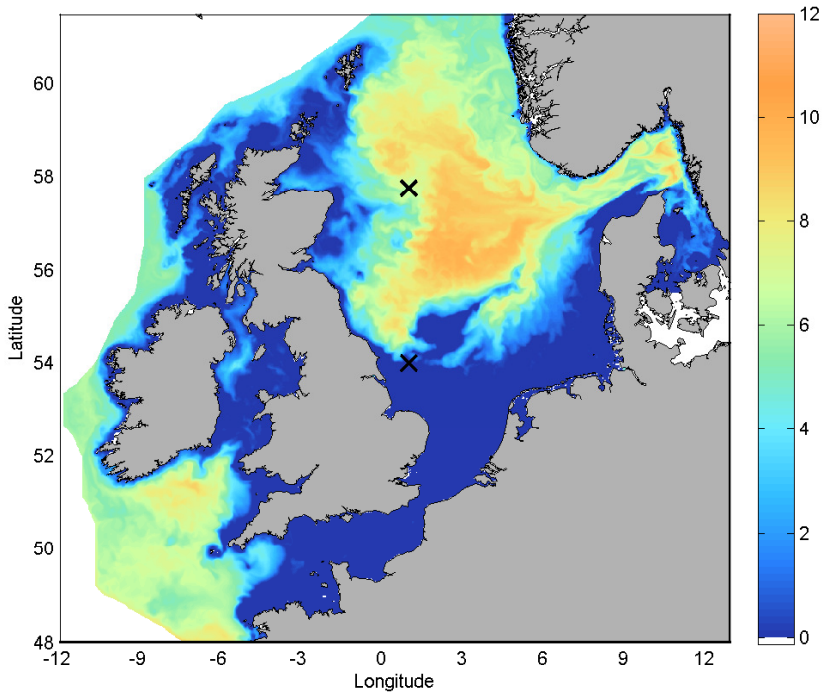

Figure A.3: (b) Surface temperature minus bottom temperature (C) on 1st September 1999 according to POLCOMS output. CO_2 leakage sites are denoted by black crosses.

well suited to maintaining sharp temperature and salinity gradients that are abundant in shelf seas. The High Resolution Continental Shelf (HRCS) setup with 32 vertical σ-coordinate layers and approximately 1.8 km horizontal resolution is used for all model simulations. This has a finer horizontal resolution than the MRCS setup (approximately 7 km horizontal resolution, 18 vertical layers) used in a previous study (Blackford et al., 2008), and is known to have some improvements, particularly in the estimation of currents near fronts and the flow entering the Skagerrak (Holt and Proctor, 2008). POLCOMS is coupled to GOTM (Umlauf and Burchard, 2003) to calculate the turbulent kinetic energy with the k-ϵ turbulence closure scheme, which is then used to derive eddy viscosity and diffusivity using the stability relations of Canuto et al. (2001).

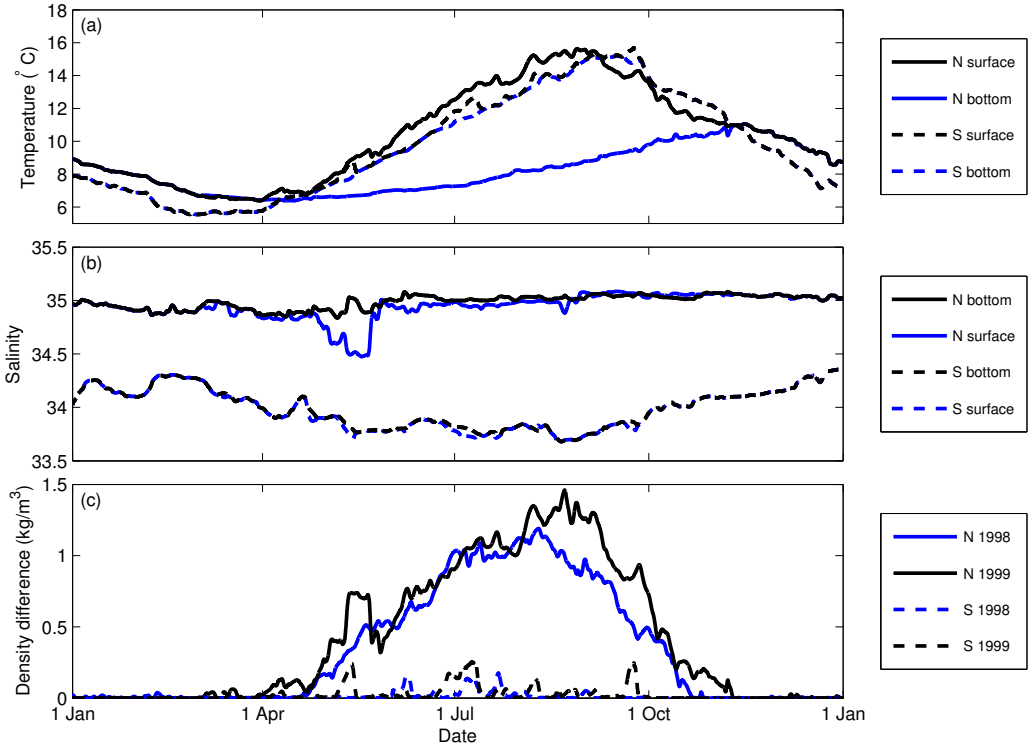

Figure A.4: Time series data at the two CO_2 release sites (N, north site; S, south site) from POLCOMS model output. (a): Surface and bottom temperature in 1999. (b): Surface and bottom salinity in 1999. (c): Comparison of stratification (bottom density minus surface density) in 1998 and 1999.

The CO_2 or carbonate system is simulated using an iterative speciation model based on HALTAFALL (Ingri et al., 1967), as applied in Blackford and Gilbert (2007); Blackford et al. (2008) and Artioli et al. (2012) with dissolved inorganic carbon (DIC) and total alkalinity (TA) as master variables. Coupled with information of the primary physical properties (temperature, salinity and pressure) delivered by POLCOMS the model derives the carbonate system parameters of interest, in particular pH and the saturation states of calcite (Ω_{cal}) and aragonite (Ω_{arg}), which are used here as metrics of impact.

For the purpose of this study DIC was divided into two components,

representing the background DIC (DIC_B) and the additional DIC as a result of a geological carbon storage leak (DIC_L). For clarity the sum of these two components will henceforth be referred to as the total DIC (DIC_T),

$$DIC_T = DIC_B + DIC_L. \tag{A.1}$$

Both DIC_B and DIC_L were treated as three dimensional scalar fields, advected and diffused within the hydrodynamic model. By separating DIC_T into two components and omitting the use of a coupled ecosystem model (such as ERSEM) the complexity of the model is reduced significantly, however this approach means that any nonlinear biological feedback caused by the injection of additional DIC_L into the ecosystem is neglected. As the North Sea marine ecosystem is not carbon limited, these nonlinear feedbacks are believed to be minimal.

Background DIC_B is initialised to zero and relaxed to monthly mean DIC data generated by the coupled hydrodynamic-ecosystem model POLCOMS-ERSEM (AMM setup) (Wakelin et al., 2012), interpolated in space onto the HRCS grid and linearly in time to each model time step, with a relaxation period of one week. This provides a reasonable proxy for the normal seasonal and spatial dynamics of DIC_B.

The small-scale dynamics of CO_2 bubble plumes are highly complex and research into the subject is ongoing. In a recent small-scale two-fluid modelling investigation into the impact of CO_2 injection in the North Sea, Dewar et al. (2013) found that CO_2 bubbles have a fast rise velocity but also a quick dissolution rate, and whilst plume height was influenced by a number of factors including tidal flow, temperature and leakage rate, all injected CO_2 dissolved within a few metres. Furthermore in a controlled CO_2 leakage experiment in a coastal loch, the QICS research consortium (QICS, 2012) observed that the majority of CO_2 bubbles dissolved in the first 10 metres of upward flow. Consequently, all DICL source terms are injected directly into to the bottom layer of a single grid cell at the two leakage sites, with various leakage scenarios as described in section A.2.3. The air-sea flux of leakage DIC_L is calculated using the scheme of (Nightingale et al., 2000) by

subtracting the background CO_2 flux (using pCO2 derived from DIC_B) from the total CO_2 flux (using pCO_2 derived from DIC_T), as air-sea fluxes of DIC_B are already accounted for in the background data.

Haugan and Drange (1992) first brought attention to the effect of dissolved CO_2 on seawater density and highlighted the fact that in extreme cases injections of dissolved CO_2 could result in sufficiently large density modifications to drive a density current. More recently there have been numerous attempts to determine the equation of state for a CO_2 solution (Ohsumi et al., 1992; Song et al., 2002; Duan and Zhang, 2006). For this research the following density modification of Song et al. (2002) is used,

$$\Delta\rho = 275.47\chi, \tag{A.2}$$

where χ represents the mass fraction of CO_2 in the solution,

$$\chi = \frac{\rho_{CO_2}}{\rho_s + \rho_{CO_2}}. \tag{A.3}$$

Here ρ_{CO_2} is taken to be the density of the freshly dissolved CO_2 due to the simulated leak and ρ_s represents the density of seawater in the absence of the added CO_2. In the model, CO_2 is a diagnostic variable that is derived from prognostic variables (DIC, TA, etc.), so the concentration of CO_2 attributed to the leakage DIC_L is assumed to be equal to the following term

$$[\Delta CO_2] = [CO_2]|_{\mathrm{DIC}_T} - [CO_2]|_{\mathrm{DIC}_B}\ (\mathrm{mmolm}^{-3}). \tag{A.4}$$

In extremely large CO_2 concentrations the density effect may be significant ($\Delta\rho \approx 0.1$ kg/m^3 at CO_2 concentrations of the order of 10 mol/m^3), however changes to density are likely to be minimal outside the vicinity of the source at the leakage rates considered in this study.

TA is considered to be the sum of a diagnostic component and a prognostic component following an improved approach for calculating TA in shelf seas (Artioli et al., 2012).

$$TA = TA_{dia} + TA_{pro}. \tag{A.5}$$

TA_{dia} is calculated from the linear relation between TA and salinity S in the Atlantic Ocean (Millero et al., 1998),

$$TA_{dia} = 51.24S + 520.1, \tag{A.6}$$

whilst TA_{pro} is treated as a conservative scalar, advected and diffused in POLCOMS with source terms at the riverine grid cells (representing the contribution of riverine TA). For further details of this approach and for the derivation of riverine TA concentrations see Artioli et al. (2012), although note that the sink terms representing the biochemical contribution to TApro are not included in the present study due to the lack of a coupled ecosystem model.

The carbonate model uses the OCMIP recommendations for the set of constants, i.e. using the Weiss (1974) formulation of Henry's constant for CO_2, the dissociation constants for carbonic acid defined by Millero (1995) using the refit of Mehrbach et al. (1973), and the borate dissociation constant from Millero (1995) using data from Dickson (1990).

A.2.3 Leakage Scenarios

A series of short-term and long-term leakage scenarios were devised to investigate the range of potential impacts of geological CO_2 release in the North Sea. During the short-term model runs CO_2 is released at the two leakage sites at a constant rate of $5,000$ t CO_2 per day for one day before being "switched of". The recovery of the carbonate system is monitored for the remainder of the month. This scenario represents a quick release of CO_2 that is quickly identified and promptly repaired, such as a pipeline failure. The release rate used here is approximately twice the CO_2 pipeline capacity at the currently operating Sleipner plant (Statoil, 2013).

During the long-term simulations, CO_2 is injected continuously for a full year, representing a failure of the carbon sequestration reservoir, such as a leak through a geological fault that may be extremely difficult to repair. The carbonate system is monitored throughout the duration of the CO_2 leak and for the initial three months of the recovery period. IEA GHG (2008)

reported a range of plausible long-term CO_2 leakage rates extending from 1 to $50,000$ t CO_2 per day. Scale analysis shows that leakages closer to the lower end of this range will scarcely be detectable at the resolution of the model used within the present study, and regional hydrodynamic models with finer resolution would be better suited to investigate the impacts of such leakages over small scales. Therefore the decision was taken to conduct the long-term simulations with constant leakage rates of $1,000$ and $10,000$ t CO_2 per day.

In order to investigate the seasonal and inter-annual variability of the impacts of CO_2 leakages, each short-term experiment is repeated with a release in January, April, July and October of 1998 and 1999, and the long-term simulations are repeated with a release beginning in January and July of 1998 and 1999. Each simulation begins on 1st January 1995, providing a minimum of a three year spin-up period to ensure that salinity, temperature, DIC_B and TA_{pro} have reached appropriate values and stabilised prior to the introduction of leakage DIC_L. Years 1998 and 1999 were selected to give two consecutive years with contrasting mean North Atlantic Oscillation (NAO) indices (National Weather Service, 2013), (figure A.5), as the NAO is believed to influence the wind driven circulation and mixing in the North Sea (Reid et al., 2001) (figure A.6).

The seasonal stratification is slightly stronger at the north site during 1999 than 1998 (figure A.4). Although the south site experiences no prolonged periods of enduring stratification in either year, the temporary periods of stratification are both more frequent and stronger during 1999. Full details of each model run are given in table A.1.

A.3 Results

We present the majority of the results by referencing the change in pH caused by the additional CO_2. Normal marine pH is in the region of 8.1 and varies naturally by around ± 0.2 units in shelf systems, although larger variations can be associated with coastal features (Blackford and Gilbert, 2007). It is established that marine biota and biogeochemical processes are sensitive

Run	Leak start	Leak duration (days)	Leak size (t CO_2 / day)
Short term leakage scenarios			
ST1	1st January 1998	1	5,000
ST2	1st April 1998	1	5,000
ST3	1st July 1998	1	5,000
ST4	1st October 1998	1	5,000
ST5	1st January 1999	1	5,000
ST6	1st April 1999	1	5,000
ST7	1st July 1999	1	5,000
ST8	1st October 1999	1	5,000
Long term leakage scenarios			
LT1	1st January 1998	365	10,000
LT2	1st July 1998	365	10,000
LT3	1st January 1999	365	10,000
LT4	1st July 1999	365	10,000
LT5	1st January 1998	365	1,000
LT6	1st July 1998	365	1,000
LT7	1st January 1999	365	1,000
LT8	1st July 1999	365	1,000

Table A.1: Details of the duration and size of the CO_2 source term for each model run. Model spin-up begins on 1st Jan 1995 for every run.

to pH, although this sensitivity is complex. In order to give context to the results presented, long term reductions in pH approaching or exceeding 1.0 unit can be considered as significantly harmful, reductions of the order of $0.2 - 0.5$ as potentially harmful whilst reductions of less than 0.1 unit are unlikely to have an impact (Widdicombe et al., 2013). Short term (hours to a few days) reductions in pH will be much less deleterious to marine biota. In terms of monitoring for leakage, current instrumentation can resolve pH changes of 0.01 unit or greater (Rerolle et al., 2013). The limiting factor in monitoring for leakage is therefore distinguishing leakage signals from natural variability.

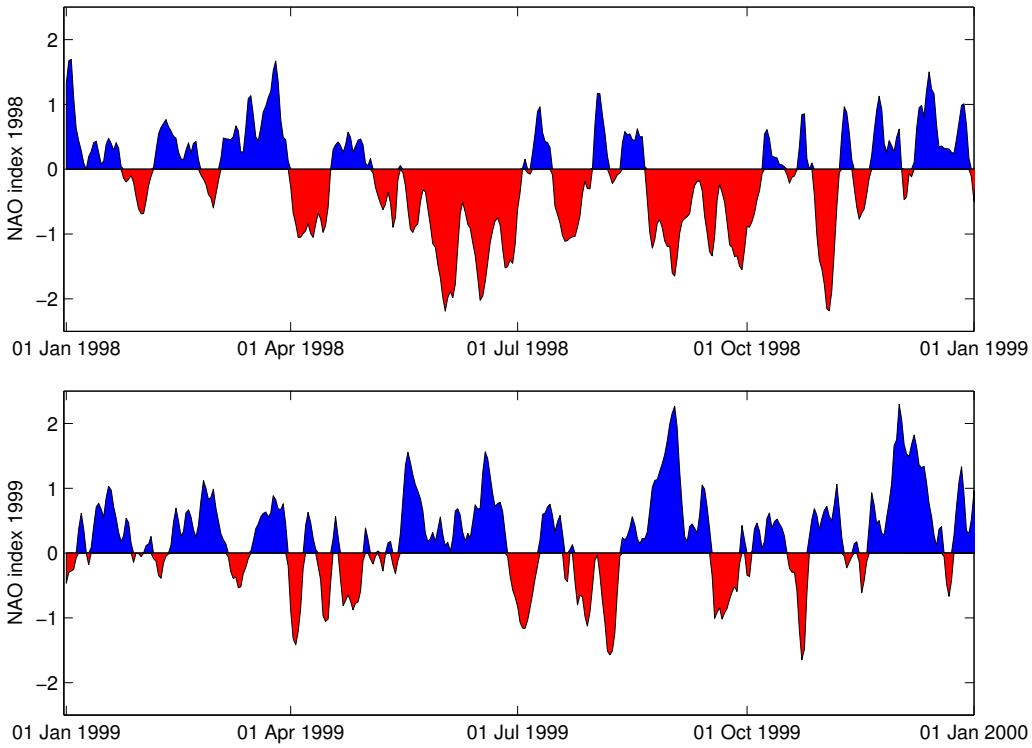

Figure A.5: Daily North Atlantic Oscillation (NAO) index in 1998 and 1999. Data from National Weather Service (2013).

A.3.1 Short-term Leakage Scenarios

Significant changes in the marine carbonate system are observed in each of the short-term leakage scenarios, however any perturbations are minimal outside the vicinity of the source. Across all eight simulations the largest recorded reductions to seawater pH are 1.92 and 1.22 pH units at the north and south site respectively, both occurring during the ST4 scenario, yet reductions are typically weaker than 0.1 pH units beyond 10 km from the release sites (see table A.2, figures A.7 and A.8). Significant perturbations to pH are generally restricted to the bottom layer, even at the vertically mixed south site, and reductions to surface pH are typically weaker than 0.1 pH units (figures A.9, A.10). It is evident that any CO_2 plumes arising from leakages of this magnitude are highly localised in the context of the North Sea.

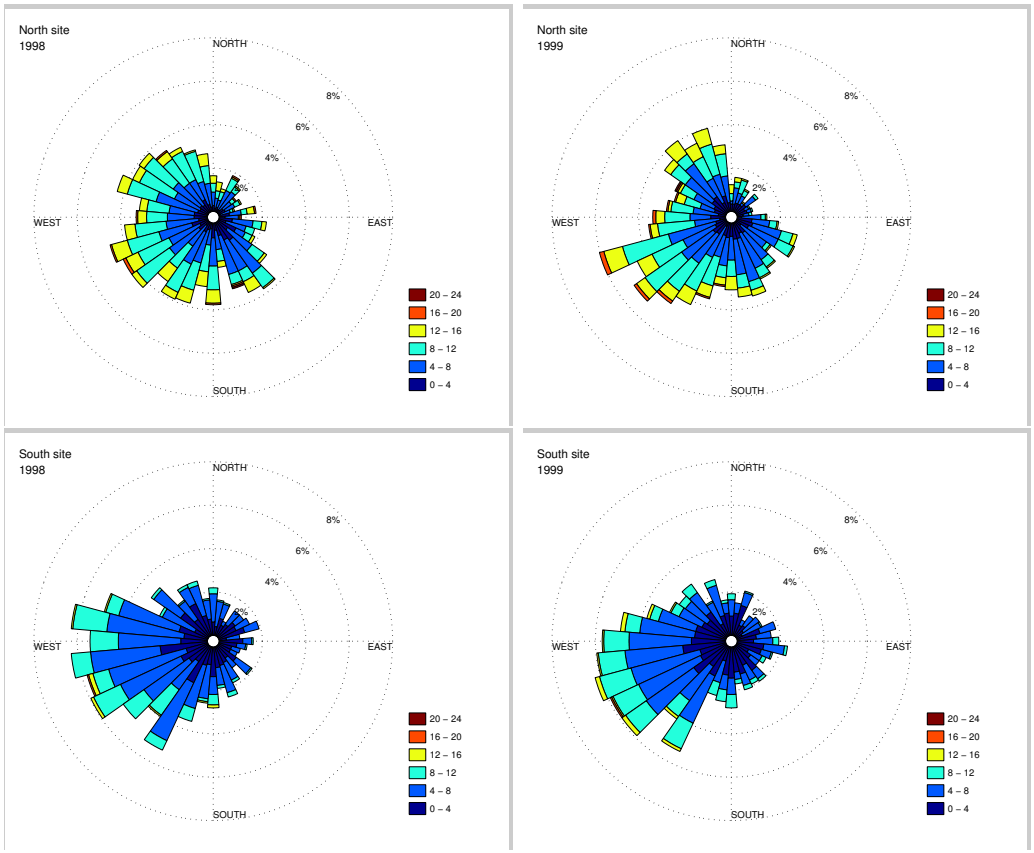

Figure A.6: Wind rose at both release sites during 1998 and 1999.

The results show that calcite is only briefly undersaturated at both sites, and this is spatially confined to the release sites and adjacent grid cells. Undersaturation of aragonite extends only slightly further at the north site, reaching approximately 4 km from the CO_2 source. Both minerals return to supersaturated levels within a single day after the end of the release period in all simulations and at both sites. It is apparent that the 1.8 km grid resolution is not sufficiently fine to properly resolve the small undersaturated region for CO_2 leakages of this magnitude.

The carbonate system at the leakage sites quickly returns to background values after the end of the CO_2 release period. This is primarily due to advection of CO_2 away from the leakage sites and tidal mixing rather than

outgasing of CO_2 at the sea surface, and a rapid recovery is also observed at the north site during the summer months when outgasing is negligible. During the recovery period the greatest reduction in seawater pH is generally not found at the release sites but at nearby locations, as the CO_2 plumes are gradually advected further away from their source point. Across all leakage scenarios the reductions to pH are weaker than 0.1 pH units within 5 days and below 0.05 pH units within 8 days within the northern CO_2 plume. In the southern CO_2 plume all reductions are weaker than 0.1 pH units within 3 days and below 0.05 pH units within 7 days. By day 30 the greatest reductions to seawater pH are less than 0.014 pH units at both sites. The concentration of CO_2 at the release sites is observed to oscillate periodically during some simulations due to semi-diurnal tidal advection.

Table A.3 displays the proportion of the injected CO_2 that had escaped into the atmosphere thirty days after the start of the CO_2 release period. Across all eight simulations an average of 25.0% outgases at the south site by the end of the thirty days, meanwhile only 6.2% typically escapes the water column at the north site over the same period. There are significant variations between release scenarios at the north site as there is minimal outgasing during the summer releases due to the sharp thermocline. By contrast, the pathway and strength of the acidified plume at the south site is more consistent between simulations. There is also considerable inter-annual variability at the north site, as the proportion of escaped CO_2 in the April and October 1998 release scenarios (ST2 and ST4) is considerably greater than the corresponding releases in 1999 (ST6 and ST8). This can be explained by the fact that stratification develops earlier and breaks down later during the 1999 run.

A.3.2 Long-term Leakage Scenarios

The long term scenarios with release rates of $10,000$ t CO_2 per day (LT1 to LT4) result in extensive plumes of highly acidified water that extend from the source locations (figure A.11). At the north site most of the CO_2 is carried initially northward then eastward by the mean circulation, broadly

Station	Δ pH	ST1	ST2	ST3	ST4	ST5	ST6	ST7	ST8
North site	0.1	6	6	17	8	8	8	8	8
	0.05	8	8	42	9	11	11	13	28
	0.01	37	102	102	61	61	61	92	93
South site	0.1	4	4	6	9	9	9	9	9
	0.05	35	35	35	20	23	23	23	23
	0.01	108	108	108	104	116	116	116	116

Table A.2: Greatest horizontal distance (rounded to nearest km) between the release sites and three critical Δ pH contours for each short term release scenario. Values represent the greatest distance over the whole simulation. Note that the horizontal grid resolution is approximately 1.8 km, therefore low values should be treated with caution as these contours will be highly dependent upon the grid resolution.

Station	ST1	ST2	ST3	ST4	ST5	ST6	ST7	ST8
North site	11.5%	12.9%	$< 0.01\%$	6.0%	14.4%	3.8%	$< 0.01\%$	0.8%
South site	31.6%	22.3%	15.2%	33.4%	39.9%	24.3%	14.2%	18.9%

Table A.3: Percentage of additional CO_2 released into atmosphere 30 days after the start of the CO_2 release, short term leakage scenarios ST1 to ST8.

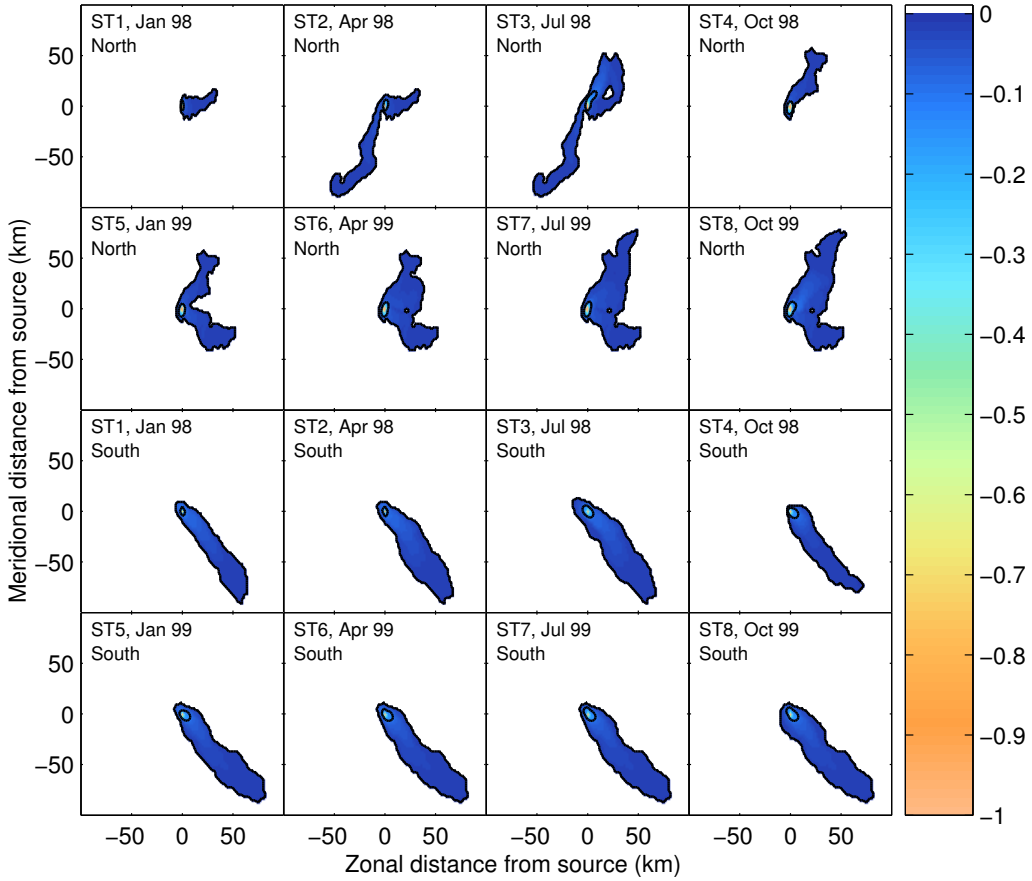

Figure A.7: Maximum perturbation to pH at the seabed over each short term simulation at the north site. Each figure shows a 200 km by 200 km grid surrounding the release site. The −0.1 and −0.01 pH unit contours are highlighted and changes of less than 0.01 pH units have been masked.

reflecting the Dooley current, and gradually spreads laterally to the north and south. However, a considerable proportion is also advected south of the release station. The pathway of CO_2 released at the south site appears to be much more persistent, initially flowing in a slow and narrow south-eastward pathway adjacent to the English coastline, then rapidly advancing north-eastward towards the Skagerrak in a much weaker concentration. The

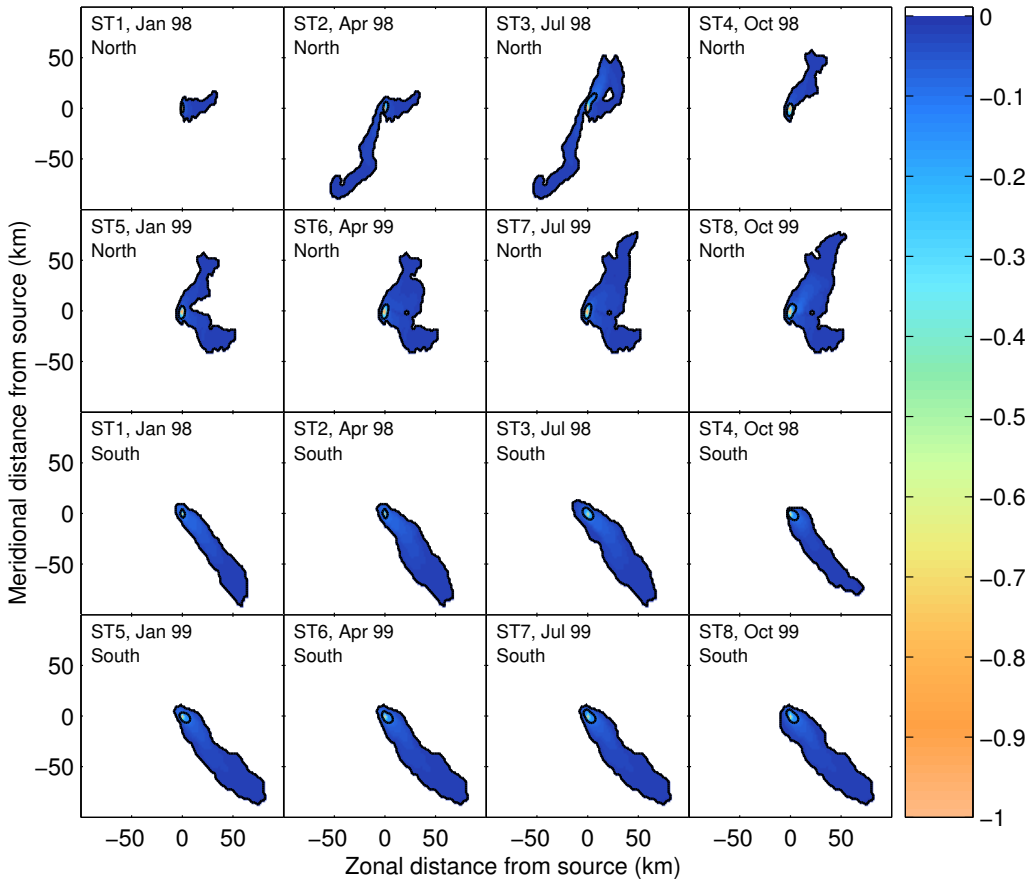

Figure A.8: Maximum perturbation to pH at the seabed over each short term simulation at the south site. Each figure shows a 200 km by 200 km grid surrounding the release site. The -0.1 and -0.01 pH unit contours are highlighted and changes of less than 0.01 pH units have been masked.

greatest reductions to pH are 2.67 and 2.32 pH units at the north and south site respectively, whilst acidification by 1.0 pH units could be found as far as 39 km from the north site, and 24 km from the south site. These scenarios result in large regions where calcite is undersaturated, extending as far as 62 km from the north site, and 70 km from the south site. Aragonite was undersaturated as far as 126 and 118 km from the north and south site respectively.

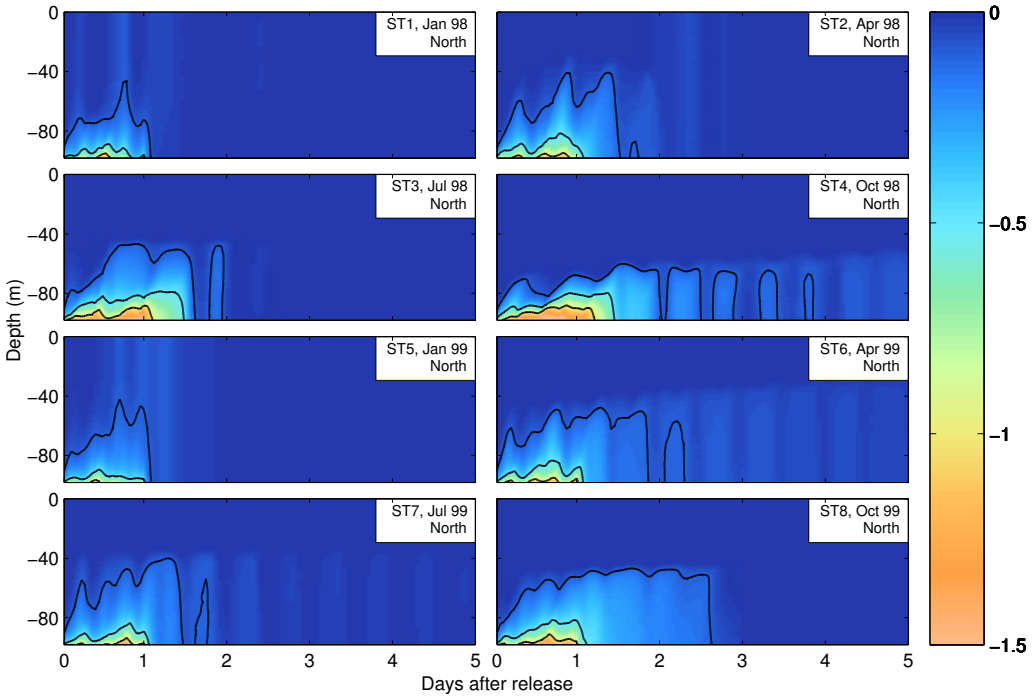

Figure A.9: Time series of the perturbation to pH throughout the water column at the north site during the first 5 days of the simulation for the short term leakage scenarios. Contours of −1.0, −0.5 and −0.1 pH units have been highlighted.

Leakages of 1,000 t CO_2 per day (LT5 to LT8) result in plumes of acidified water that follow identical pathways to those described for the larger release rate, however reductions to seawater pH are generally an order of magnitude weaker throughout most of the domain (figure A.11). The largest reductions to seawater pH across these four scenarios are 1.19 and 0.98 pH units at the north site and south site respectively. These scenarios cause no undersaturation of calcite outside the CO_2 source grid cells, and only minimal undersaturation of aragonite, extending no further than 6 km from either site.

The carbonate system at both release sites returns to natural values almost instantly after the end of the CO_2 release period (figure A.12), how-

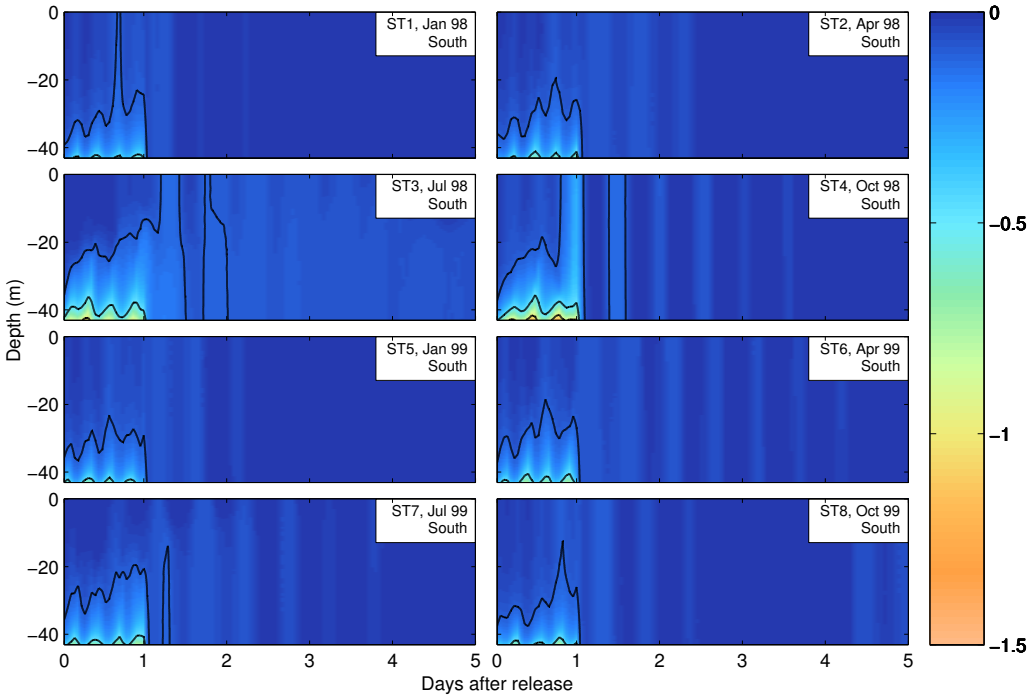

Figure A.10: Time series of the perturbation to pH throughout the water column at the south site during the first 5 days of the simulation for the short term leakage scenarios. Contours of −1.0, −0.5 and −0.1 pH units have been highlighted.

ever this is misleading as once again the rapid recovery is due to advection away from the source rather than outgasing, and acidified water continues to linger in the North Sea for some time afterwards (figure A.13). Figure A.12 demonstrates the influence of stratification upon the fate of released CO_2 as the impact on bottom pH is intensified at the north site during the summer months, whilst the influence on surface pH is negligible. Another feature that is particularly apparent at the south site is a regular oscillation in pH in synchronisation with the spring-neap cycle. Strong tidal advection during spring tides mean the CO_2 is injected into a larger volume of water in weaker concentrations, and the energetic turbulence ensures the CO_2 is well mixed. In contrast neap tides allow CO_2 to accumulate at the release site in

large concentrations, causing greater reductions to seawater pH.

On average 40.2% of the CO_2 added at the north site outgases by the end of the ninety days, whereas the average figure is 86.4% at the south site (table A.5). There is little variability in the proportion of outgased CO_2 between different leakage scenarios because long release durations ensure that each simulation contains similar periods when the water column is stratified and vertically mixed.

There is significant seasonal variability in the rate of CO_2 outgasing within each individual simulation, and this is particularly evident at the north site (figure A.14). The air-sea flux of CO_2 is generally slightly greater during 1998 than 1999 at the north site due to the shorter duration of stratification, whereas there is no significant inter-annual variability in outgasing at the south site. At the south site a greater proportion of CO_2 escapes the water column during the first four leakage scenarios with the larger CO_2 source term, this can be explained by the buffering of CO_2 in seawater. This variability according to the magnitude of the CO_2 source term is less pronounced at the north site as the large depths and strong summer stratification mean that the added CO_2 is well mixed and somewhat diluted before it reaches the surface layer.

A.4 Discussion

Leakage scenarios ranging from pipeline leakages (with a release rate of $1,000$ t CO_2 per day) to the complete failure of a carbon sequestration facility (with a release rate of $10,000$ t CO_2 per day) were simulated for a modelling investigation into the effects of large geological CO_2 leakages on the North Sea carbonate system. Short-term leakages of $5,000$ t CO_2 over a single day result in significant acidification at the release sites, reducing pH by as much as 1.92 pH units. Perturbations of 0.1 pH units and greater were generally confined to a restricted region at any point in time (in the context of the size of the study region), typically smaller than 10 km in diameter, however strong mean circulation and semi-diurnal tidal advection meant that such re-

Station	Δ pH	LT1	LT2	LT3	LT4	LT5	LT6	LT7	LT8
North site	1.0	39	21	34	30	0	X	X	0
	0.5	61	49	54	54	0	0	0	0
	0.25	117	103	108	141	6	4	2	2
	0.1	354	306	378	347	26	16	18	16
	0.01	570	575	580	58	299	334	303	322
South site	1.0	23	22	24	24	X	X	X	X
	0.5	62	61	62	57	X	0	0	0
	0.25	122	100	99	108	2	2	2	2
	0.1	166	156	165	160	35	22	33	33
	0.01	693	670	461	437	193	186	196	18

Table A.4: Greatest horizontal distance (rounded to nearest km) between the release sites and five critical ΔpH contours for each long term release scenario. Values represent the greatest distance over the whole simulation. A value of 0.0 indicates that such perturbations are found at the release site only. An 'X' indicates that no such perturbations are found anywhere.

Station	LT1	LT2	LT3	LT4	LT5	LT6	LT7	LT8
North site	46.0%	38.8%	40.2%	38.0%	44.7%	37.2%	39.1%	37.2%
South site	90.7%	84.5%	92.9%	85.6%	87.3%	79.5%	90.3%	80.7%

Table A.5: Table 5: Percentage of additional CO_2 released into atmosphere 90 days after the end of the CO_2 release (455 days after the initial CO_2 injection), long term leakage scenarios LT1 to LT8.

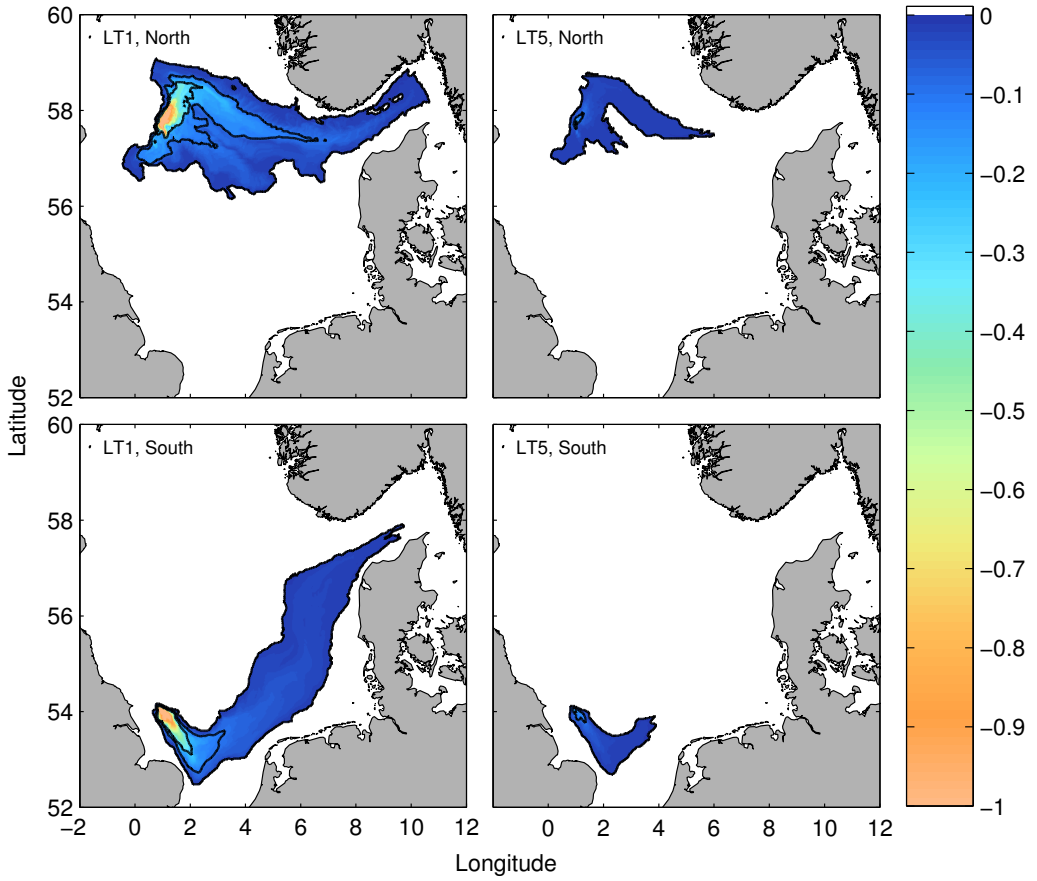

Figure A.11: Maximum perturbation pH at the seabed over the long term simulations LT1 (10,000 t CO_2/day, January 1998 start) and LT5 (1,000 t CO_2/day, January 1998 start), with the −0.25, −0.1 and −0.01 pH unit contours highlighted. The colour bar has been capped at 1 pH units. Changes of less than 0.01 pH units have been masked.

ductions in pH were found as far as 17 km from the source point. By contrast long-term leakages of 1,000 t CO_2 per day for a year only reduced the pH by a maximum of 1.19 pH units at the release site, and local perturbations were considerably weaker than those in the short-term leakage scenarios. This highlights the fact that added CO_2 is rapidly flushed away from the source, and a single burst of CO_2 at a high rate will result in greater perturba-

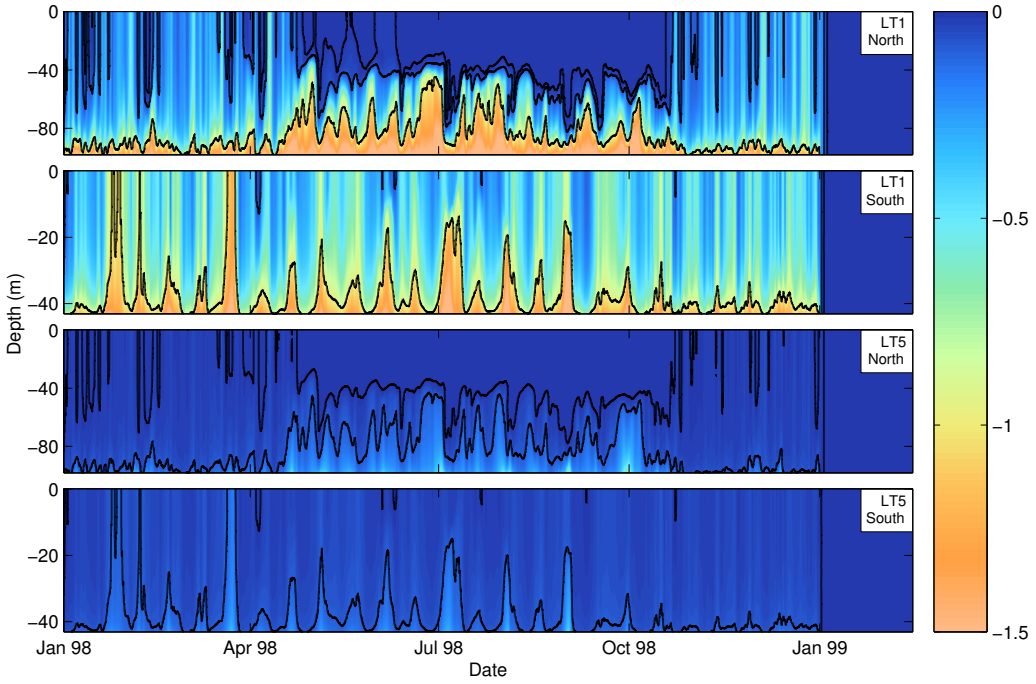

Figure A.12: Time series of perturbation to pH over the LT1 scenario (10, 000 t CO_2/day, January 1998 start) and LT_5 scenario (1,000 t CO_2/day, January 1998 start) at the north and south sites. Hourly output has been smoothed with a moving average filter (span of 25 hours) to reduce diurnal variability. The 1.0, 0.1 and 0.01 pH contours have been highlighted.

tions to the carbonate system over short distances than a slower sustained release. Over greater spatial scales the long-term leakages had a much more significant impact upon the carbonate system than the short-term releases, causing reductions of 0.1 pH units as far as 35 km from the release point, and reductions of 0.01 pH units over several hundred kilometres. Finally the long-term leakages of 10, 000 t CO_2 per day for a full year caused widespread acidification across the North Sea, reducing pH by up to 2.67 pH units at the release sites and causing reductions of 0.25 pH units as far as 141 km away from the source (figure A.15). It should be emphasized though that this is a very unlikely scenario.

Any predicted acidification should be considered in the context of natural

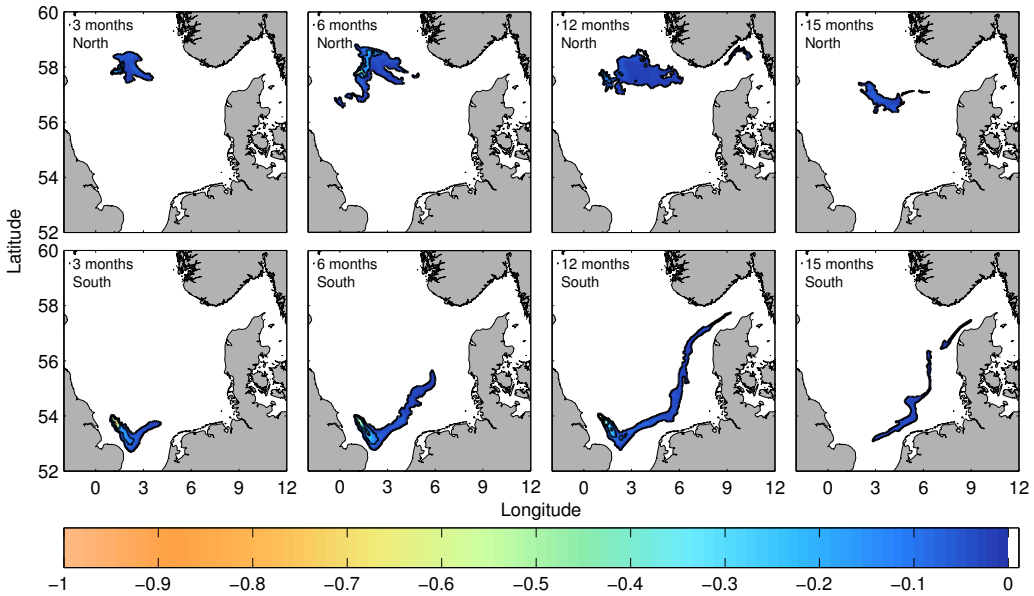

Figure A.13: Snapshots of the perturbation to pH at the seabed during the LT1 scenario at both release sites. The −0.25, −0.1 and −0.01 pH unit contours are highlighted and perturbations of less than 0.01 pH units have been masked. The colour bar has been capped at 1 pH units. Labels (3, 6, 9, 15 months) indicate the length of time elapsed since the start of the initial CO_2 injection. The 15 month snapshot shows the pH perturbation after 3 months of recovery.

variability of pH in the North Sea, which can exceed 1.0 pH units in coastal regions of freshwater influence, although further offshore in regions of low biological activity annual variability is typically around 0.1 to 0.2 pH units (Blackford and Gilbert, 2007). Furthermore, the North Sea is expected to acidify by an average of 0.2 pH units compared to pre-industrial levels by the year 2050 due to anthropogenic CO_2 emissions, and by an additional 0.13 to 0.28 pH units by 2100 (Blackford and Gilbert, 2007). Therefore throughout most of the North Sea, continued unmitigated CO_2 emissions will result in greater, ubiquitous and more long-lived acidification over the next few decades than even the worst case scenario investigated here. It should be highlighted however that any acidification due to CO_2 leakages would be in

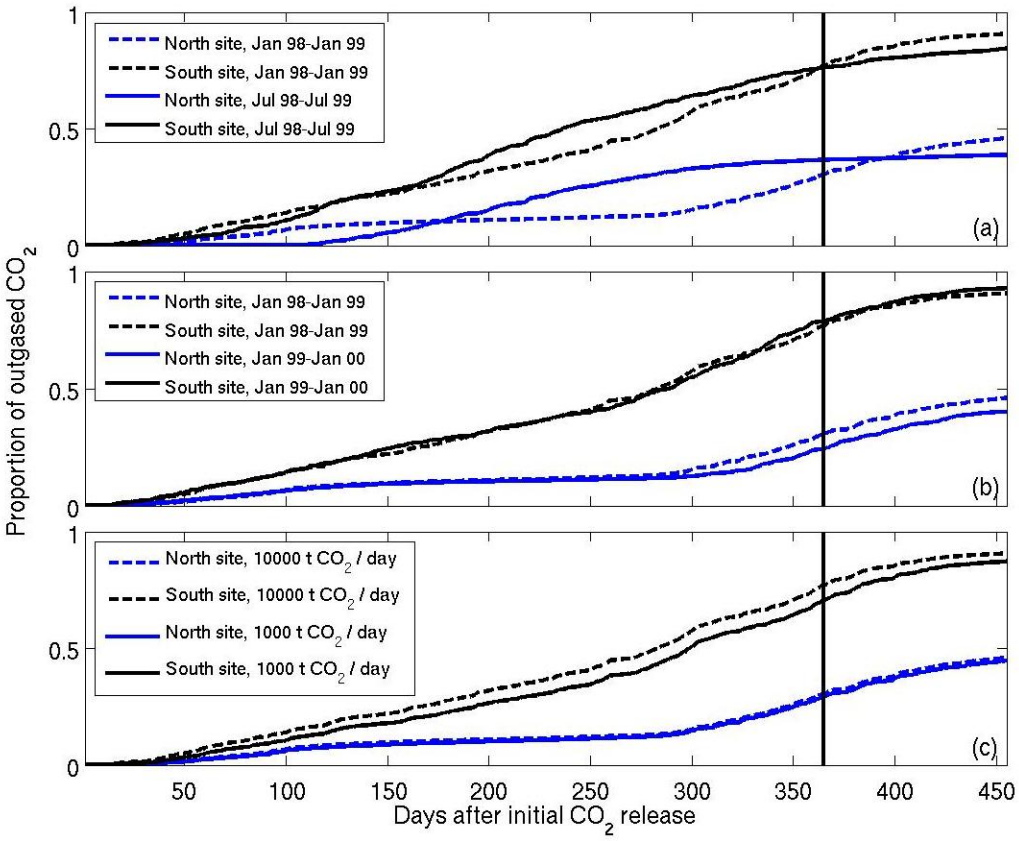

Figure A.14: Comparison of CO_2 outgasing rates. (a): Seasonal variability (LT1 and LT2). (b): Inter-annual variability (LT1 and LT3). (c) Variability due to CO_2 leakage rate (LT1 and LT5).

addition to natural variability, and the rate of acidification would be considerably faster than the long term trend associated with rising atmospheric CO_2.

It is difficult to determine precisely how the carbonate system would react to CO_2 leakages under the environmental conditions of the future, when CCS is conducted on a larger scale. It is anticipated that atmospheric pCO_2 will continue to increase, and seawater pH will decrease, shifting the partitioning of DIC in favour of CO_2. As the ratio of CO_2 to DIC rises, any additional CO_2 injected into the water column will outgas at a faster rate.

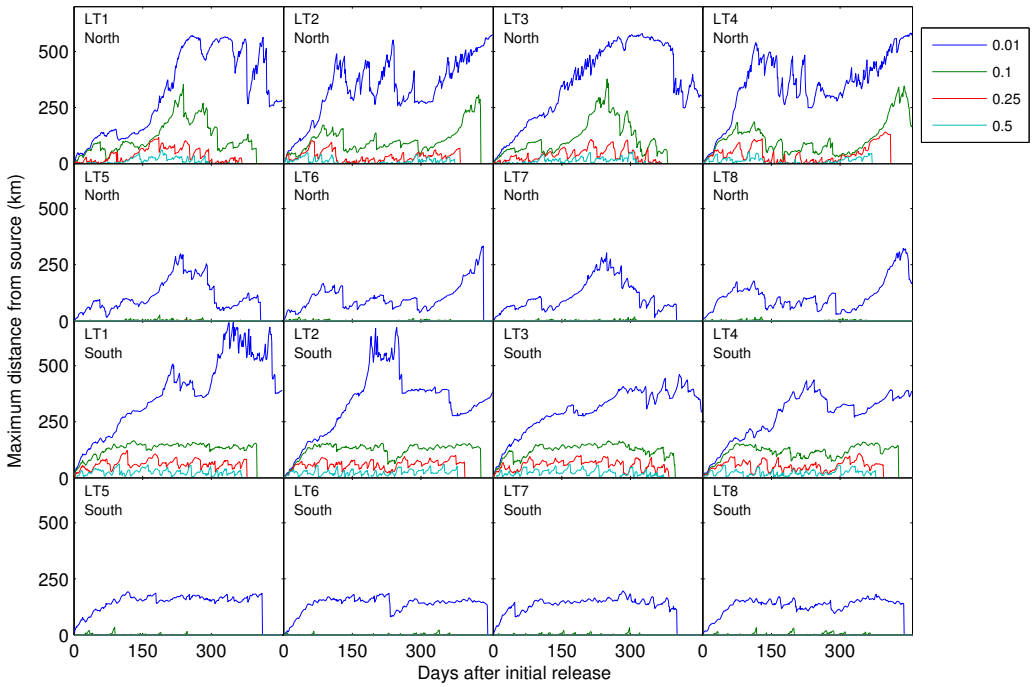

Figure A.15: Greatest distance of four critical pH perturbation contours from the source over time for long-term leakage simulations.

Furthermore, any increase in surface temperatures will lead to a decrease in the solubility of CO_2 in seawater, potentially increasing the rate of outgasing further. Therefore it may be reasonable to expect that any perturbations to seawater pH in the future could be relatively short-lived compared to these simulations, however the magnitude of the total perturbation to seawater pH (due to both the uptake of atmospheric CO_2 and seabed CO_2 leakages) would be greater compared to pre-industrial levels. This is somewhat speculative due to the complex nature of the carbonate system, and other factors such as potential changes to wind intensity could complicate this matter further. There is clearly a need for further research to focus upon the response of the carbonate system to CO_2 leakages under projected future climate conditions.

Whilst the results presented here give considerable insight into the impact of large CO_2 additions upon the physical and chemical environment, the

impact of acidification upon the marine ecosystem would ultimately depend upon the tolerance and adaptive capacity of resident biota to perturbations to pH and the saturation states of calcite and aragonite, and a detailed assessment of this is beyond the scope of this article. With the exception of the worst case scenarios, LT1 to LT4, the simulations investigated here generally only caused significant perturbations to the carbonate system over spatial scales of the order of 50 km, and whilst release rates of $1,000$ t CO_2 per day caused reductions of 0.01 pH units over hundreds of kilometres from the source, in reality such small changes would be indistinguishable from background variability, and they would have no deleterious consequences for marine fauna and flora. It would therefore appear sensible for future modelling studies to utilise local hydrodynamic models with finer horizontal resolution to investigate the impacts of smaller CO2 leakages over more confined spatial scales.

The influence of stratification upon the fate of a CO_2 plume was evident in every set of release scenarios considered here. Strong seasonal thermoclines are able to inhibit the exchange of CO_2 between surface and bottom waters, and ultimately prevent outgasing of CO_2 into the atmosphere. Overall the carbonate system at the south site would appear to be considerably less sensitive to CO_2 additions than the north site, primarily because the shallow depths and generally well mixed vertical profile mean CO_2 can readily escape to the atmosphere, and strong tidal currents ensure that CO_2 is well mixed within the water column. Although seasonal variability to the air-sea flux was significant at both sites, on average the CO_2 injected at the south site reached the atmosphere twice as fast as the corresponding CO_2 at the north site. Furthermore Thomas et al. (2004) reported that on average the southern North Sea is super-saturated with CO_2 whereas the northern North Sea is generally under-saturated, and this is particularly clear during the summer. Although pCO_2 is not replicated particularly well by the POLCOMS-ERSEM-HALTAFALL model (Artioli et al., 2012), in reality this pattern would reinforce the spatial variability highlighted by this study, as added CO_2 would leave the water column faster in an outgasing regime. Al-

though there are many additional factors to consider when assessing potential carbon sequestration sites, including the biodiversity of the environment, the feasibility and cost of installation and maintenance, and the likelihood of sequestered CO_2 entering the water column, this investigation would suggest that if all other factors are equal, the physical marine environment of the shallow, well-mixed southern North Sea is less sensitive to CO_2 inputs than the deeper, seasonally stratified northern North Sea. However such leakages may be more difficult to detect in the southern North Sea as a result of weaker perturbations to the marine carbonate system.

The results of this investigation are broadly in good agreement with Blackford et al. (2008), however there are some notable differences between the two studies due to the model improvements, particularly in the local pH perturbations. For example, in their high long-term seepage scenario (3.02×10^5 t CO_2 over a year), Blackford et al. (2008) found that that perturbations to pH reached a maximum of 0.12 pH units, whereas the LT5 to LT8 scenarios in the present study (3.65×10^5 t CO_2 over a year) show perturbations exceeding 1 pH unit at the seabed. Similarly the previous investigation reports that low short-term leaks (1.49×10^4 t CO_2 over a single day) result in reductions of up to 0.2 pH units, whereas short-term scenarios ST1 to ST8 (5×10^3 t CO_2 over a single day) in the current investigation show perturbations reaching 1.92 pH units, despite the much smaller release. This can be explained by the improvements in model resolution, and the fact that CO_2 is injected only into the bottom grid cell in this study. The volume of seawater receiving the CO_2 source term is approximately two orders of magnitude smaller than the volume in the previous investigation, and as a result CO_2 concentrations are much greater, and local pH reductions are far more significant. This supports the assertion of the previous study that it is likely that such events would have a catastrophic impact on the environment on a localised scale (< 1 km).

This study confirms previous work that suggests that only the largest conceivable leakage events would have significant environmental impact over large spatial scales. In the largest release scenarios investigated here, reduc-

tions of 0.1 pH units were detected 10 km downstream of the source within a couple of days of the start of the CO_2 release, and were found 50 km downstream within a month. Such events should be readily detectable and conversely, lack of detection of such events, given good monitoring practice, could be taken as conclusive proof that such an event was not occurring.

Bibliography

Adams, T. P., Miller, R. G., Aleynik, D., and Burrows, M. T. Offshore marine renewable energy devices as stepping stones across biogeographical boundaries. *Journal of Applied Ecology*, 51(2):330–338, 2014.

Agardy, T., Bridgewater, P., Crosby, M. P., Day, J., Dayton, P. K., Kenchington, R., Laffoley, D., McConney, P., Murray, P. A., Parks, J. E., and Peau, L. Dangerous targets? Unresolved issues and ideological clashes around marine protected areas. *Aquatic Conservation - Marine and Freshwater Ecosystems*, 13(4):353–367, 2003.

Almany, G. R., Berumen, M. L., Thorrold, S. R., Planes, S., and Jones, G. P. Local replenishment of coral reef fish populations in a marine reserve. *Science*, 316(5825):742–744, 2007.

Arakawa, A. and Lamb, V. R. Computational design of the basic dynamical processes of the UCLA generic circulation model. *Methods of Compututional Physics*, 17:173–265, 1977.

Artioli, Y., Blackford, J. C., Butenschoen, M., Holt, J., Wakelin, S. L., Thomas, H., Borges, A. V., and Allen, J. I. The carbonate system in the North Sea: Sensitivity and model validation. *Journal of Marine Systems*, 102:1–13, 2012.

Beck, M. W., Heck, K. L., Able, K. W., Childers, D. L., Eggleston, D. B., Gillanders, B. M., Halpern, B., Hays, C. G., Hoshino, K., Minello, T. J., Orth, R. J., Sheridan, P. F., and Weinstein, M. R. The identification,

conservation, and management of estuarine and marine nurseries for fish and invertebrates. *Bioscience*, 51(8):633–641, 2001.

Berumen, M. L., Almany, G. R., Planes, S., Jones, G. P., Saenz-Agudelo, P., and Thorrold, S. R. Persistence of self-recruitment and patterns of larval connectivity in a marine protected area network. *Ecology and Evolution*, 2(2):444–452, 2012.

Bishop, M. W. H. Establishment of an immigrant barnacle in British coastal waters. *Nature*, 159(4041):501–502, 1947.

Black, K. P. The relative importance of local retention and inter-reef dispersal of neutrally buoyant material on coral reefs. *Coral Reefs*, 12(1):43–53, 1993.

Blackford, J. C. and Gilbert, F. J. pH variability and CO2 induced acidification in the North Sea. *Journal of Marine Systems*, 64(1-4):229–241, 2007. Symposium on Advances in Marine Ecosystem Modelling Research, Plymouth England, Jun 27-29, 2005.

Blackford, J. C., Jones, N., Proctor, R., and Holt, J. Regional scale impacts of distinct CO2 additions in the North Sea. *Marine Pollution Bulletin*, 56 (8):1461–1468, 2008.

Boehlert, G. W. and Gill, A. B. Environmental and ecological effects of ocean renewable energy development a current synthesis. *Oceanography*, 23(2, SI):68–81, 2010.

Bolle, L. J., Dickey-Collas, M., van Beek, J. K. L., Erftemeijer, P. L. A., Witte, J. I. J., van der Veer, H. W., and Rijinsdorp, A. D. Variability in transport of fish eggs and larvae. III. Effects of hydrodynamics and larval behaviour on recruitment in plaice. *Marine Ecology Progress Series*, 390: 195–211, 2009.

Bowden, K. F. Processes affecting the salinity of the Irish Sea. *Monthly Notices of the Royal Astronomical Society Geophysical*, 6(2):63–90, 1950.

Bowden, K. F. Physical oceanography of the Irish Sea. *Fishery Investigation Series 2*, 18(8):1–67, 1955.

Bowden, K. F. Horizontal mixing in the sea due to a shearing current. *Journal of Fluid Mechanics*, 21(Part 1):83–95, 1965.

Bowden, K. F. and Fairbairn, L. A. A determination of the frictional forces in a tidal current. *Proceedings of the Royal Society of London Series A - Mathematical and Physical Sciences*, 214(1118):371–392, 1952.

Branch, G. M. and Steffani, C. N. Can we predict the effects of alien species? A case-history of the invasion of South Africa by Mytilus galloprovincialis (Lamarck). *Journal of Experimental Marine Biology and Ecology*, 300(1-2): 189–215, 2004.

Brickman, D. and Smith, P. C. Lagrangian stochastic modeling in coastal oceanography. *Journal of Atmospheric and Oceanic Technology*, 19(1): 83–99, 2002.

Briggs, R. P., Armstrong, M. J., Dickey-Collas, M., Allen, M., McQuaid, N., and Whitmore, J. The application of fecundity estimates to determine the spawning stock biomass of Irish Sea Nephrops norvegicus (L.) using the annual larval production method. *ICES Journal of Marine Science*, 59(1): 109–119, 2002.

Brochier, T., Lett, C., Tam, J., Freon, P., Colas, F., and Ayon, P. An individual-based model study of anchovy early life history in the northern Humboldt Current system. *Progress in Oceanography*, 79(2-4, SI):313–325, 2008.

Brown, J. and Gmitrowicz, E. M. Observations of the transverse structure and dynamics of the low-frequency flow through the North Channel of the Irish Sea. *Continental Shelf Research*, 15(9):1133–1156, 1995.

Brown, J., Carrillo, L., Fernand, L., Horsburgh, K. J., Hill, A. E., Young, E. F., and Medler, K. J. Observations of the physical structure and seasonal

jet-like circulation of the Celtic Sea and St. George's Channel of the Irish Sea. *Continental Shelf Research*, 23(6):533–561, 2003.

Brown, J. M., Amoudry, L. O., Souza, A. J., and Rees, J. Fate and pathways of dredged estuarine sediment spoil in response to variable sediment size and baroclinic coastal circulation. *Journal of Environmental Management*, 149:209–221, 2015.

Burchard, H. and Bolding, K. Comparative analysis of four second-moment turbulence closure models for the oceanic mixed layer. *Journal of Physical Oceanography*, 31(8):1943–1968, 2001.

Butler, M. J., Paris, C. B., Goldstein, J. S., Matsuda, H., and Cowen, R. K. Behavior constrains the dispersal of long-lived spiny lobster larvae. *Marine Ecology Progress Series*, 422:223–237, 2011.

Canuto, V. M., Howard, A., Cheng, Y., and Dubovikov, M. S. Ocean turbulence. Part I: One-point closure model - momentum and heat vertical diffusivities. *Journal of Physical Oceanography*, 31(6):1413–1426, 2001.

Carlton, J. T. and Geller, J. B. Ecological roulette : the global transport of nonindigenous marine organsims. *Science*, 261(5117):78–82, 1993.

Carr, M. H. and Reed, D. C. Conceptual issues relevant to marine harvest refuges - examples from temperate reef fishes. *Canadian Journal of Fisheries and Aquatic Sciences*, 50(9):2019–2028, 1993.

Carson, H. S., Lopez-Duarte, P. C., Cook, G. S., Fodrie, F. J., Becker, B. J., DiBacco, C., and Levin, L. A. Temporal, spatial, and interspecific variation in geochemical signatures within fish otoliths, bivalve larval shells, and crustacean larvae. *Marine Ecology Progress Series*, 473:133–148, 2013.

CEH. Derivation of daily outflows from Hydrometric Areas. Technical report, CEH Wallingford, 2003. National River Flow Archive.

Christie, M. R., Tissot, B. N., Albins, M. A., Beets, J. P., Jia, Y., Ortiz, D. M., Thompson, S. E., and Hixon, M. A. Larval connectivity in an effective network of marine protected areas. *PLOS ONE*, 5(12):1–8, 2010.

Colella, P. and Woodward, P. R. The piecewise parabolic method (PPM) for gas-dynamical simulations. *Journal of Computational Physics*, 54(1): 174–201, 1984.

Cowen, R. K. and Sponaugle, S. Larval dispersal and marine population connectivity. *Annual Review of Marine Science*, 1:443–466, 2009.

Cowen, R. K., Lwiza, K. M. M., Sponaugle, S., Paris, C. B., and Olson, D. B. Connectivity of marine populations: Open or closed? *Science*, 287(5454): 857–859, 2000.

Cowen, R. K., Paris, C. B., and Srinivasan, A. Scaling of connectivity in marine populations. *Science*, 311(5760):522–527, JAN 27 2006.

Crisp, D. J. The spread of Elminius modestus Darwin in north-west Europe. *Journal of the Marine Biological Association of the United Kingdom*, 37 (2):483–520, 1958.

Cronin, T. W. and Forward, R. B. Tidal vertical migration - endogenous rhythm in estuarine crab larvae. *Science*, 205(4410):1020–1022, 1979.

Cushing, D. H. The vertical migration of planktonic crustacea. *Biological Reviews of the Cambridge Philosophical Society*, 26(2):158–192, 1951.

Cuveliers, E. L., Geffen, A. J., Guelinckx, J., Raeymaekers, J. A. M., Skadal, J., Volckaert, F. A. M., and Maes, G. E. Microchemical variation in juvenile Solea solea otoliths as a powerful tool for studying connectivity in the North Sea. *Marine Ecology Progress Series*, 350:117–126, 2010.

Dabrowski, T. and Hartnett, M. Modelling travel and residence times in the eastern Irish Sea. *Marine Pollution Bulletin*, 57(1-5):41–46, 2008.

Dabrowski, T., Hartnett, M., and Olbert, A. I. Influence of seasonal circulation on flushing of the Irish Sea. *Marine Pollution Bulletin*, 60(5):748–758, 2010.

Davidson, F. J. M. and deYoung, B. Modeling advection of cod eggs and larvae on the Newfoundland shelf. *Fisheries Oceanography*, 4(1):33–51, 1995.

Degraer, S. and Brabant, R. Offshore wind farms in the Belgian part of the North Sea: State of the art after two years of environmental monitoring. In *Royal Belgian Institute for Natural Sciences, Management Unit of the North Sea Mathematical Models. Marine ecosystem management unit* , pages 1–287. 2009.

Deleersnijder, E., Campin, J. M., and Delhez, E. J. M. The concept of age in marine modelling I. Theory and preliminary model results. *Journal of Marine Systems*, 28(3-4):229–267, 2001.

Delhez, E. J. M. and Deleersnijder, E. The concept of age in marine modelling II. Concentration distribution function in the English Channel and the North Sea. *Journal of Marine Systems*, 31(4):279–297, 2002.

Delhez, E. J. M., Campin, J. M., Hirst, A. C., and Deleersnijder, E. Toward a general theory of the age in ocean modelling. *Ocean Modelling*, 1(1): 17–27, 1999.

Delhez, E. J. M., Heemink, A. W., and Deleersnijder, E. Residence time in a semi-enclosed domain from the solution of an adjoint problem. *Estuarine Coastal and Shelf Science*, 61(4):691–702, 2004.

DeVries, M. C., Tankersley, R. A., Forward, R. B., Kirbysmith, W. W., and Luettich, R. A. Abundance of estuarine crab larvae is associated with tidal hydrologic variables. *Marine Biology*, 118(3):403–413, 1994.

Dewar, M., Wei, W., McNeil, D., Nishio, M., and Chen, B. Simulation of the near field physiochemical impact of CO2 leakage into shallow water in the North Sea. *Energy Procedia*, 37:413 – 3423, 2013. GHGT-11.

Dickey-Collas, M., Brown, J., Fernand, L., Hill, A. E., Horsburgh, K. J., and Garvine, R. W. Does the western Irish Sea gyre influence the distribution of pelagic juvenile fish? *Journal of Fish Biology*, 51(A):206–229, 1997. Fisheries-Society-of-the-British-Isles Annual Symposium on Ichthyoplankton Ecology, Galway, Ireland, Jul 08-11, 1997.

Dickey-Collas, M., Briggs, R. P., Armstrong, M. J., and Milligan, S. P. Production of Nephrops norvegicus larvae in the Irish Sea. *Marine Biology*, 137(5-6):973–981, 2000a.

Dickey-Collas, M., McQuaid, N., Armstrong, M. J., Allen, M., and Briggs, R. P. Temperature-dependent stage durations of Irish sea Nephrops larvae. *Journal of Plankton Research*, 22(4):749–760, 2000b.

Dickson, A. G. Thermodynamics of the dissociation of boric-acid in synthetic seawater from 273.15-K TO 318.15-K. *Deep-Sea Research Part A - Oceanographic Research Papers*, 37(5):755–766, 1990.

Dight, I. J., James, M. K., and Bode, L. Modeling the larval dispersal of Acanthaster-planci .2. patterns of reef connectivity. *Coral Reefs*, 9(3): 125–134, 1990.

Duan, Z. H. and Zhang, Z. G. Equation of state of the H2O, CO2, and H2O-CO2 systems up to 10 GPa and 2573.15 K: Molecular dynamics simulations with ab initio potential surface. *Geochimica et Cosmoahimica Acta*, 70(9): 2311–2324, 2006.

Emsley, S. M., Tarling, G. A., and Burrows, M. T. The effect of vertical migration strategy on retention and dispersion in the Irish Sea during spring-summer. *Fisheries Oceanography*, 14(3):161–174, 2005.

Fairall, C. W., Bradley, E. F., Hare, J. E., Grachev, A. A., and Edson, J. B. Bulk parameterization of air-sea fluxes: Updates and verification for the COARE algorithm. *Journal of Climate*, 16(4):571–591, 2003.

Farmer, A. S. D. Synopsis of the biological data on the Norway Lobster (Nephrops norvegicus, Linnaeus 1758). *FAO Fisheries Synopsis No. 112*, FIRS/S112:1–97, 1975.

Fisher, R., Leis, J. M., Clark, D. L., and Wilson, S. K. Critical swimming speeds of late-stage coral reef fish larvae: variation within species, among species and between locations. *Marine Biology*, 147(5):1201–1212, 2005.

Fodrie, F. J., Becker, B. J., Levin, L. A., Gruenthal, K., and McMillan, P. A. Connectivity clues from short-term variability in settlement and geochemical tags of mytilid mussels. *Journal of Sea Research*, 65(1):141–150, 2011.

Forteath, G. N. R., Picken, G. B., Ralph, R., and Williams, J. Marine growth studies on the North Sea oil platform Montrose Alpha. *Marine Ecology Progress Series*, 8(1):61–68, 1982.

Forward, R. B. and Tankersley, R. A. Selective tidal-stream transport of marine animals. In Gibson, R. B. and Barnes, M. and Atkinson, R. J. A., editor, *Oceanography and Marine Biology, Vol 39*, volume 39 of *Oceanography and Marine Biology*, pages 305–353. 2001.

Forward, R. B., Cronin, T. W., and Stearns, D. E. Control of diel vertical migration - photoresponses of a larval crustacean. *Limnology and Oceanography*, 29(1):146–154, 1984.

Fox, C. J., McCloghrie, P., Young, E. F., and Nash, R. D. M. The importance of individual behaviour for successful settlement of juvenile plaice (Pleuronectes platessa L.): a modelling and field study in the eastern Irish Sea. *Fisheries Oceanography*, 15(4):301–313, 2006.

Fox, C. J., McCloghrie, P., and Nash, R. D. M. Potential transport of plaice eggs and larvae between two apparently self-contained populations in the Irish Sea. *Estuarine Coastal and Shelf Science*, 81(3):381–389, 2009.

Galindo, H. M., Pfeiffer-Herbert, A. S., McManus, M. A., Chao, Y., Chai, F., and Palumbi, S. R. Seascape genetics along a steep cline: using genetic patterns to test predictions of marine larval dispersal. *Molecular Ecology*, 19(17, SI):3692–3707, 2010.

Gell, F. R. and Roberts, C. M. Benefits beyond boundaries: the fishery effects of marine reserves. *Trends in Ecology & Evolution*, 18(9):448–455, 2003.

Gilg, M. R. and Hilbish, T. J. Patterns of larval dispersal and their effect on the maintenance of a blue mussel hybrid zone in southwestern England. *Evolution*, 57(5):1061–1077, 2003a.

Gilg, M. R. and Hilbish, T. J. The geography of marine larval dispersal: Coupling genetics with fine-scale physical oceanography. *Ecology*, 84(11): 2989–2998, 2003b.

Glasby, T. M., Connell, S. D., Holloway, M. G., and Hewitt, C. L. Non-indigenous biota on artificial structures: could habitat creation facilitate biological invasions? *Marine Biology*, 151(3):887–895, 2007.

Gleason, M., McCreary, S., Miller-Henson, M., Ugoretz, J., Fox, E., Merrifield, M., McClintock, W., Serpa, P., and Hoffman, K. Science-based and stakeholder-driven marine protected area network planning: A successful case study from north central California. *Ocean & Coastal Management*, 53(2):52–68, 2010.

Gliwicz, M. Z. Predation and the evolution of vertical migration in zooplankton. *Nature*, 320(6064):746–748, 1986.

Gowen, R. J. and Stewart, B. M. The Irish Sea: Nutrient status and phytoplankton. *Journal of Sea Research*, 54(1):36–50, 2005. Workshop

on Contrasting Approaches to Understanding Eutrophication Effects on Phytoplankton, RIKZ Lab Netherlands Rijkswaterstaat, Rijkswaterstaat, Netherlands, Mar, 2002.

Gowen, R. J., Mills, D. K., Trimmer, M., and Nedwell, D. B. Production and its fate in two coastal regions of the Irish Sea: the influence of anthropogenic nutrients. *Marine Ecology Progress Series*, 208:51–64, 2000.

Gowen, R. J., Tett, P., Kennington, K., Mills, D. K., Shammon, T. M., Stewart, B. M., Greenwood, N., Flanagan, C., Devlin, M., and Wither, A. The Irish Sea: Is it eutrophic? *Estuarine Coastal and Shelf Science*, 76 (2):239–254, 2008.

Greenwood, N., Hydes, D. J., Mahaffey, C., Wither, A., Barry, J., Sivyer, D. B., Pearce, D. J., Hartman, S. E., Andres, O., and Lees, H. E. Spatial and temporal variability in nutrient concentrations in Liverpool Bay, a temperate latitude region of freshwater influence. *Ocean Dynamics*, 61 (12):2181–2199, 2011.

Hallegraeff, G. M. A Review of Harmful Algal Blooms and their Apparent Global Increase. *Phycologia*, 32(2):79–99, 1993.

Haugan, P. M. and Drange, H. Sequestration of CO2 in the deep ocean by shallow injection. *Nature*, 357(6376):318–320, 1992.

Hays, G. C. A review of the adaptive significance and ecosystem consequences of zooplankton diel vertical migrations. *Hydrobiologia*, 503(1-3):163–170, 2003. 37th European Marine Biology Symposium, Reykjavik, Iceland, Aug 05-09, 2002.

Hays, G. C., Warner, A. J., and Lefevre, D. Long-term changes in the diel vertical migration behaviour of zooplankton. *Marine Ecology Progress Series*, 141(1-3):149–159, 1996.

Heaps, N. S. Estimation of Density Currents in the Liverpool Bay Area of the Irish Sea. *Geophys. J. R. Astr. Soc.*, 30(4):415–132, 1972.

Heaps, N. S. and Jones, J. E. Density currents in the Irish Sea. *Geophysical Journal of the Royal Astronomical Society*, 51(2):393–429, 1977.

Hedgecock, D., Barber, P. H., and Edmands, S. Genetic approaches to measuring connectivity. *Oceanography*, 20(3):70–79, 2007.

Hellberg, M. E., Burton, R. S., Neigel, J. E., and Palumbi, S. R. Genetic assessment of connectivity among marine populations. *Bulletin of Marine Science*, 70(1, S):273–290, 2002.

Hill, A. E. Pelagic dispersal of norway lobster nephrops-norvegicus larvae examined using an advection-diffusion-mortality model. *Marine Ecology Progress Series*, 64(3):217–226, 1990.

Hill, A. E. Vertical migration in tidal currents. *Marine Ecology Progress Series*, 75(1):39–54, 1991.

Hill, A. E. Spin-down and the dynamics of dense pool gyres in shallow seas. *Journal of Marine Research*, 54(3):471–486, 1996.

Hill, A. E. Diel vertical migration in stratified tidal flows: Implications for plankton dispersal. *Journal of Marine Research*, 56(5):1069–1096, 1998.

Hill, A. E., Durazo, R., and Smeed, D. A. Observations of a cyclonic gyre in the western Iish Sea. *Continental Shelf Research*, 14(5):479–490, 1994.

Hill, A. E., Brown, J., and Fernand, L. The western Irish Sea gyre: A retention system for Norway lobster (Nephrops norvegicus)? *Oceanologica Acta*, 19(3-4):357–368, 1996. Colloquium on Biotic and Abiotic Interactions Regulating Life Cycle of Marine Invertebrates, Villefranche-sur-mer, France, Sep 19-23, 1994.

Hill, A. E., Brown, J., and Fernand, L. The summer gyre in the western Irish Sea: Shelf sea paradigms and management implications. *Estuarine Coastal and Shelf Science*, 44(A):83–95, 1997. 25th Annual Symposium of the Estuarine-and-Coastal-Sciences-Association on Science for Management in

Coastal and Estuarine Waters, Trinity Coll, Univ Dublin, Dublin, Ireland, Sep 11-16, 1995.

Hillis, J. P. Field observations on larvae of the Dublin Bay prawn *Nephrops norvegicus* (L.) in the western Irish Sea. *Irish Fisheries Investigations*, B 13:1–24, 1974.

Holt, J. and Proctor, R. The seasonal circulation and volume transport on the northwest European continental shelf: A fine-resolution model study. *Journal of Geophysical Research-Oceans*, 113(C6), 2008.

Holt, J. T. and James, I. D. An s coordinate density evolving model of the northwest European continental shelf - 1, Model description and density structure. *Journal of Geophysical Research - Oceans*, 106(C7):14015–14034, 2001.

Holt, J. T., Allen, J. I., Proctor, R., and Gilbert, F. Error quantification of a high-resolution coupled hydrodynamic-ecosystem coastal-ocean model: Part 1 model overview and assessment of the hydrodynamics. *Journal of Marine Systems*, 57(1-2):167–188, 2005.

Horsburgh, K. J. and Hill, A. E. A three-dimensional model of density-driven circulation in the Irish Sea. *Journal of Physical Oceanography*, 33 (2):343–365, 2003.

Horsburgh, K. J., Hill, A. E., Brown, J., Fernand, L., Garvine, R. W., and Angelico, M. M. P. Seasonal evolution of the cold pool gyre in the western Irish Sea. *Progress in Oceanography*, 46(1):1–58, 2000.

Howarth, J. and Palmer, M. The Liverpool Bay Coastal Observatory. *Ocean Dynamics*, 61(11):1917–1926, 2011. 15th Biennial Joint Numerical Sea Modelling Group Conference (JONSMOD), Deltares-Delft Hydraulics, Delft, Netherlands, May, 2010.

Howarth, M. J. Currents in the eastern Irish Sea. *Oceanography and Marine Biology*, 22:11–53, 1984.

Huggett, J., Freon, P., Mullon, C., and Penven, P. Modelling the transport success of anchovy Engraulis encrasicolus eggs and larvae in the southern Benguela: the effect of spatio-temporal spawning patterns. *Marine Ecology Progress Series*, 250:247–262, 2003.

Hunter, J. R., Craig, P. D., and Phillips, H. E. On the use of random-walk models with spatially-variable diffusivity. *Journal of Computational Physics*, 106(2):366–376, 1993.

IEA GHG. Assessment of sub sea ecosystem impacts. Technical report, IEA Greenhouse Gas R&D Programme, AUG 2008.

Ingri, N., Kakolowi, W., Sillen, L. G., and Warnqvis, B. High-speed computers as a supplement to graphical methods - V: Haltafall , a general program for calculating composition of equilibrium mixtures. *Talanta*, 14 (11):1261–&, 1967.

Irigoien, X., Conway, D. V. P., and Harris, R. P. Flexible diel vertical migration behaviour of zooplankton in the Irish Sea. *Marine Ecology Progress Series*, 267:85–97, 2004.

James, I. D. Advection schemes for shelf sea models. *Journal of Marine Systems*, 8(3-4):237–254, 1996.

Jefferies, D. F., Steele, A. K., and Preston, A. Further studies on the distribution of CS-137 in British coastal waters .1. Irish Sea. *Deep-Sea Research Part A-Oceanographic Research Papers*, 29(6):713–738, 1982.

Jenkins, G. P., Black, K. P., Wheatley, M. J., and Hatton, D. N. Temporal and spatial variability in recruitment of a temperate, seagrass-associated fish is largely determined by physical processes in the pre- and post-settlement phases. *Marine Ecology Progress Series*, 148(1-3):23–35, 1997.

Jones, G. P., Milicich, M. J., Emslie, M. J., and Lunow, C. Self-recruitment in a coral reef fish population. *Nature*, 402(6763):802–804, 1999.

Jones, G. P., Planes, S., and Thorrold, S. R. Coral reef fish larvae settle close to home. *Current Biology*, 15(14):1314–1318, 2005.

Jones, G. P., Almany, G. R., Russ, G. R., Sale, P. F., Steneck, R. S., van Oppen, M. J. H., and Willis, B. L. Larval retention and connectivity among populations of corals and reef fishes: history, advances and challenges. *Coral Reefs*, 28(2):307–325, 2009. Workshop on Connectivity and Resilience Sustaining Coral Reefs during the coming Century, Townsville, Australia, Oct 13-16, 2007.

Kingsford, M. J., Leis, J. M., Shanks, A., Lindeman, K. C., Morgan, S. G., and Pineda, J. Sensory environments, larval abilities and local self-recruitment. *Bulletin of Marine Science*, 70(1, S):309–340, 2002.

Knight, P. J. and Howarth, M. J. The flow through the north channel of the Irish Sea. *Continental Shelf Research*, 19(5):693–716, APR 1999.

Knights, A. M., Crowe, T. P., and Burnell, G. Mechanisms of larval transport: vertical distribution of bivalve larvae varies with tidal conditions. *Marine Ecology Progress Series*, 326:167–174, 2006.

Kramer, D. L. and Chapman, M. R. Implications of fish home range size and relocation for marine reserve function. *Environmental Biology of Fishes*, 55 (1-2):65–79, 1999. Annual meeting of the society-for-conservation-biology, Victoria, Canada, Jun 07, 1997.

Kvalseth, T. O. Cautionary note about R2. *American Statistician*, 39(4): 279–285, 1985.

Lalli, C. M. and Parsons, T. R. *Biological Oceanography: An Introduction*. Butterworth-Heinemann, Second edition edition, 1997.

Langhamer, O., Wilhelmsson, D., and Engstrom, J. Artificial reef effect and fouling impacts on offshore wave power foundations and buoys - a pilot study. *Estuarine Coastal and Shelf Science*, 82(3):426–432, 2009.

Leech, D. M. and Williamson, C. E. In situ exposure to ultraviolet radiation alters the depth distribution of Daphnia. *Limnology and Oceanography*, 46 (2):416–420, 2001.

Leis, J. M. and Carson-Ewart, B. M. In situ swimming speeds of the late pelagic larvae of some Indo-Pacific coral-reef fishes. *Marine Ecology Progress Series*, 159:165–174, 1997.

Leis, J. M., Sweatman, H. P. A., and Reader, S. E. What the pelagic stages of coral reef fishes are doing out in blue water: Daytime field observations of larval behavioural capabilities. *Marine and Freshwater Research*, 47(2): 401–411, 1996. International Larval Fish Conference, Sydney, Australia, 1995.

Levin, L. A. Recent progress in understanding larval dispersal: new directions and digressions. *Integrative and Comparative Biology*, 46(3):282–297, 2006. Annual Meeting of the Society-for-Integrative-and-Comparative-Biology, San Diego, CA, Jan 04-08, 2004.

Lindley, J. A., Williams, R., and Conway, D. V. P. Variability in dry-weight and vertical distributions of decapod larvae in the Irish-Sea and North-Sea during the spring. *Marine Biology*, 120(3):385–395, 1994.

Mack, R. N., Simberloff, D., Lonsdale, W. M., Evans, H., Clout, M., and Bazzaz, F. A. Biotic invasions: Causes, epidemiology, global consequences, and control. *Ecological Applications*, 10(3):689–710, 2000.

Marta-Almeida, M., Dubert, J., Peliz, A., and Queiroga, H. Influence of vertical migration pattern on retention of crab larvae in a seasonal upwelling system. *Marine Ecology Progress Series*, 307:1–19, 2006.

Martin, G. B., Thorrold, S. R., and Jones, C. M. Temperature and salinity effects on strontium incorporation in otoliths of larval spot (Leiostomus xanthurus). *Canadian Journal of Fisheries and Aquatic Sciences*, 61(1): 34–42, 2004.

McLaren, I. A. Effects of temperature on growth of zooplankton, and the adaptive value of vertical migration . *Journal of the Fisheries Research Board of Canada*, 20(3):685–727, 1963.

McQuaid, C. D. and Phillips, T. E. Limited wind-driven dispersal of intertidal mussel larvae: in situ evidence from the plankton and the spread of the invasive species Mytilus galloprovincialis in South Africa. *Marine Ecology Progress Series*, 201:211–220, 2000.

Mehrbach, C., Culberso, C. H., Hawley, J. E., and Pytkowic, R. M. Measurement of apparent dissociation-constants of carbonic-acid in seawater at atmospheric-pressure. *Limnology and Oceanography*, 18(6):897–907, 1973.

Mercier, C. H. and Delhez, E. J. M. Consistent computation of the age of water parcels using CART. *Ocean Modelling*, 35(1-2):67–76, 2010.

Millero, F. J. Thermodynamics of the carbon-dioxide system in the oceans. *Geochimica et Cosmochimica Acta*, 59(4):661–677, 1995.

Millero, F. J., Lee, K., and Roche, M. Distribution of alkalinity in the surface waters of the major oceans. *Marine Chemistry*, 60(1-2):111–130, FEB 1998. 1st International Meeting on Carbon Dioxide in the Oceans, Mayaguez, PR, Jan, 1996.

Molnar, J. L., Gamboa, R. L., Revenga, C., and Spalding, M. D. Assessing the global threat of invasive species to marine biodiversity. *Frontiers in Ecology and the Environment*, 6(9):485–492, 2008.

Monsen, N. E., Cloern, J. E., Lucas, L. V., and Monismith, S. G. A comment on the use of flushing time, residence time, and age as transport time scales. *Limnology and Oceanography*, 47(5):1545–1553, 2002.

Murakami, K. Tidal exchange mechanism in enclosed regions. *Proceedings of the Second International Conference on Hydraulic Modelling of Coast Estuary and River Waters*, 2:111–120, 1991.

National Research Council, C. *Improving the safety of marine pipelines*. National Academy Press, Washington D. C., 1994.

National Weather Service, N. Climate prediction center - teleconnections: North atlantic oscillation, 2013. http://www.cpc.ncep.noaa.gov/products/precip/CWlink/pna/nao.shtml.

Neill, W. E. Induced vertical migration in copepods as a defence against invertebrate predation. *Nature*, 345(6275):524–526, 1990.

Nichols, J. H., Bennett, D. B., Symonds, D. J., and Grainger, R. Estimation of the stock size of adult Nephrops-norvegicus (L) from larvae surveys in the western Irish Sea in 1982. *Journal of Natural History*, 21(6):1433–1450, 1987.

Nicolle, A., Dumas, F., Foveau, A., Foucher, E., and Thiebaut, E. Modelling larval dispersal of the king scallop (Pecten maximus) in the English Channel: examples from the Bay of Saint-Brieuc and the Bay of Seine. *Ocean Dynamics*, 63(6):661–678, 2013.

Nightingale, P. D., Malin, G., Law, C. S., Watson, A. J., Liss, P. S., Liddicoat, M. I., Boutin, J., and Upstill-Goddard, R. C. In situ evaluation of air-sea gas exchange parameterizations using novel conservative and volatile tracers. *Global Biogeochemical Cycles*, 14(1):373–387, 2000.

North, E., Gallego, A., and Petitgas, P. Manual of recommended practices for modelling physical-biological interactions during fish early life. *ICES Cooperative Research Report*, 295:1–111, 2009.

North, E. W., Schlag, Z., Hood, R. R., Li, M., Zhong, L., Gross, T., and Kennedy, V. S. Vertical swimming behavior influences the dispersal of simulated oyster larvae in a coupled particle-tracking and hydrodynamic model of Chesapeake Bay. *Marine Ecology Progress Series*, 359:99–115, 2008.

O'Connor, M. I., Bruno, J. F., Gaines, S. D., Halpern, B. S., Lester, S. E., Kinlan, B. P., and Weiss, J. M. Temperature control of larval dispersal and the implications for marine ecology, evolution, and conservation. *Proceedings of the National Academy of Sciences of the United States of America*, 104(4):1266–1271, 2007.

Officer, C. B. *Physical oceanography of estuaries (and associated coastal waters)*. Wiley & Sons, New York, 1976.

Ohman, M. D., Frost, B. W., and Cohen, E. B. Reverse diel vertical migration - an escape from invertebrate predators. *Science*, 220(4604):1404–1407, 1983.

Ohsumi, T., Nakashiki, N., Shitashima, K., and Hirama, K. Density change of water due to dissolution of carbon-dioxide and near-field behavior of CO2 from a source on deep-sea floor. *Energy Conversion and Management*, 33(5-8):685–690, 1992. 1st international conf on carbon dioxide removal (ICCDR), Amsterdam, Netherlands, Mar 04-06, 1992.

Olbert, A. I., Hartnett, M., Dabrowski, T., and Mikolajewicz, U. Long-term inter-annual variability of a cyclonic gyre in the western Irish Sea. *Continental Shelf Research*, 31(13):1343–1356, 2011.

O'Neill, C. K., Polton, J. A., Holt, J. T., and O'Dea, E. J. Modelling temperature and salinity in Liverpool Bay and the Irish Sea: sensitivity to model type and surface forcing. *Ocean Science*, 8(5):903–913, 2012.

OSPAR Commission. OSPAR Recommendation 2003/3 adopted by OSPAR 2003 (OSPAR 03/17/1, Annex 9), amended by OSPAR Recommendation 2010/2 (OSPAR 10/23/1, Annex 7), 2003.

OSPAR Commission. 2012 Status Report on the OSPAR Network of Marine Protected Areas, 2012.

OSPAR Commission. OSPAR inventory of offshore installations, 2013.

Ospina-Alvarez, A., Parada, C., and Palomera, I. Vertical migration effects on the dispersion and recruitment of European anchovy larvae: From spawning to nursery areas. *Ecological Modelling*, 231:65–79, 2012.

Palmer, M. R. The modification of current ellipses by stratification in the Liverpool Bay ROFI. *Ocean Dynamics*, 60(2, SI):219–226, 2010.

Palmer, M. R. and Polton, J. A. A strain-induced freshwater pump in the Liverpool Bay ROFI. *Ocean Dynamics*, 61(11):1905–1915, 2011. 15th Biennial Joint Numerical Sea Modelling Group Conference (JONSMOD), Deltares-Delft Hydraulics, Delft, Netherlands, May, 2010.

Palumbi, S. R. Population genetics, demographic connectivity, and the design of marine reserves. *Ecological Applications*, 13(1, S):S146–S158, 2003.

Panton, A., Mahaffey, C., Greenwood, N., Hopkins, J., Montagnes, D., and Sharples, J. Short-term and seasonal variation in metabolic balance in Liverpool Bay. *Ocean Dynamics*, 62(2):295–306, 2012.

Paris, C. B. and Cowen, R. K. Direct evidence of a biophysical retention mechanism for coral reef fish larvae. *Limnology and Oceanography*, 49(6): 1964–1979, 2004.

Paris, C. B., Cowen, R. K., Claro, R., and Lindeman, K. C. Larval transport pathways from Cuban snapper (Lutjanidae) spawning aggregations based on biophysical modeling. *Marine Ecology Progress Series*, 296:93–106, 2005.

Paris, C. B., Cherubin, L. M., and Cowen, R. K. Surfing, spinning, or diving from reef to reef: effects on population connectivity. *Marine Ecology Progress Series*, 347:285–300, 2007. Workshop on Advancements in Modelling Physical-Biological Interactions in Fish Early-Life History, Nantes, France, Apr, 2006.

Peliz, A., Marchesiello, P., Dubert, J., Marta-Almelda, M., Roy, C., and Queiroga, H. A study of crab larvae dispersal on the Western Iberian

Shelf: Physical processes. *Journal of Marine Systems*, 68(1-2):215–236, 2007.

Pennington, J. T. and Emlet, R. B. Ontogenic and diel vertical migration of a planktonic echinoid larva, dendraster-excentricus (eschscholtz) - occurrence, causes, and probable consequences. *Journal of Experimental Marine Biology and Ecology*, 104(1-3):69–95, 1986.

Phelps, J. J. C., Polton, J. A., Souza, A. J., and Robinson, L. A. Hydrodynamic timescales in a hyper-tidal region of freshwater influence. *Continental Shelf Research*, 63:13–22, 2013.

Phelps, J. J. C., Polton, J. A., Souza, A. J., and Robinson, L. A. The influence of behaviour on larval dispersal in shelf sea gyres: Nephrops norvegicus in the Irish Sea. *Marine Ecology Progress Series*, 518:177–191, 2015a.

Phelps, J. J. C., Blackford, J. C., Holt, J. T., and Polton, J. A. Modelling large-scale CO2 leakages in the North Sea. *International Journal of Greenhouse Gas Control*, 38:210–220, 2015b.

Pineda, J., Hare, J. A., and Sponaugle, S. Larval Transport and Dispersal in the Coastal Ocean and Consequences for Population Connectivity. *Oceanography*, 20(3):22–39, 2007.

Planes, S., Jones, G. P., and Thorrold, S. R. Larval dispersal connects fish populations in a network of marine protected areas. *Proceedings of the National Academy of Sciences of the United States of America*, 106(14): 5693–5697, 2009.

Polton, J. A., Palmer, M. R., and Howarth, M. J. Physical and dynamical oceanography of Liverpool Bay. *Ocean Dynamics*, 61(9):1421–1439, 2011.

Polton, J. A., Palmer, M. R., and Howarth, M. J. The vertical structure of time-mean estuarine circulation in a shallow, rotating, semi-enclosed

coastal bay: A Liverpool Bay case study with application for monitoring. *Continental Shelf Research*, 59:115–126, 2013.

Powell, A. and Eriksson, S. P. Reproduction: Life cycle, larvae and larviculture. In Johnson, M. L. and Johnson, M. P., editor, *Ecology and Biology of Nephrops Norvegicus*, volume 64 of *Advances in Marine Biology*, pages 201–245. Elsevier Academic Press Inc, 2013. ISBN 978-0-12-410533-1. doi: 10.1016/B978-0-12-410466-2.00006-6.

Puckett, B. J., Eggleston, D. B., Kerr, P. C., and Luettich, R. A., Jr. Larval dispersal and population connectivity among a network of marine reserves. *Fisheries Oceanography*, 23(4):342–361, 2014.

QICS. Quantifying and monitoring potential ecosystem impacts of geological carbon storage., 2012. http://www.bgs.ac.uk/qics/home.html.

Qiu, Z., Doglioli, A. M., He, Y., and Carlotti, F. Lagrangian model of zooplankton dispersion: numerical schemes comparisons and parameter sensitivity tests. *Chinese Journal of Oceanology and Limnology*, 29(2): 438–445, 2011.

Ramsden, D. and Holloway, G. Timestepping lagrangian particles in two dimensional eulerian flow fields. *Journal of Computational Physics*, 95(1): 101–116, 1991.

Reid, P. C., Borges, M. D., and Svendsen, E. A regime shift in the North Sea circa 1988 linked to changes in the North Sea horse mackerel fishery. *Fisheries Research*, 50(1-2):163–171, 2001.

Rerolle, V. M. C., Floquet, C. F. A., Harris, A. J. K., Mowlem, M. C., Bellerby, R. R. G. J., and Achterberg, E. P. Development of a colorimetric microfluidic pH sensor for autonomous seawater measurements. *Analytica Chimica Acta*, 786:124–131, 2013.

Rijnsdorp, A. D., van Stralen, M., and van der Veer, H. W. Selective tidal transport of North-Sea plaice larvae Pleuronectes-platessa in coastal nurs-

ery areas. *Transactions of the Americal Fisheries Society*, 114(4):461–470, 1985.

Roberts, C. M. Connectivity and management of Caribbean coral reefs. *Science*, 278(5342):1454–1457, 1997.

Roberts, C. M., Bohnsack, J. A., Gell, F., Hawkins, J. P., and Goodridge, R. Effects of marine reserves on adjacent fisheries. *Science*, 294(5548): 1920–1923, 2001.

Roberts, C. M., Hawkins, J. P., Fletcher, J., Hands, S., K., R., and Ward, S. Guidance on the size and spacing of marine protected areas in England. Technical report, Natural England, 2010. Natural England commissioned report NECR037.

Robins, P. E., Neill, S. P., Gimenez, L., Jenkins, S. R., and Malham, S. K. Physical and biological controls on larval dispersal and connectivity in a highly energetic shelf sea. *Limnology and Oceanography*, 58(2):505–524, 2013.

Roe, H. S. J. The diel migrations and distributions within a mesopelagic community in the northeast Atlantic .2. vertical migrations and feeding of mysids and decapod crustacea. *Progress in Oceanography*, 13(3-4):269–318, 1984.

Ross, O. N. and Sharples, J. Recipe for 1-D Lagrangian particle tracking models in space-varying diffusivity. *Limnology and Oceanography - Methods*, 2:289–302, 2004.

Ruiz, G. M., Fofonoff, P. W., Carlton, J. T., Wonham, M. J., and Hines, A. H. Invasion of coastal marine communities in North America: Apparent patterns, processes, and biases. *Annual Review of Ecology and Systematics*, 31:481–531, 2000.

Schindler, D. W. Recent advances in the understanding and management of eutrophication. *Limnology and Oceanography*, 51(1, Part 2):356–363, 2006.

Shanks, A. L. Vertical migration and cross-shelf dispersal of larval Cancer spp and Randallia ornata (Crustacea, Brachyura) off the coast of southern California. *Marine Biology*, 92(2):189–199, 1986.

Shanks, A. L. Pelagic Larval Duration and Dispersal Distance Revisited. *Biological Bulletin*, 216(3):373–385, 2009.

Shanks, A. L., Grantham, B. A., and Carr, M. H. Propagule dispersal distance and the size and spacing of marine reserves. *Ecological Applications*, 13(1, S):S159–S169, 2003.

Simons, R. D., Siegel, D. A., and Brown, K. S. Model sensitivity and robustness in the estimation of larval transport: A study of particle tracking parameters. *Journal of Marine Systems*, 119:19–29, 2013.

Simpson, J. H. Physical processes in the ROFI regime. *Journal of Marine Systems*, 12(1-4):3–15, 1997.

Simpson, J. H. and Hunter, J. R. Fronts in Irish Sea. *Nature*, 250(5465): 404–406, 1974.

Simpson, J. H., Brown, J., Matthews, J., and Allen, G. Tidal straining, density currents, and stirring in the control of estuarine stratification. *Estuaries*, 13(2):125–132, 1990.

Smith, N. P. and Stoner, A. W. Computer-simulation of larval transport through tidal channels - role of vertical migration. *Estuarine Coastal and Shelf Science*, 37(1):43–58, 1993.

Smith, R. S. M. *The biology of larval and juvenile Nephrops norvegicus (L) in the Firth of Clyde*. PhD thesis, University of Glasgow, Glasgow, Scotland, 1987.

Song, Y. C., Nishio, M., Chen, B. X., Someya, S., Uchida, T., and Akai, M. Measurement of the density of CO2 solution by Mach-Zehnder interferometry. In Sideman, S and Landesberg, A, editor, *Visualization and imaging in transport phenomena*, volume 972 of *Annals of the New York Academy of Sciences*, pages 206–212, 2002. International Symposium on Visualization and Imaging in Transport Phenomena, Antalya, Turkey, May 05-10, 2002.

Souza, A. J. and Lane, A. Effects of freshwater inflow on sediment transport. *Journal of Operational Oceanography*, 6(1):27–31, 2013.

Souza, A. J. and Simpson, J. H. The modification of tidal ellipses by stratification in the Rhine ROFI. *Continental Shelf Research*, 16(8):997–1007, 1996.

Staaterman, E. and Paris, C. B. Modelling larval fish navigation: the way forward. *ICES Journal of Marine Science*, 71(4):918–924, 2014.

Starrs, D., Davis, J. T., Schlaefer, J., Ebner, B. C., Eggins, S. M., and Fulton, C. J. Maternally transmitted isotopes and their effects on larval fish: a validation of dual isotopic marks within a meta-analysis context. *Canadian Journal of Fisheries and Aquatic Sciences*, 71(3):387–397, 2014.

Statoil. Sleipner West, 2013. http://www.statoil.com/en/technologyinnovation/newenergy/co2capturestorage/pages/sleipnervest.aspx.

Sundelof, A. and Jonsson, P. R. Larval dispersal and vertical migration behaviour - a simulation study for short dispersal times. *Marine Ecology - an Evolutionary Perspective*, 33(2):183–193, 2012.

Svane, I. and Petersen, J. K. On the problems of epibioses, fouling and artificial reefs, a review. *Marine Ecology*, 22(3):169–188, 2001. doi: 10.1046/j.1439-0485.2001.01729.x.

Svendsen, E., Saetre, R., and Mork, M. Features of the northern North-Sea circulation. *Continental Shelf Research*, 11(5):493–508, 1991.

Takeoka, H. Fundamental concepts of exchange and transport time scales in a coastal sea. *Continental Shelf Research*, 3(3):311–326, 1984.

Thiyagarajan, V., Harder, T., and Qian, P. Y. Combined effects of temperature and salinity on larval development and attachment of the subtidal barnacle Balanus trigonus Darwin. *Journal of Experimental Marine Biology and Ecology*, 287(2):223–236, 2003.

Thomas, H., Bozec, Y., Elkalay, K., and de Baar, H. J. W. Enhanced open ocean storage of CO2 from shelf sea pumping. *Science*, 304(5673):1005–1008, 2004.

Thompson, B. M. and Ayers, R. A. Laboratory studies on the development of Nephrops-norvegucus larvae. *Journal of the Marine Biological Association of the United Kingdom*, 69(4):795–801, 1989.

Thorpe, S. A. On the biological connectivity of oil and gas platforms in the North Sea. *Marine Pollution Bulletin*, 64(12):2770–2781, 2012.

Thorrold, S. R., Jones, C. M., Swart, P. K., and Targett, T. E. Accurate classification of juvenile weakfish Cynoscion regalis to estuarine nursery areas based on chemical signatures in otoliths. *Marine Ecology Progress Series*, 173:253–265, 1998.

Thorrold, S. R., Jones, G. P., Hellberg, M. E., Burton, R. S., Swearer, S. E., Neigel, J. E., Morgan, S. G., and Warner, R. R. Quantifying larval retention and connectivity in marine populations with artificial and natural markers. *Bulletin of Marine Science*, 70(1, S):291–308, 2002.

Thorrold, S. R., Jones, G. P., Planes, S., and Hare, J. A. Transgenerational marking of embryonic otoliths in marine fishes using barium stable isotopes. *Canadian Journal of Fisheries and Aquatic Sciences*, 63(6):1193–1197, 2006.

Thorrold, S. R., Zacherl, D. C., and Levin, L. A. Population Connectivity and Larval Dispersal Using Geochemical Signatures in Calcified Structures. *Oceanography*, 20(3, SI):80–89, 2007.

Todd, C. D. and Doyle, R. W. Reproductive strategies of marine benthic invertebrates - a settlement-timing hypothesis. *Marine Ecology Progress Series*, 4(1):75–83, 1981.

Umlauf, L. and Burchard, H. A generic length-scale equation for geophysical turbulence models. *Journal of Marine Research*, 61(2):235–265, 2003.

van der Molen, J., Rogers, S. I., Ellis, J. R., Fox, C. J., and McCloghrie, P. Dispersal patterns of the eggs and larvae of spring-spawning fish in the Irish Sea, UK. *Journal of Sea Research*, 58(4):313–330, 2007.

Vance, R. R. Reproductive strategies in marine benthic invertebrates. *American Naturalist*, 107(955):339–352, 1973.

Vasconcelos, R. P., Reis-Santos, P., Tanner, S., Fonseca, V., Latkoczy, C., Guenther, D., Costa, M. J., and Cabral, H. Discriminating estuarine nurseries for five fish species through otolith elemental fingerprints. *Marine Ecology Progress Series*, 350:117–126, 2007.

Verspecht, F., Rippeth, T. P., Howarth, M. J., Souza, A. J., Simpson, J. H., and Burchard, H. Processes impacting on stratification in a region of freshwater influence: Application to Liverpool Bay. *Journal of Geophysical Research-Oceans*, 114, 2009a.

Verspecht, F., Rippeth, T. P., Simpson, J. H., Souza, A. J., Burchard, H., and Howarth, M. J. Residual circulation and stratification in the Liverpool Bay region of freshwater influence. *Ocean Dynamics*, 59(5):765–779, 2009b.

Verspecht, F., Simpson, J. H., and Rippeth, T. P. Semi-diurnal tidal ellipse variability in a region of freshwater influence. *Geophysical Research Letters*, 37(L18602), 2010.

Vikebo, F., Sundby, S., Adlandsvik, B., and Fiksen, O. The combined effect of transport and temperature on distribution and growth of larvae and pelagic juveniles of Arcto-Norwegian cod. *ICES Journal of Marine Science*, 62(7):1375–1386, 2005. ICES Symposium on Influence of Climate Change on North Atlantic Fish Stocks, Bergen, Norway, May 11-14, 2004.

Vikebo, F., Jorgensen, C., Kristiansen, T., and Fiksen, O. Drift, growth, and survival of larval Northeast Arctic cod with simple rules of behaviour. *Marine Ecology Progress Series*, 347:207–219, 2007. Workshop on advancements in modelling physical-biological interactions in fish early-life history, Nantes, France, Apr, 2006.

Visser, A. W. Using random walk models to simulate the vertical distribution of particles in a turbulent water column. *Marine ecology progress series*, 158:275–281, 1997.

Wakelin, S. L., Holt, J. T., Blackford, J. C., Allen, J. I., Butenschoen, M., and Artioli, Y. Modeling the carbon fluxes of the northwest European continental shelf: Validation and budgets. *Journal of Geophysical Research-Oceans*, 117, 2012.

Waugh, D. W., Haine, T. W. N., and Hall, T. M. Transport times and anthropogenic carbon in the subpolar North Atlantic Ocean. *Deep-Sea Research Part I-Oceanographic Research Papers*, 51(11):1475–1491, 2004.

Weiss, R. F. Carbon dioxide in water and seawater: the solubility of a non-ideal gas. *Marine Chemistry*, 2(3):203 – 215, 1974.

White, R. G., Hill, A. E., and Jones, D. A. Distribution of nephrops-norvegicus (l) larvae in the western Irish Sea - an example of advective control on recruitment. *Journal of Plankton Research*, 10(4):735–747, 1988.

Widdicombe, S., Blackford, J. C., and Spicer, J. I. Assessing the environmental consequences of CO2 leakage from geological CCS: Generating evidence to support environmental risk assessment. *Marine Pollution Bulletin*, 73 (2, SI):399–401, 2013.

Wilhelmsson, D. and Malm, T. Fouling assemblages on offshore wind power plants and adjacent substrata. *Estuarine Coastal and Shelf Science*, 79(3): 459–466, 2008.

Williamson, D. H., Jones, G. P., Thorrold, S. R., and Frisch, A. J. Transgenerational marking of marine fish larvae: stable-isotope retention, physiological effects and health issues. *Journal of Fish Biology*, 74(4):891–905, 2009.

Willis, J. Modelling swimming aquatic animals in hydrodynamic models. *Ecological Modelling*, 222(23-24):3869–3887, 2011.

Wilson, T. R. S. Caesium-137 as a water movement tracer in St. Georges Channel. *Nature*, 248(5444):125–127, 1974.

Xing, J. X. and Davies, A. M. A three-dimensional baroclinic model of the Irish Sea: Formation of the thermal fronts and associated circulation. *Journal of Physical Oceanography*, 31(1):94–114, 2001.

Zaret, T. M. and Suffern, J. S. Vertical migration in zooplankton as a predator avoidance mechanism. *Limnology and Oceanography*, 21(6):804–813, 1976.

Zhang, W. G., Wilkin, J. L., and Schofield, O. M. E. Simulation of water age and residence time in New York Bight. *Journal of Physical Oceanography*, 40(5):965–982, 2010.

Zimmerman, J. T. F. Mixing and flushing of tidal embayments in the western Dutch Wadden Sea, Part .1. Distribution of salinity and calculation of mixing time scales. *Netherlands Journal of Sea Research*, 10(2):149–191, 1976.